Dissecting the phenotype and functionality of different malaria-induced regulatory T cell subsets

Dissertation with the aim of achieving a doctoral degree at the Faculty of Mathematics, Informatics and Natural Sciences

Department of Biology

Universität Hamburg

Submitted by Lea Kaminski

Hamburg, 2023

Date of the oral defense: 18.08.2023

Referees

Prof. Dr. Tim Gilberger

CSSB Centre for Structural Systems Biology

c/o Deutsches Elektronen-Synchrotron DESY

Notkestraße 85, Building 15, 22607 Hamburg

PD Dr. Thomas Jacobs

Bernhard Nocht Institute for Tropical Medicine

Department Protozoa Immunology

Bernhard-Nocht-Straße 74, 20359 Hamburg

Table of Contents

Eidesstattliche Versicherung/ Declaration on oath

Hiermit erkläre ich an Eides statt, dass ich die vorliegende Dissertationsschrift selbst verfasst und keine anderen als die angegebenen Quellen und Hilfsmittel benutzt habe.

I hereby declare upon oath that I have written the present dissertation independently and have not used further resources and aids than those stated.

Hamburg, den | Hamburg, date   Unterschrift | Signature

Publications

(1)   Kaminski, L.-C., Riehn, M., Abel, A., Steeg, C., Yar, D. D., Addai-Mensah, O., Aminkiah, F., Owusu Dabo, E., Jacobs, T., and Mackroth, M. S. (2019). Cytotoxic T Cell-Derived Granzyme B Is Increased in Severe Plasmodium Falciparum Malaria. Front Immunol, 10(2917), 2917. https://doi.org/10.3389/fimmu.2019.02917

(2)   Brandi, J., Lehmann, C., Kaminski, L. C., Schulze Zur Wiesch, J., Addo, M., Ramharter, M., Mackroth, M., Jacobs, T., and Riehn, M. (2021). T cells expressing multiple co-inhibitory molecules in acute malaria are not exhausted but exert a suppressive function in mice. Eur J Immunol, 52, 312-327. https://doi.org/10.1002/eji.202149424

Abbreviations

APC	Antigen-presenting cell
	Also: Allophycocyanin (fluorophore)
AF700	Alexa fluor 700 (fluorophore)
AMP	Adenosine monophosphate
ATP	Adenosine triphosphate
BCR	B cell receptor
BUV395	Brilliant ultra violet 395 (fluorophore)
BV421	Brilliant violet 421 (fluorophore)
CD	Cluster of differentiation
CM	Cerebral malaria
CO_2	Carbon dioxide
cRPMI	Complete Roswell Park Memorial Institute cell culture medium
CTL	Cytotoxic T lymphocyte
CTLA-4	Cytotoxic T lymphocyte-associated protein 4
Cy7	Cyanine 7
DC	Dendritic cell
DMSO	Dimethyl sulfoxide
EDTA	Ethylenediaminetetraacetic acid
eF450	Cell proliferation dye eFluor^{TM} 450
FACS	Fluorescence-activated cell sorting
FCS	Fetal calf serum
FGL1	Fibrinogen-like protein 1
FITC	Fluorescein isothiocyanate (fluorophore)
FMO	Fluorescence minus one
FoxP3	Forkhead Box P3
FSC	Forward scatter
Gy	Gray (unit of radiation quantity)
HBV	Hepatitis B virus
HCV	Hepatitis C virus
HIV	Human immunodeficiency virus

ICOS	Inducible T cell costimulator
IFN	Interferon
Ig	Immunoglobulin
IL	Interleukin
ITIM	Immunoreceptor tyrosine-based inhibitory motif
iTreg	Induced regulatory T cell
ITSM	Immunoreceptor tyrosine-based switch motif
LAG-3	Lymphocyte-activation gene 3
LCMV	Lymphocytic choriomeningitis virus
MACS	Magnetic activated cell separation
MFI	Median fluororescence intensity
MHC	Major histocompatibility complex
min	minute(s)
n/a	Not available
NK cell	Natural killer cell
NKT cell	Natural killer T cell
nTreg	Natural FoxP3$^+$ regulatory T cells
PAMP	Pathogen-associated molecular pattern
*Pb*A	*Plasmodium berghei* ANKA
PBMCs	Peripheral blood mononuclear cells
PBS	Dulbecco's phosphate buffered saline
PD-1	Programmed Death-1
PD-L1/2	Programmed Death Ligand 1/2
PE	Phycoerythrin (fluorophor)
PerCP	Peridinin chlorophyll protein (fluorophor)
Pf	*Plasmodium falciparum*
PRR	Pattern recognition receptor
PtdSer	Phosphatidylserine
rad	Radiation absorbed dose
RBC	Red blood cell
rpm	Revolutions per minute
RT	Room temperature

SSC	Side scatter
TGF-β	Transforming growth factor beta
TIGIT	T cell immunoreceptor with Ig and ITIM domains
Th cell	T helper cell
TIM-3	T cell immunoglobulin and mucin-domain containing-3
TNF-α	Tumor necrosis factor alpha
Tr1 cell	Type 1 regulatory T cell
Treg	Regulatory T cell
TCR	T cell receptor
WHO	World Health Organization
xg	Relative centrifugal force

List of figures

List of tables

Abstract

In infectious diseases like malaria, maintaining a balance between pro-inflammatory and anti-inflammatory immune reactions is crucial to ensure successful control of the pathogen without causing immunopathology. Pro-inflammatory-acting cytotoxic CD8$^+$GrzB$^+$ T cells have been shown to be a main contributor to experimental cerebral malaria. However, their role in patients with acute *Plasmodium falciparum* (*Pf*) malaria remains incompletely understood. The induction of co-inhibitory molecules on T cells is one mechanism, which might counteract this T cell-mediated immunopathology. Regulatory CD4$^+$FoxP3$^-$PD-1$^+$ T cells with characteristics of type 1 regulatory T cells (Tr1 cells) have shown to be induced in patients suffering from *Pf* malaria. However, whether they have an influence on the disease outcome of malaria remains unclear. Thus, this study aimed to understand the role of cytotoxic CD8$^+$ T cells and potentially counteracting regulatory T cell subsets induced during *Pf* malaria. To this end, T cells of adults and Ghanaian children suffering from malaria, as well as corresponding healthy donors were analyzed via flow cytometry. Furthermore, different subsets of malaria-induced regulatory CD4$^+$FoxP3$^-$PD-1$^+$ T cells were isolated from peripheral blood of malaria patients and healthy donors and incubated with autologous responder cells to elucidate their suppressive function. Here, we showed that the proportion of CD8$^+$GrzB$^+$ T cells correlates significantly with disease severity in Ghanaian children suffering from *Pf* malaria, underlining their contribution to the development of severe malaria in humans. Furthermore, when analyzing different subsets of regulatory CD4$^+$FoxP3$^-$PD-1$^+$ T cells, we identified a malaria-induced subset that co-expresses LAG-3 and CD49b, which are markers for type 1 regulatory T cells (Tr1 cells). While their frequency did not differ between Ghanaian children suffering from severe or mild malaria, phenotypic analyses revealed a significant upregulation of TIGIT and TIM-3 in children with severe malaria compared to children with mild malaria. Besides PD-1, we identified CCR5 as an additional surface marker of malaria-induced CD4$^+$LAG-3$^+$CD49b$^+$ T cells. Because of the low amount of CD4$^+$LAG-3$^+$CD49b$^+$ T cells in the peripheral blood of malaria patients, we instead analyzed the suppressive function of different subsets of CD4$^+$FoxP3$^-$PD-1$^+$ T cells, which contained the CD4$^+$LAG-3$^+$CD49b$^+$ T cell population. Interestingly, the CCR5$^+$ subset showed a more activated phenotype and exerted a stronger suppressive function than the CCR5$^-$ population. In contrast, expression of TIGIT led to diminished suppressive capacities and a less activated phenotype. Strikingly, the frequency of CD4$^+$PD-1$^+$TIGIT$^+$ T cells correlated with

disease severity in Ghanaian children suffering from malaria, indicating that higher numbers of those dysfunctional regulatory T cells favor immunopathology in malaria patients.

In conclusion, this study further emphasizes the critical role of GrzB-producing CD8$^+$ T cells in the development of severe clinical malaria and indicates that also a failure of regulatory T cell functions might contribute to immunopathology. Further analysis of the interplay between cytotoxic CD8$^+$ T cells and malaria-induced regulatory T cells and the mechanisms regulating their functionality could be of great importance to treat malaria and improve the clinical outcome of severe cases in the future.

Zusammenfassung

Bei Infektionskrankheiten wie der Malaria ist die Aufrechterhaltung eines Gleichgewichts zwischen entzündungsfördernden und entzündungshemmenden Immunreaktionen von entscheidender Bedeutung, um eine erfolgreiche Bekämpfung des Erregers zu gewährleisten, ohne Immunpathologie zu verursachen. Es hat sich gezeigt, dass pro-inflammatorisch-wirkende, zytotoxische $CD8^+GrzB^+$ T-Zellen eine wesentliche Rolle bei der Entstehung von experimenteller zerebraler Malaria spielen. Ihre Rolle bei Patienten mit akuter *Plasmodium falciparum* (*Pf*) Malaria ist jedoch noch nicht vollständig geklärt. Die Induktion von ko-inhibitorischen Molekülen auf T-Zellen ist ein Mechanismus, der dieser T-Zell-vermittelten Immunpathologie entgegenwirken könnte. Es wurde gezeigt, dass regulatorische $CD4^+FoxP3^-PD-1^+$ T-Zellen mit Merkmalen von Typ 1 regulatorischen T- (Tr1) Zellen bei Patienten mit *Pf*-Malaria induziert sind. Ob sie jedoch einen Einfluss auf den Krankheitsverlauf der Malaria haben, wurde bisher nicht hinreichend geklärt. Ziel dieser Studie war es daher, die Rolle zytotoxischer $CD8^+$ T-Zellen und potenziell entgegenwirkender, malaria-induzierter regulatorischer T-Zell-Populationen zu untersuchen. Zu diesem Zweck wurden T-Zellen von Erwachsenen und Ghanaischen Kindern, die an Malaria erkrankt waren, sowie von gesunden Spendern durchflusszytometrisch analysiert. Darüber hinaus wurden verschiedene Untergruppen der Malaria-induzierten regulatorischen $CD4^+FoxP3^-PD-1^+$ T-Zellen aus dem peripheren Blut von Malariapatienten und gesunden Spendern isoliert und mit autologen Responderzellen inkubiert, um ihre suppressive Funktion zu untersuchen.

Wir konnten zeigen, dass der Anteil der $CD8^+GrzB^+$ T-Zellen bei, an *Pf*-Malaria erkrankten Ghanaischen Kindern, signifikant mit dem Schweregrad der Erkrankung korreliert, was ihre Rolle bei der Entwicklung einer schweren Malaria beim Menschen unterstreicht. Bei der Analyse verschiedener Untergruppen regulatorischer $CD4^+FoxP3^-PD-1^+$ T-Zellen identifizierten wir außerdem eine Malaria-induzierte Population, die LAG-3 und CD49b ko-exprimiert. LAG-3 und CD49b sind Marker für Tr1-Zellen. Während sich die Anzahl dieser Zellen nicht zwischen Ghanaischen Kindern mit schwerer und leichter Malaria unterschied, zeigten phänotypische Analysen eine signifikante Hochregulierung von TIGIT und TIM-3 bei Kindern mit schwerer Malaria im Vergleich zu Kindern mit milder Malaria. Neben PD-1 identifizierten wir CCR5 als einen weiteren Oberflächenmarker von Malaria-induzierten $CD4^+LAG-3^+CD49b^+$ T-Zellen. Aufgrund der geringen Menge an $CD4^+LAG-3^+CD49b^+$ T-Zellen im peripheren Blut von

Malariapatienten analysierten wir stattdessen die suppressive Funktion verschiedener Populationen von CD4$^+$FoxP3$^-$PD-1$^+$ T-Zellen, die die CD4$^+$LAG-3$^+$CD49b$^+$ T-Zellpopulation enthalten. Interessanterweise zeigten die CCR5$^+$ Zellen einen aktiveren Phänotyp und übten eine stärkere suppressive Funktion aus als die CCR5$^-$ Zellen. Im Gegensatz dazu führte die Expression von TIGIT zu verminderten suppressiven Fähigkeiten und einem weniger aktivierten Phänotyp. Bemerkenswerterweise korrelierte die Anzahl an CD4$^+$PD-1$^+$TIGIT$^+$ T-Zellen mit dem Schweregrad der Erkrankung bei an Malaria erkrankten Ghanaischen Kindern, was darauf hindeutet, dass eine höhere Anzahl dieser dysfunktionalen regulatorischen T-Zellen die Immunpathologie bei Malariapatienten begünstigt.

Zusammenfassend unterstreicht diese Studie die kritische Rolle der GrzB-produzierenden CD8$^+$ T-Zellen bei der Entwicklung einer schweren klinischen Malaria und zeigt, dass auch ein Versagen der regulatorischen T-Zellfunktionen zur Immunpathologie beitragen könnte. Eine weitere Analyse des Zusammenspiels zwischen zytotoxischen CD8$^+$ T-Zellen und Malaria-induzierten regulatorischen T-Zellen und der Regulierung ihrer Funktionalität könnte in Zukunft von Bedeutung für die Behandlung von Malaria und die Verbesserung des klinischen Verlaufs von schwerer Malaria sein.

1   Introduction

1.1   Malaria

The mosquito-borne disease malaria remains a major threat, mainly to people living in resource-limited countries and areas. In 2021, 84 countries were malaria-endemic with an estimated 247 million cases and 619,000 deaths (1). Africa accounted for 95 % of all global malaria cases and 96 % of deaths and is therefore the region most affected by malaria, followed by the Eastern Mediterranean Region (2.5 % cases, 2 % deaths), South-East Asia (2 % cases, 1.5 % deaths), the Western Pacific Region (< 1 % cases and deaths) and Central and South America (< 1 % cases and deaths) (Figure 1).
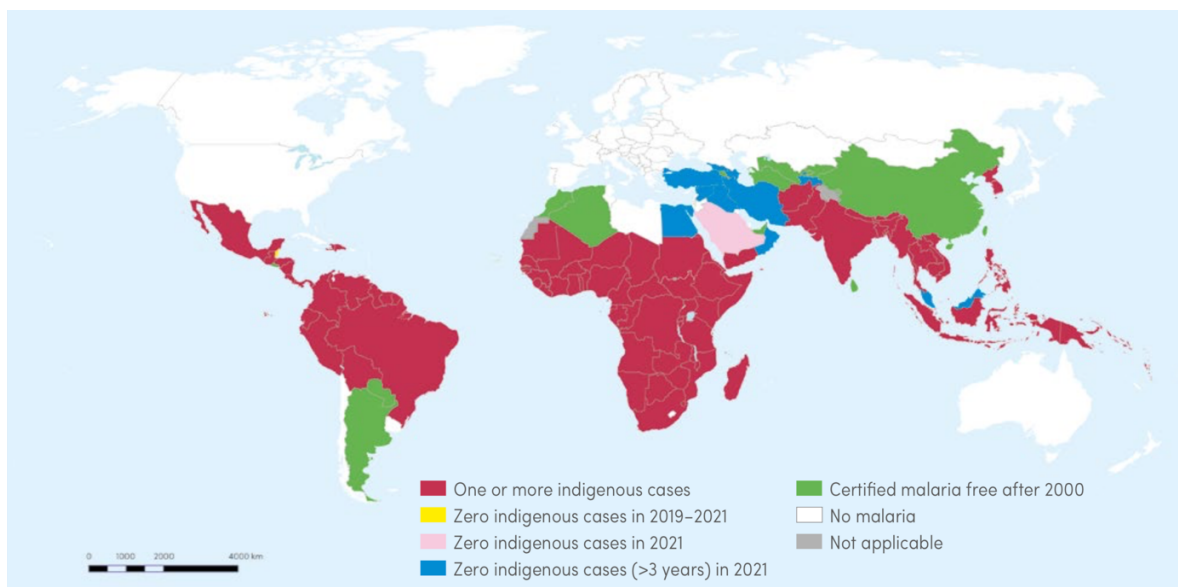
Figure 1: Countries with indigenous malaria cases between 2000 and 2021.

The map shows all countries that had reported indigenous malaria cases in 2000 and their status in the year 2021. According to the World Health Organization (WHO), all countries that had no reported indigenous case in three consecutive years are considered to have eliminated malaria. The European region has been malaria-free since 2015. Source of the map: World malaria report 2022 of the WHO (1).

Due to improved preventive measures, like the distribution of insecticide-treated mosquito nets, seasonal malaria chemoprevention, better diagnosis and easier access to medication, the number of global death cases has declined over the last years, from 897,000 in 2000 to 568,000 in 2019 (2). Between 2019 and 2021, the number of malaria cases increased from around 229

million to 247 million cases. In addition, the number of malaria deaths increased by 10 % between 2019 and 2020 from 568,000 to 625,000, mainly due to service disruptions caused by the ongoing COVID-19 pandemic (3). Although malaria deaths slightly decreased again between 2020 and 2021, malaria is still far from being under control and further measures are needed to cope with this threat.

The most vulnerable groups affected by malaria are pregnant women and their fetuses as well as children under the age of 5. Young children account for approximately 60-70 % of death cases each year and children born to infected mothers often suffer from low birth weight, which is associated with an increased infant mortality rate (2, 4).

Malaria is caused by single-celled, eukaryotic, protozoan parasites of the genus *Plasmodium*. There are 5 different human pathogenic strains of *Plasmodium* with different characteristics with regard to their pathogenicity and disease severity. *Plasmodium falciparum* (*Pf*) and *Plasmodium vivax* are the most prevalent parasite strains. *Plasmodium vivax* predominantly occurs in Central and South America and normally causes milder symptoms than *Pf*. Other strains are *Plasmodium malariae*, *Plasmodium ovale* and the zoonotic parasite *Plasmodium knowlesi* (5). *Plasmodium falciparum* is responsible for over 99 % of the infections in sub-Saharan Africa (2). It causes the most severe form of malaria, the malaria tropica, and accounts for the vast majority of annual malaria deaths. Due to its relevance, this work focuses on infections with *Plasmodium falciparum*.

Generally, the disease malaria is divided into three groups based on disease severity: asymptomatic, mild (uncomplicated) and severe (complicated). In the beginning, malaria leads to unspecific symptoms like headaches, fever, respiratory distress, nausea, joint pain, coughing and diarrhea, which makes it difficult to distinguish them from those of other infectious diseases (6, 7). As the disease progresses, many patients also develop anemia which can become severe, especially in infections with *Pf*. Symptoms of severe malaria include severe anemia, respiratory distress, hyperparasitemia (parasitemia > 10 %) and acidosis (8). In a particularly severe course of *Pf*-malaria, some patients develop cerebral malaria (CM), with symptoms including neuronal deficits, paralysis, seizures and coma (9). Approximately 1 % of patients develop CM, of which 90 % occur in children in sub-Saharan Africa (2). At 15-20 %, the mortality rate of CM is quite high and around 10-20 % of patients suffer from long-term complications after surviving it (9, 10). Multiple factors are involved in the development of CM, and not all mechanisms are fully understood yet. The main factor causing CM in humans is the

sequestration of *Pf*-infected erythrocytes in vascular endothelial cells of the brain (11). Other factors are increased inflammation caused by an exacerbated proinflammatory cytokine response in the brain, and widespread coagulation in blood vessels of the brain (12, 13). All of these events lead to a disruption of the blood-brain barrier, thus causing severe neurological complications.

People living in a malaria-endemic region with a high transmission rate – where the antigen is constantly present – develop partial immunity over time. After several malaria episodes during their childhood, adults are partly immune and are more likely to develop only mild or no symptoms after an infection with *Pf* (14). However, this immunity is only temporary and fades as soon as people are no longer exposed to the antigen (for example when they leave the country for a longer period of time).

1.1.1   Plasmodia life cycle

Plasmodia are transmitted to the human host as sporozoites by female *Anopheles* mosquitos during a blood meal, where they undergo a complex life cycle (Figure 2). The sporozoites migrate quickly from the skin through blood vessels into the liver, where they invade hepatocytes (15). Here they multiply asexually and develop into merozoites. One sporozoite thus gives rise to several thousand merozoites. This liver stage lasts 6-7 days and is usually asymptomatic (16). The merozoite-filled hepatocytes, called schizonts, eventually rupture and the merozoites are released into the blood stream where they infect red blood cells (RBC) and the blood stage begins (17). *Plasmodium vivax* and *Plasmodium ovale* can persist in the liver in a dormant stage known as hypnozoites, and thus can cause relapses even months or years after the initial infection (18). The merozoites multiply inside the RBC and undergo different developmental stages. First, they develop into the ring stage, followed by the trophozoite stage. Finally, they form schizonts that rupture and release merozoites into the blood stream, where they infect RBC and the cycle starts over again (19). The rupture of RBC causes a strong inflammatory response characterized by the onset of symptoms, most notably fever. The developmental cycle of merozoites inside RBC takes 36-72 hours, which results in recurrent, regular episodes of fever (16). Some parasites develop from the ring stage into sexual stages (male and female gametocytes) that can be taken up by an *Anopheles* mosquito during a blood feed to undergo sexual development inside the mosquito and infect a new human host, fulfilling the whole life cycle (20).
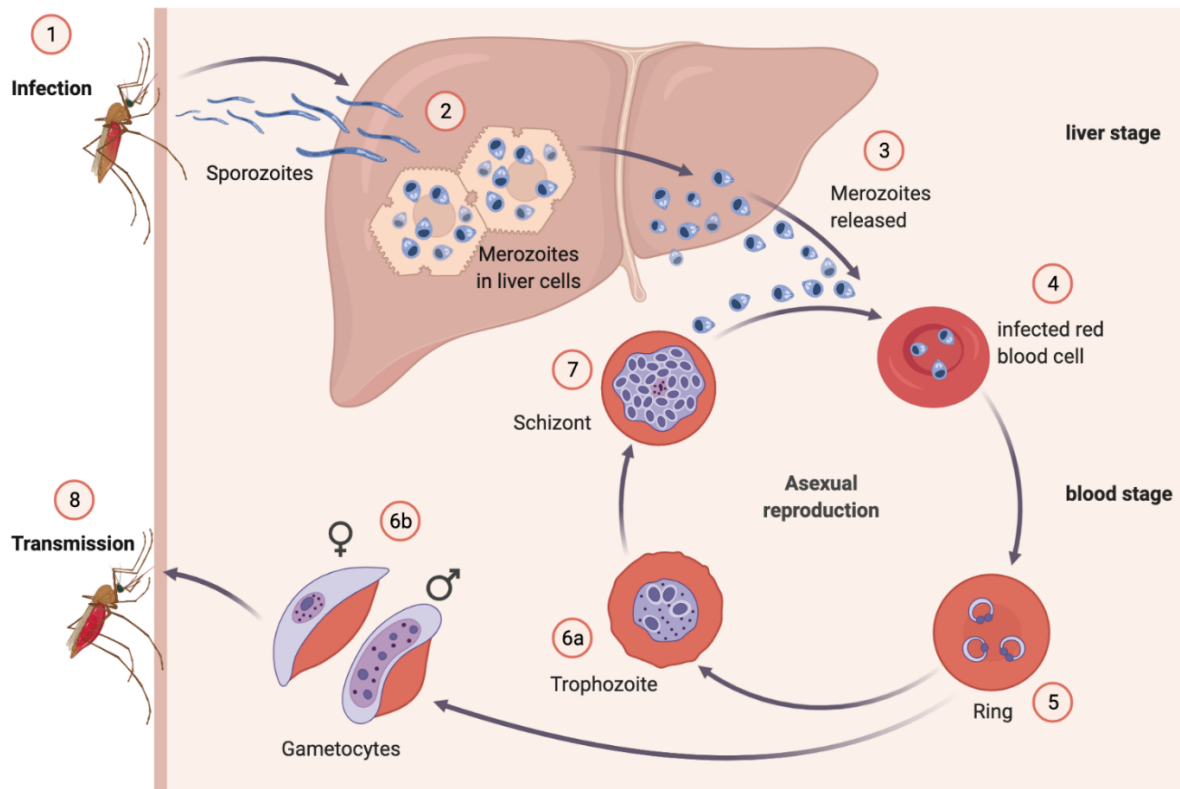
Figure 2: Asexual life cycle of *Plasmodium falciparum* inside the human host.

Female *Anopheles* mosquitos transmit *Plasmodium falciparum* (*Pf*) parasites during a blood feed (1). These sporozoites migrate quickly to the liver where they infect hepatocytes and the liver stage begins (2). The parasites develop into schizonts that eventually rupture and release thousands of merozoites into the blood stream (3). They infect red blood cells (RBC) and the blood stage takes place (4). Inside the RBC, the parasites undergo different developmental stages: the ring stage (5), the trophozoite stage (6a) and finally the schizont stage (7). The schizonts rupture and release merozoites, which again infect RBCs and the cycle starts from the beginning. Some parasites develop from the ring stage into gametocytes (6b) – the sexual stages – which can be ingested by another *Anopheles* mosquito during a blood meal (8). Sexual development of the parasites then takes place inside the mosquito's gut.

Adapted from "Malaria Transmission Cycle", by BioRender.com (2021). Retrieved from https://app.biorender.com/biorender-templates.

1.2   The immune system

1.2.1   Innate immunity

The immune system protects humans from pathogens such as bacteria, viruses, fungi and parasites through complex defense mechanisms. In this process, a non-specific immune response by the innate immune system forms one of the first lines of defense. Cellular components of the innate immune system include natural killer (NK) cells, macrophages and dendritic cells. While NK cells can induce apoptosis of infected cells by secreting cytotoxic granules, macrophages and dendritic cells are so-called professional antigen-presenting cells

(APC) that can phagocytose pathogens (21, 22). After intracellular processing, these APC present small parts of the pathogens as antigens on their cell surface via major histocompatibility complexes (MHC). These MHC-antigen complexes are recognized by cells of the adaptive immune system. Cellular responses of the innate immune system to pathogens result in the release of messenger substances, such as cytokines and chemokines, which recruit additional immune cells to the site of inflammation. The cellular and humoral (soluble) components of the innate immune system interact with the cells of the adaptive immune system to initiate a specific and selective immune response.

1.2.2 Adaptive immunity

The cells of the adaptive immune system are the B and T lymphocytes, which recognize antigens via their specific surface receptors – the B and T cell receptor (BCR and TCR). While T cells initiate the cellular immune response, activated B cells provide a humoral immune response by releasing antigen-specific antibodies. B cells mature inside the bone marrow and subsequently migrate through the blood to secondary lymphoid organs, such as the spleen and lymph nodes (23). T cells develop inside the thymus and, depending on the structure of their TCR, a distinction is made between αβ-T cells, which account for 90-95% of circulating T cells, and γδ-T cells that are mostly tissue-resident (24). Since this work is limited to studies on αβ-T cells, only these will be described in more detail here. During the maturation of αβ-T cells, an antigen-specific receptor complex is formed, consisting of the TCR, cluster of differentiation 3 (CD3), and a co-receptor (25). As a co-receptor, mature αβ-T cells express either CD4 or CD8, dividing them into CD4$^+$ and CD8$^+$ T cells. The TCR specifically binds antigens presented by APC via MHC molecules. In this process, CD4 binds to MHC class II (MHCII) and CD8 to MHC class I molecules (MHCI). Three signals are required for full T cell activation. Recognition of antigens presented on MHC by APC forms the first signal and binding of co-stimulatory molecules is required as the second signal (26). One of the best-characterized costimulatory signals is caused by the binding of CD28 to CD80 (27, 28) and CD86 (29-31). CD28 is constitutively expressed on T cells (32) and CD80 and CD86 are expressed by APCs such as macrophages, DCs and B cells (33). The expression of CD80 and CD86 is induced by activation of APCs, for example during infection with certain microbes. The signal mediated by CD28 supports TCR signaling pathways by inducing survival signals and the production of IL-2, which leads to T cell proliferation (34, 35).

Cytokine-mediated signals derived, for example, from activated dendritic cells, macrophages, NK cells or other T cells are critical for T cell differentiation and form the third signal required for full T cell activation. Naïve T cells differentiate into T effector cells or memory T cells after activation. While T effector cells induce inflammatory processes by activating B cells and cells of the innate immune system, regulatory T cells (Treg) are responsible for regulating and inhibiting these processes, as described in more detail in section 1.2.4. In response to an infection, some antigen-specific activated T cells develop into memory T cells, which are rapidly activated upon re-exposure to the same antigen, often ensuring a rapid elimination of the pathogen (36).

1.2.3   Effector T cells

Activated T cells differentiate into different effector T cell types. CD8+ T cells differentiate into cytotoxic T cells (CTL). Their main function is to recognize and eliminate infected and malignant endogenous cells by secreting cytotoxic molecules such as granzymes and perforin (37). CD4+ T effector cells, also called T helper (Th) cells, are divided into several subgroups, including Th1, Th2 and Th17 cells. Naïve CD4+ T cells produce very small amounts of cytokines. Shortly after activation, they produce interleukin 2 (IL-2), which stimulates their proliferation. The release of IL-12 and interferon gamma (IFN-γ) by activated macrophages, dendritic cells and NK cells results in the development of Th1 cells, which in turn mainly produce IFN-γ and induce further activation of macrophages (38). Th2 cells develop, for example, in response to helminth infections or allergens at high concentrations of IL-4, which is secreted by mast cells and Th2 cells themselves (39). Th2 cells mainly produce IL-4, IL-5 and IL-13 and stimulate the activation of mast cells and eosinophils and the release of immunoglobulin (Ig) E (40). Infections with various bacteria and fungi lead to activation of dendritic cells and production of IL-6, IL-1 and IL-23, inducing differentiation of Th17 cells (41). These produce IL-17 and IL-22 and recruit and activate neutrophil granulocytes, which, like macrophages, can ingest pathogens by phagocytosis and are also an important component of the innate immune system.

1.2.4   Regulatory T cells

The proinflammatory responses of T effector cells to combat and eliminate pathogens can be harmful to the host and may lead to tissue damage and other unwanted complications. It is necessary to prevent endogenous or harmless exogenous antigens (for example food-

associated allergens) from being recognized as harmful. Therefore, it is of great importance to regulate the reactions of T effector cells and other immune cells. This is essentially done by natural regulatory CD4$^+$ T cells (nTreg), which already develop in the thymus and can be characterized by the expression of the IL-2 receptor α-chain (CD25) and the transcription factor forkhead box P3 (Foxp3) (42, 43). There is evidence that their regulatory function is mainly based on the release of the immunomodulatory cytokines IL-10 and TGF-β (44-48). By expressing high levels of CD25, nTreg might also regulate effector T cell functions through IL-2 consumption (49). During acute infections, another population of Treg cells differentiates from naïve CD4$^+$ T cells. These cells are referred to as induced regulatory T cells (iTreg) (50-52). The interplay between both Treg populations is important for maintaining immune homeostasis (53).

Another type of regulatory CD4$^+$ T cells are type 1 regulatory T cells (Tr1 cells), which were first described in an immunodeficient patient who had received a stem cell transplant (54). In contrast to nTreg, they only transiently express low levels of FoxP3 upon activation (55). They show high suppressive activity during various immune-mediated diseases and maintain immune tolerance (56, 57). They mainly regulate effector cell responses by releasing IL-10 and TGF-β and eliminating APC by granzyme B (58, 59). Tr1 cells express the ectonuclease CD39, which exerts anti-inflammatory effects by degrading extracellular adenosine triphosphate (ATP) (60). CD49b, the α2 subunit of very late activation antigen 2 (VLA-2), and the co-inhibitor lymphocyte-activation gene 3 (LAG-3), have both been described as markers for both murine and human Tr1 cells (61, 62). It has been shown that in different contexts Tr1 cells can develop from naïve and memory CD4$^+$ T cells as well as from Th1, Th2 and Th17 cells (63). In malaria, the conversion of Th1 cells into Tr1 cells was suggested through a combination of single-cell RNA sequencing and computational analysis (64).

1.3 T cell exhaustion

Under steady state conditions, CD8$^+$ T cells recognize antigens presented by APC and kill them effectively. This controls the outgrowth of mutated cells and the expansion of pathogens within infected cells. Effector T cells either die after potential agitators have been eliminated or they transition into memory cells, ensuring a rapid immune response after reinfection with the same pathogen or cancer relapses. In contrast, in certain chronic viral infections and tumors, constant

antigen exposure can lead to a dysfunctional T cell state (65). This state, where T cell function, activity and cytokine production is impaired, is termed T cell exhaustion. This mechanism is important to maintain immune homeostasis during chronic infections by preventing severe damage to the host but also ensuring further pathogen elimination. Initially, T cell exhaustion was discovered in mice infected with the lymphocytic choriomeningitis virus (LCMV), in which CD8$^+$ T cells lost their ability to kill infected cells and thus prevent proper viral clearance (66). Furthermore, in certain tumors, T cell exhaustion has been found to be responsible for impaired tumor growth control (67-69). A key characteristic of exhausted T cells is the expression of so-called co-inhibitory molecules which will be described in detail in the following chapter (1.4 Co-Inhibitory molecules). In short, these are molecules that are able to downregulate effector functions of other immune cells. Antibody-mediated blockade of co-inhibitory molecules to regain or improve T cell function was first successfully implemented in cancer therapy (70). The antibodies are designed to block the interaction between the co-inhibitory molecule and its respective ligand without conferring the otherwise-induced downstream signal. Accordingly, T cell function is restored, leading to higher levels of pro-inflammatory cytokines and increased effector T cell proliferation. Immune therapy with antibodies targeting PD-1 or CTLA-4 were successfully implemented as a therapeutic approach against certain tumors, restoring effector functions of tumor-specific T cells (71). The effectiveness of such immune checkpoint inhibitors in infectious diseases has been less intensively studied than for cancer. However, several studies suggest that administration of blocking antibodies against one or multiple co-inhibitory receptors can enhance the T cell response, providing immune protection during, for example, HIV infection, HBV infection, HCV infection, tuberculosis and malaria (72). Recently, a Phase II clinical trial with HIV-infected patients showed that administration of an anti-PDL-1 antibody led to enhanced HIV-1-specific immunity in most study participants. So far, this has been the only study with an immune checkpoint inhibitor in HIV patients without cancer (73). These results clearly show that immunotherapy with immune checkpoint inhibitors that restore T effector functions can be a potential therapy approach not only in cancer but also in infectious diseases.

Of note, most studies investigating T cell exhaustion have been focused on CD8$^+$ T cells. However, CD4$^+$ T cells also show diminished production of IL-2, IFN-γ and TNF-α and express high levels of co-inhibitory molecules during chronic infections, indicating T cell exhaustion (74, 75).

In malaria, the role of T cell exhaustion during the anti-parasitic immune response is controversially discussed. Increased expression of several co-inhibitory molecules on both CD4+ and CD8+ T cells has been described in human as well as rodent malaria (76, 77). Accordingly, co-blockade of LAG-3 and PD-L1 in mice infected with *Plasmodium yoelii* enhanced CD4+ T cell cytokine production and antibody responses, which led to a more rapid parasite clearance (74). In case of the lethal infection of mice with *Plasmodium berghei* ANKA, the blockade of CTLA-4 led also to an increased activation and proliferation of CD4+ T cells (78). However, instead of a more protective immune response, the treatment led to enhanced immunopathology and earlier death of the mice. Studies addressing T cell exhaustion in human malaria have focused mainly on the phenotypic characteristics of exhausted T cells, such as the expression of co-inhibitory molecules, but lack the investigation of effector functions of those T cells. However, in human as well as in mouse malaria it has been shown that CD4+ T cells that express PD-1 and CTLA-4 co-express the activation marker inducible T cell co-stimulator (ICOS) and the proliferation marker CD69 (76, 79-81). This indicates a more activated state of co-inhibitory molecule-expressing T cells in malaria rather than an exhausted phenotype. Concurrent with that, a recent study found that co-inhibitory rich CD8+ T cells of mice infected with *P. berghei ANKA* produce high levels of cytokines and effector molecules and exert enhanced cytotoxic activity, indicating that these cells are indeed not exhausted but highly activated (82). Taken together, the expression of co-inhibitory molecules on T cells plays an important role in sustaining the quality and effectiveness of the anti-malarial T cell response and further investigation is needed to fully dissect their influence on the development of immunity in the context of malaria.

1.4   Co-inhibitory molecules

The fine-tuning of the immune reaction to a pathogen is of crucial importance for the outcome of disease. The induction of co-inhibitory molecules on T cells may play a key role in regulating overwhelming immune responses and thus preventing immunopathology. In a multifaceted disease like malaria, the interplay between immune activation and inhibition may be of utmost importance to balance the immune response. In the following chapter, the co-inhibitory molecules most relevant for this work are described in more detail (Figure 3).
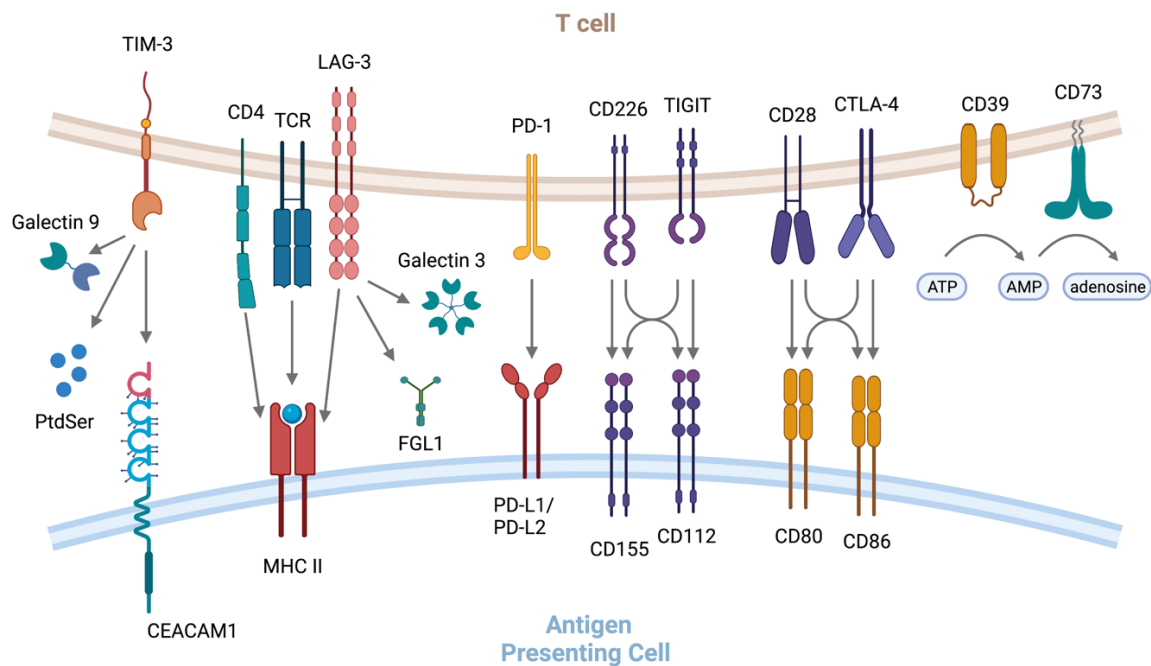
Figure 3: Schematic overview of co-inhibitory and regulatory molecules and their respective ligands relevant for this work.

Co-inhibitory molecules play an important role in maintaining immune homeostasis. They are also referred to as immune checkpoint molecules and can be expressed by T cells. Examples of such co-inhibitory molecules are TIM-3, LAG-3, PD-1, TIGIT and CTLA-4, which engage their immune suppressive function by binding to their ligands. These ligands can either be surface-bound, for example on antigen-presenting cells, or soluble, as in the case of Galectins, FGL1 and PtdSer. CD39 is an example of a membrane-bound molecule that, together with CD73, regulates immune responses by degrading pro-inflammatory extracellular ATP to anti-inflammatory-acting adenosine.

PtdSer: Phosphatidylserine, FGL1: Fibrinogen-like protein 1, TCR: T cell receptor, ATP: Adenosine triphosphate, AMP: Adenosine monophosphate. Created with BioRender.com.

1.4.1 PD-1

Programmed cell death protein 1 (PD-1 or CD279) is a membrane protein and one of the best characterized co-inhibitory molecules. It consists of an extracellular immunoglobulin-like variable (IgV) domain and is a member of the immunoglobulin superfamily (83). The cytoplasmic domain of PD-1 has an immunoreceptor tyrosine-based inhibitory motif (ITIM) and an immunoreceptor tyrosine-based switch motif (ITSM). Binding of PD-1 to one of its ligands, programmed cell death ligand 1 (PD-L1) or 2 (PD-L2), phosphorylates the ITIM and the ITSM (84, 85). This recruits the Src homology 2 domain-containing phosphatases 1 and 2 (SHP-1 and SHP-2), which subsequently dephosphorylate signaling molecules of the TCR signaling cascade and thereby inactivate them (86, 87). Thus, the interaction of PD-1 with its ligands leads to

inhibition of TCR-mediated T cell activation. Additionally, it has also been described that SHP-2 phosphatase recruited by PD-1 is responsible for inhibition of CD28-mediated signaling (88). PD-1 expression has mainly been described on T cells, but it may be also found on B cells, dendritic cells and activated monocytes (89). While it is only expressed at low to undetectable levels by non-activated T cells, it is upregulated on the surface of T cells shortly after stimulation via the TCR or different cytokines like interleukin 2 (IL-2), interleukin 7 (IL-7) or type I interferons (90). Therefore, the expression of PD-1 has been considered an activation marker of T cells. Expression of PD-1 on T cells can be induced in vitro; for example, by stimulation with α-CD3 and α-CD28 antibodies and with persistent antigen exposure or stimulation, the expression of PD-1 remains stable (91, 92).

PD-L1 is constitutively expressed on T cells, B cells, macrophages and dendritic cells, as well as non-lymphoid tissue cells in the heart and lung, on parenchymal cells and on tumor cells (84, 93-95). PDL-1 expression on T cells, B cells and epithelial cells can be induced by interferon α (IFN-α), IFN-β, IFN-γ, and tumor necrosis factor α (TNF-α). In vitro stimulation with anti-CD3 and anti-CD28 antibodies also leads to an upregulation of PD-L1 on T cells (91, 92). PD-L2 is expressed on activated dendritic cells and macrophages. On dendritic cells, PD-L2 expression can be induced by IL-4, IFN-α, IFN-β and IFN-γ (96).

Interestingly, in both human and experimental malaria, PD-1 is known to be upregulated on $CD4^+$ as well as $CD8^+$ T cells (74, 76, 77, 80, 97). In chronic diseases, expression of PD-1 on T cells has been associated with reduced T cell function (98-100). Accordingly, $CD4^+$ T cells co-expressing PD-1 and LAG-3 have been shown to display reduced cytokine production and an anergic phenotype in cancer as well as in malaria (74, 101). In contrast, other studies have found that in both murine and human malaria, PD-1 and CTLA-4-expressing $CD4^+$ T cells express higher levels of activation markers, such as ICOS and CD69, and of the proliferation marker Ki67 than their PD-1$^-$ counterparts (80, 81, 102). A similar finding was recently discovered in experimental malaria, where $CD8^+$ T cells expressing high levels of PD-1 had a higher cytotoxic capacity than PD-1^{lo} and PD-1$^-$ cells (82). These results suggest that, in the context of malaria, PD-1 can be considered a marker of T cell activation rather than dysfunction.

1.4.2 TIGIT

The co-inhibitory receptor T cell immunoreceptor with Ig and ITIM domains (TIGIT) also belongs to the Ig superfamily (103, 104). It was first identified in 2009 and is expressed on activated T

cells, memory T cells and Tregs (105). In addition to T cells, TIGIT is constitutively expressed by human NK cells. In contrast, murine NK cells express TIGIT only after prior activation (106). Together with CD226, TIGIT features a signaling pathway similar to that of CD28 and CTLA-4. While CD226 is a co-stimulatory molecule, TIGIT acts in an inhibitory manner. Both molecules bind to the ligands CD155 and CD112, resulting in competition for binding partners. TIGIT binds to CD155 with a significantly higher affinity than CD226. CD226 is expressed by macrophages, T cells and NK cells, and CD155 and CD112 are expressed by dendritic cells, T cells and also tumor cells (107).

TIGIT can regulate T cell responses both cell-intrinsically via its intracellular ITIM domain or cell-extrinsically via binding to CD155, which has its own ITIM. The interaction of TIGIT with CD155 expressed by dendritic cells leads to increased production of IL-10 and decreased production of IL-12 by the respective dendritic cell (103). Thus, the T cell response is indirectly inhibited by the emergence of tolerogenic dendritic cells. TIGIT's cell-intrinsic mode of action has been confirmed by several studies. By activating the TIGIT pathway in vitro using an agonistic anti-TIGIT monoclonal antibody, human CD4$^+$ T cells showed limited proliferation and reduced production of IFN-γ (108). This was independent of the signals mediated by CD155. Furthermore, stimulation of T cells with agonistic anti-TIGIT antibodies induced the production of regulatory effector molecules such as IL-10, also highlighting the cell-intrinsic regulation of TIGIT (109, 110).

1.4.3 LAG-3

Another co-inhibitor studied in this work is the lymphocyte-activation gene 3 (LAG-3 or CD223). It is similar in structure to the T cell co-receptor CD4 and is expressed on activated T and NK cells. LAG-3 binds to MHCII with a higher affinity than CD4 does (111, 112). However, LAG-3 also affects the function of CD8$^+$ T cells and NK cells, which do not interact with MHCII, suggesting interaction with additional ligands. Recently, fibrinogen-like protein 1 (FGL1), a liver-secreted protein, was identified as one of these ligands (113). Another ligand is the liver sinusoidal endothelial cell lectin (LSECtin), which is expressed by liver cells and tumor cells (114). LAG-3 inhibits T cell proliferation by interacting with CD3, resulting in reduced cytokine production and calcium flux (115).

LAG-3 is expressed on natural Tregs as well as on induced Tregs and Tr1 cells (61, 62, 116). Blockade of LAG-3 leads to abrogation of the regulatory function of Tregs while inducing

proliferation of CD4+ T effector cells, their production of IL-2 and thus the development of Th1 cells. Tregs show a stronger suppressive effect on CD4+ effector T cells expressing LAG-3 than on those not expressing LAG-3 (117, 118). These results confirm the role of LAG-3 in Treg-based regulation of T cell homeostasis.

1.4.4   TIM-3

The co-inhibitor T-cell immunoglobulin and mucin-domain containing-3 (TIM-3 or CD366) is expressed mainly by activated Th1 cells, but also by regulatory T cells, Th17 cells and cytotoxic T cells (CTL) (119-121). In addition, monocytes, dendritic cells and NK cells can express TIM-3 on their cell surface (105, 122). One ligand of TIM-3 is the C-type lectin galectin-9. The interaction of TIM-3 with galrectin-9 has been shown to promote the selective loss of IFN-γ-producing Th1 cells and thus ameliorate experimental autoimmune encephalomyelitis (EAE) – an experimental mouse model for multiple sclerosis (123). TIM-3 also interacts with phosphatidylserine (PtSer) on apoptotic cells, promoting their uptake and cross-presentation of antigens by TIM-3-expressing DCs (124). The most recently identified ligand of TIM-3 is CEACAM-1, which has been shown to promote the stability of TIM-3 on the cell surface and thus is important for the regulatory function of TIM-3 (125). The discovery of TIM-3 led to the identification of the TIM gene family, which is associated with gene loci linked to immune-mediated diseases such as asthma, allergies and atopy in both humans and mice (126). Like LAG-3, TIM-3 does not possess a classical cytoplasmic signaling motif, but five conserved tyrosine residues that can be phosphorylated for example by Src kinases. Thus, through a SHP 2-mediated signaling cascade, the activating TCR-mediated signal is prevented (127).

Blockade of TIM-3 results in increased production of IFN-γ, IL-17, IL-2 and IL 6 but not IL-4, IL-10 or TNF-α, confirming the inhibitory effect of TIM-3 (120). Peripheral blood T cells from patients with multiple sclerosis, rheumatoid arthritis and psoriasis express only little TIM-3, whereas TIM-3 expression on CD8+ T cells is markedly increased during chronic viral infections such as HIV, HBV and HCV or cancers and is associated with T cell exhaustion (123, 128, 129). TIM-3 is also induced on Tregs localized in tissues with acute inflammation (105). Thus, the functions of TIM-3 affect both regulatory and effector T cells and thus influence the course of various diseases.

1.4.5 CD39

The ectonucleotidase CD39 (ectonucleoside triphosphate diphosphohydrolase 1/ NTPDase 1) is an integral membrane protein that catalyzes the conversion of extracellular adenosine triphosphate (eATP) and adenosine diphosphate (ADP) to adenosine monophosphate (AMP) (130). AMP is subsequently dephosphorylated to adenosine by CD73, another ectonucleotidase (131). ATP is the main energy source for cells and is crucial for nearly all cellular biological processes. During, for example, apoptosis or necrosis, ATP is released to the extracellular space. This eATP acts in a pro-inflammatory manner while adenosine has immune-inhibitory functions (132). Thus, CD39 acts as an immune regulator by breaking down the pro-inflammatory eATP. Accordingly, this molecule is often found on cells with immunosuppressive capacity, such as nTregs and Tr1 cells (133, 134). Additionally, CD39 has been described as a marker of exhausted CD8^{+} T cells in chronic viral infections (135).

1.5 Immunity to malaria and vaccine strategies

The patients' immune system faces several challenges when combating an infection with *Plasmodium* parasites. First, it has to deal with an intracellular parasite that infects cells of an immune-tolerogenic organ (the liver) and subsequently infects red blood cells that lack any MHC molecules, preventing them from being recognized by cells of the adaptive immune system. Secondly, the enormous replication rate of the parasite inside the infected cells enables it to successfully establish an infection even when the number of initially inoculated sporozoites is very low (136). In addition, the parasites express different proteins in their various developmental stages, some of which also exhibit polymorphisms, leading to a huge variety of possible antigens (137). Nevertheless, the various components of the immune system interact with each other to fight the infection.

After a bite from an infected *Anopheles* mosquito, some sporozoites also enter the skin draining lymph nodes, where they are phagocytosed by resident dendritic cells (138). These dendritic cells process and cross-present plasmodial antigens, which is essential for priming of cytotoxic CD8^{+} T cells that can then recognize and kill infected hepatocytes (139). Together with CD4^{+} T cells, this priming of CD8^{+} T cells by skin draining lymph node-resident dendritic cells is crucial for the formation of central and effector CD8^{+} memory T cells (140). However, the main target organ of the sporozoites is the liver, where they infect hepatocytes. Liver-resident cells

of the innate immune compartment may recognize specific molecules of the parasites (for example RNA) as pathogen-associated molecular patterns (PAMPs) via their own pattern recognition receptors (PRRs) (141). Upon recognition, they induce a type I interferon response, which in turn recruits other lymphocytes to the infected liver. Activated NK cells as well as NKT cells have been shown to have an at least partially protective function by inhibiting parasite development in infected hepatocytes (142, 143). Furthermore, through the help of antigen-presenting cells, CD4+ T cells recognize antigen presented through the MHCII, leading them to become activated and produce IFN-γ. This antigen-specific Th1 response has been shown to be important to reduce the parasite burden and disease severity in naturally exposed and experimentally vaccinated individuals (144). In combination with other Th1 associated cytokines such as IL-2, it aids the activation of both adaptive and innate immune cells like macrophages and NK cells (145, 146). This IFN-γ, produced by Th1 cells among others, is a key cytokine in liver stage immunity (147). Because of the tolerogenic nature of the liver milieu and the small number of antigens, this immune response is limited and the liver stage progresses asymptomatically. However, with the transition to the blood stage, this changes. The blood stage is accompanied by fever, induced by the pro-inflammatory response of multiple immune compartments. On the innate side, activated NK cells are able to directly lyse infected red blood cells (146), while activated macrophages accumulate in the spleen, phagocytosing infected red blood cells, and further promote a Th1 response by producing IL-12 (148, 149). This Th1 response is a hallmark characteristic of malaria, and is marked by increased serum IFN-γ levels (150). Whereas CD4+ T cells interact with professional antigen-presenting cells which present peptides over MHCII, CD8+ T cells can interact with almost all cell types in the body via antigens presented by MHCI. While hepatocytes express MHCI molecules, enabling them to present antigens to cytotoxic CD8+ T cells, erythrocytes lack any MHC molecules. Accordingly, the liver stage presents a potential target for T cell-mediated immunity, while the blood stage mainly requires an antibody-mediated immune response (151, 152). This is provided by B cells, which, upon recognition of antigen, mature to express B cell receptors with increasing affinity and secreting plasmodium-specific antibodies. These antibodies are a key factor in controlling the infection by, for example, opsonization of merozoites with subsequent complement activation or antibody-dependent cellular inhibition in cooperation with monocytes and macrophages (151, 153, 154). Despite CD8+ T cells not being able to directly kill infected red blood cells, they significantly influence disease progression in malaria. Multiple experiments, including depletion

or knock out of CD8^{+} T cells or their effector molecules in mice, have demonstrated their direct involvement in the development of experimental cerebral malaria (155-157). Although similar studies are difficult to perform in humans, increased numbers of CD8^{+} T cells in the brains of malaria-deceased children indicate a similar involvement in human malaria (158). It is hypothesized that brain endothelial cells uptake plasmodium antigen and cross-present it via their own MHCI, which in turn leads to their killing by cytotoxic CD8^{+} T cells (159, 160).

While some CD4^{+} T cells fulfill a pro-inflammatory role, they are a very plastic cell type which may also act in an anti-inflammatory manner. It has been shown that CD4^{+} Treg, as well as other non-Treg CD4^{+} T cells, are able to produce anti-inflammatory cytokines like IL-10 and TGF-β and are capable of suppressing other effector T cells in vivo (44, 161, 162). Multiple studies found increased IL-10 levels in the sera of malaria patients, indicating the induction of immunoregulatory mechanisms during malaria (163, 164). Taken together, the immune response to malaria is complex and multifaceted. A balance is required between an effective immune response and an overwhelming activation of immune cells, which can lead to immunopathology and ultimately be lethal.

Interestingly, despite experiencing multiple infections per year, people living in malaria-endemic regions do not seem to develop a sterile, long-lasting immunity against *Plasmodium* parasites (165). However, it has been shown that people living in malaria-endemic regions with a high transmission rate gain the ability to tolerate the infection without developing severe disease or even experience asymptomatic infections (14). This indicates a fine-tuned immune response that balances pathogen control and immunopathology. The exact mechanisms for the control of the immune response are not yet completely understood; it is conceivable that expression of co-inhibitory molecules, induction of regulatory T cell subsets or a combination of both contribute to the suppression of an overwhelming immune response. However, this downregulation of *Plasmodium*-specific immune responses might also prevent the development of a long-lasting or even sterile immunity against malaria. Nevertheless, over half a million people, mostly young children under the age of 5, succumb to malaria each year without achieving this balance, making the development of an effective anti-malaria vaccine imperative.

Due to their important role in controlling the blood stage infection, targeting B cell-mediated immunity against malaria is a promising vaccination strategy. Because of their primary focus against the blood stage, these vaccines are often referred to as blood stage vaccines. However,

blood stage vaccines suffer from a number of issues. First, the parasites are known for their ability to express high numbers of var genes, leading to antigenic polymorphism (137). This results in multiple invasion pathways ensuring redundancy if other receptors are blocked by antibodies. In addition, free merozoites only spend seconds between rupture of one erythrocyte and invading another. This combined with the sheer number of parasites in the blood during infection makes it difficult to stop an emerging blood stage infection via B cell-targeted vaccines. Therefore, despite several challenges, the majority of current vaccine strategies target pre-erythrocytic stages (166). Stopping the infection during the liver stage would be ideal, as the numbers of parasites are still very low and the infection progresses asymptomatically. However, despite multiple attempts, the development of effective vaccines has proven to be difficult. There are multiple reasons that might explain this phenomenon. Since only a few hundred sporozoites are transmitted during the bite of a mosquito, the probability of antigen-specific CD8$^+$ T cells to recognize and kill an infected hepatocyte is relatively low (167). Combined with the fact that the liver stage only lasts for a limited time, and the need to essentially kill all infected hepatocytes to prevent the transition to the blood stage, inducing long-lasting T cell-mediated immunity through natural infections or vaccinations is difficult to achieve. To induce a stronger activation of antigen-specific T cells, several attempts have been proposed. One promising attempt was the use of radiation-attenuated sporozoites (168). These are able to infect hepatocytes but lack the ability to transition to the blood stage. Therefore, immunization with large amounts of radiation-attenuated sporozoites makes large amounts of antigen available for a longer time span. The vaccination with P. falciparum sporozoites (*Pf*SPZ), a live radiation-attenuated whole organism vaccine, has been shown to induce high numbers of antigen-specific CD4$^+$ as well as CD8$^+$ T cells and provide protection from recurring infections in initial trials (169, 170). However, the necessary cost-effective scale-up of mosquito-derived sporozoites, combined with the need of constant cryopreservation, would be a large challenge in malaria-endemic regions, which often lack the required infrastructure to provide stable storage conditions of this potential vaccine.

In addition, the initial euphoria about the effectiveness of the vaccine was diminished by studies in malaria-endemic areas. The vaccine was found to be much less effective in adults who were previously exposed to malaria compared to malaria-naïve individuals (171). This led to the hypothesis that previous malaria episodes prevent a robust immune response to vaccination. The reasons for this are not yet fully understood.

A possible solution to these challenges is the immunization with artificially synthesized sporozoite-derived proteins, such as the RTS,S/AS01 malaria vaccine (172). This vaccine consists of a component of the circumsporozoite protein of *P. falciparum* which is fused to hepatitis B surface antigen and is given along with the adjuvant AS01 to boost the immune response. The vaccine consists of a combination of both B and T cell epitopes contributing to both humoral and cellular immunity. RTS,S/AS01 has recently been studied in a phase 3 trial in 7 African countries where, after 4 doses, it showed only a 36.5 % protection against clinical malaria in children aged 5-17 months (173). While this is a promising step in the eradication of malaria as a deadly disease, more effective vaccines are required to lessen the impact of malaria on global health.

1.6 Study aims

The balance between pro-inflammatory, pathogen-controlling immune responses and regulatory, immunopathology-preventing mechanisms is crucial to manage the infection with *Plasmodium* parasites while simultaneously protecting the host. However, whilst the mechanisms of pathogen clearance have been studied extensively, the exact mechanisms that control the immune response are poorly understood. Therefore, the goal of this work was to further elucidate the role of regulatory T cell subsets as well as the expression of co-inhibitory molecules in the context of malaria and disease progression. To this end, samples of Ghanaian children suffering from mild or severe malaria as well as adult travelers infected with *P. falciparum* were analyzed. A particular focus was laid on Tr1 cells and their role and plasticity in malaria. Lastly, similar cells from healthy donors were studied to investigate the potential mechanisms of their immune regulation.

2 Material

2.1 Laboratory equipment

Table 1: Laboratory equipment

Equipment	Company
Analytical scale	Sartorius AG
Centrifuges	
Heraeus Multifuge X3R	Thermo Fisher Scientific
5415 C	Eppendorf
CO_2 incubator Hera Cell 150	Thermo Fisher Scientific
Flow cytometers	
LSRII	BD Bioscience
LSR Fortessa	BD Bioscience
Cell sorter FACSariaIIIµ	BD Bioscience
CytoFLEX S	Beckman Coulter
Laminar flow hoods	
LaminAir HB2448	Heraeus Instruments
UVF 6.18S	BDK
Microscope Axiostar plus	Zeiss
Milli-Q purification system	Merck Millipore
Mr. Frosty freezing container	Thermo Fisher Scientific
Multichannel pipettes	Eppendorf
Microliter pipettes	Gilson, HTL, Eppendorf
Pipetus	Hirschmann Laborgeräte
Vortex V-1 plus	Kisker Biotech
Waterbath Eco ET 6S	Lauda

2.2 Glass and plastic consumables

Table 2: Glass and plastic consumables

Material	Company
Cell culture plates (U- and F-bottom, 96-well)	Greiner bio-one

Combitips advanced (0,5 ml, 2,5 ml)	Eppendorf
Cryo tubes	Nunc
FACS tubes with polystyrene lid	Greiner bio-one
FACS tubes	Sarstedt
Filter CellTrics 30 µm	Sysmex Partec
Glass bottles Schott Duran (250 ml, 500 ml, 1 L)	Schott AG
Glass pipettes (2 ml, 5ml, 10 ml, 20 ml)	Brand GmbH
LS and LD columns	Miltenyi Biotec
Neubauer counting chamber (0.1 mm x 0.0025 mm)	Hecht-Assistent
Pipette tips	Sarstedt
Safety-Multifly® needle 21G 200 mm	Sarstedt
SepMate™- 50 tubes	Stemcell Technologies
Serological pipettes	Merck
S-Monovette™ 9 ml LH	Sarstedt
Sterile filters (0,22 µm, Stericup & Steritop)	Millipore
Tubes (0,5 ml, 1,5 ml, 2 ml)	Eppendorf
Tubes (15 ml, 50 ml)	Sarstedt

2.3 Reagents

Table 3: Reagents

Reagent	Company
BD GolgiStop™ (containing monensin)	BD Bioscience
Brefeldin A (1,000 x)	BioLegend
Cohn II (mix of human immunoglobulins)	Sigma-Aldrich
Dulbecco's phosphate buffered saline (DPBS) 1x	PAN-Biotech
Dimethyl sulfoxide (DMSO)	Sigma-Aldrich
Ethylenediaminetetraacetic acid (EDTA)	Ultrol Grade EMD Millipore
FACSFlow™ sheath fluid	BD Bioscience
Ficoll-Paque™ PLUS	GE Healthcare
Gentamicin sulphate	Lonza

Giemsa Solution	Sigma-Aldrich
HEPES buffer solution (1 M)	PAA
L-Glutamine	PAA
Methanol	Sigma-Aldrich
PBS tablets	Life Technologies
RBC Lysis/Fixation solution 10x	BioLegend
Sodium azide ≥ 99 %	Carl Roth
Trypan blue (0,4%)	Sigma-Aldrich

2.4   Media and sera

Table 4: Media and sera

Media/Serum	Company
Fetal bovine serum (FBS) advanced collected in South America, sterile-filtered	Capricorn Scientific
Human serum AB, male, seraclot	PAN-Biotech
X-VIVO 15, serum free	Lonza
RPMI 1640 (without L-glutamine)	PAN-Biotech

2.5   Prepared media and buffers

All media and buffers used for cell culture were sterile filtered before use and stored at 4 °C.

Table 5: Self-prepared media and buffers

Medium/Buffer	Composition
Complete RPMI (cRPMI)	RPMI 1640 (without L-glutamine)
	10 % human serum A/B
	2.5 % HEPES buffer solution
	1 % L-glutamine
	0.5 % gentamicin
FACS buffer	1x DPBS

	2 % FCS
	0.1 % sodium azide
MACS buffer	1x DPBS
	0.5 % human serum AB
	2 mM EDTA
1x PBSS	1x PBS
	1 % human serum A/B

2.6 Kits

Table 6: Commercial kits

Kit	Company
eBioscience FoxP3 staining buffer set	Thermo Fisher Scientific
MACS CD4 T cell isolation kit human	Miltenyi Biotec
MACS CD8 T cell isolation kit human	Miltenyi Biotec

2.7 Dyes and antibodies

All antibodies used for flow cytometry or cell stimulation protocols were directed against human epitopes.

Table 7: Cell dyes for flow cytometry

Dye	Company
LIVE/DEAD^{TM} Fixable Blue Dead Cell Stain	Thermo Fisher Scientific
Zombie NIR^{TM} Fixable Viability Kit	BioLegend
Cell Proliferation Dye eFluor^{TM} 450	Thermo Fisher Scientific

Table 8: Antibodies for flow cytometry

Epitope	Fluorochrome	Clone	Panel	Dilution	Company
CCR5	PE	J418F1	REG, Sort1	1:200	BioLegend
CCR5	PerCP-Cy5.5	J418F1	ICS	1:100	BioLegend
CD3	APC/Cy7	HIT3a	REG	1:400	BioLegend
			GrzB	1:4,000	
CD3	BUV737	SK7	ICS	1:100	BD Bioscience
CD4	APC	RPA-T4	Sort1	1:100	BioLegend
CD4	BV510	RPA-T4	REG, ICS	1:100	BioLegend
CD4	BV510	OKT4	GrzB	1:100	BioLegend
CD4	APC/Cy7	RPA-T4	Sort2	1:100	BioLegend
CD8a	AF700	RPA-T8	REG	1:500	BioLegend
			GrzB	1:400	
CD8a	APC	RPA-T8	Proli2	1:500	BioLegend
CD8a	BUV395	RPA-T8	ICS	1:800	BD Bioscience
CD25	PE/Cy7	BC96	REG, Sort1, Proli1	1:100	BioLegend
CD25	PE	BC96	Sort2, Proli2	1:100	BioLegend
CD38	PE	HB-7	GrzB	1:40	BioLegend
CD39	PE-Dazzle	A1	REG	1:200	BioLegend
CD39	BV711	A1	ICS	1:200	BioLegend
CD39	BV421	A1	GrzB	1:100	BioLegend
CD49b	FITC	P1E6-C5	REG, ICS	1:100	BioLegend
CD69	FITC	FN50	GrzB	1:40	BioLegend
CD127	AF488	A019D5	Sort1+2, Proli1+2	1:100	BioLegend
CD127	PerCP-Cy5.5	A019D5	REG	1:100	BioLegend
FoxP3	AF647	259D	ICS	1:50	BioLegend
GrzB	AF700	GB11	ICS	1:200	BD Bioscience
GrzB	AF647	GB11	GrzB	1:100	BioLegend
IFNγ	BV785	4S.B3	ICS	1:100	BioLegend
IL-10	PE-Dazzle	JES3-19F1	ICS	1:100	BioLegend

LAG-3	APC	3DS223H	REG	1:50	eBioscience
LAG-3	PE	11C3C65	ICS	1:50	BioLegend
PD-1	PerCP/Cy5.5	EH12.2H7	GrzB, Sort1+2, Proli1+2	1:160 1:100	BioLegend
PD-1	BV421	EH12.2H7	REG, ICS	1:100	BioLegend
TIGIT	BV605	A15153G	REG, ICS	1:400	BioLegend
TIGIT	PE-Dazzle	A15153G	Sort2, Proli2	1:100	BioLegend
TIM-3	BV650	F38-2E2	REG, ICS	1:50	BioLegend
TNF-α	PE/Cy7	MAb11	ICS	1:200	BioLegend

Table 9: Antibodies for cell culture

Epitope	Clone	Company
CD3	UCHT1	eBioscience
CD28	CD28.2	eBioscience

2.8 Study populations in Hamburg, Germany

A total of 19 adult malaria patients, 18 adult healthy volunteers and 7 adult COVID-19 patients were included in this study (Table 10). All malaria patients became infected with *P. falciparum* in endemic areas and developed symptoms after their return to Germany. They were included in the study during their inpatient treatment at the University Medical Centre Hamburg Eppendorf, Hamburg, Germany. An ongoing *P. falciparum* infection was determined by a thick or thin blood smear. The COVID-19 patients were enrolled in Hamburg, Germany and suffered from acute, symptomatic SARS-CoV-2 infection, which was detected by a specific PCR. All healthy adults were enrolled at the Bernhard Nocht Institute for Tropical Medicine, Hamburg, Germany.

Table 10: Characteristics of the adult study participants

Group	Count	Mean Age [years]	Sex female	Malaria slide	Mean parasitemia
Healthy	18	35.7	11 (61.1 %)	-	-
Malaria	19	40.8	7 (36.8 %)	all positive	4.6 %
COVID-19	7	66.0, 2 n/a	0 (0.0 %), 2 n/a	-	-

2.9 Study populations in Ghana

For the study concerning the cytotoxic CD8$^+$ T cells, the participants' characteristics have been published before (76) and are stated again below (Table 11). The study took place in the village Jachie-Pramso, Bosomtwi District, Ashanti Region, Ghana and samples were collected between June and August 2015. Blood samples of 82 afebrile, healthy children were taken at Jachie D/A Primary school. An ongoing *Pf* infection was determined by HRP2-rapid diagnostic test. 41 of the children were malaria-negative (healthy) and 41 were asymptomatically infected with *Pf*. Children with acute, symptomatic malaria were enrolled at St Michael's Hospital. 35 children were admitted to the outpatient department and treated with oral artemisinin combination drug for uncomplicated, mild malaria. 32 children were admitted to the hospital as inpatients with complicated, severe malaria and were treated intravenously with artesunate.

Table 11: Ghanaian study population for the analysis of cytotoxic CD8$^+$ T cells

Adapted from (76).

Group	No. of children	Mean age [years]	Sex female	Rapid test	Malaria slide	Mean parasitemia of positive [%]
Healthy	41	8.5	27 (65.9 %)	All negative	-	-
Asymptomatic	41	9.1	24 (58.5 %)	All positive	15 positive, 26 n/a	0.1 %
Mild malaria	35	5.8	17 (48.6 %)	All positive	23 positive, 12 n/a	1.5 %
Severe malaria	32	4.8	16 (50.0 %)	All positive	25 positive, 7 n/a	4.7 %

For the regulatory T cell studies, all children were enrolled from the Asante Akim North District, Ashanti Region, Ghana between November 2018 and November 2020 (Table 12). 32 afebrile,

healthy children were enrolled during household visits. Children with acute, symptomatic malaria, febrile seizures or bronchopneumonia were enrolled at the Agogo Presbyterian Hospital. 20 children were admitted to the outpatient department and treated for uncomplicated, mild malaria. 30 children were admitted to the hospital as inpatients with complicated, severe malaria. Of the children admitted to the inpatient department but diagnosed with a condition other than malaria, 5 suffered from febrile seizures with different causes and 11 from acute bronchopneumonia. An ongoing *Pf* infection was determined by HRP2-rapid diagnostic test and/or a malaria slide. The children were divided into the groups based on their medical diagnosis.

Table 12: Ghanaian study population for the analysis of regulatory T cells

Group	No. of children	Mean age [years]	Sex female	Rapid test	Malaria slide	Mean parasitemia of positive [%]
Healthy	32	1.0	13 (40.6 %)	-	-	-
Mild Malaria	20	5.3	6 (30.0 %), 1 n/a	15 pos, 1 neg, 4 n/a	15 pos, 2 neg, 3 n/a	2.7
Severe Malaria	30	2.6	11 (36.7 %)	28 pos, 2 n/a	19 pos, 11 neg	3.4
Seizures	5	2.2	2 (40.0 %)	4 neg, 1 pos	All neg	n/a
Bronchopneumonia	11	0.7	4 (36.4 %)	10 neg, 1 n/a	n/a	n/a

2.10 Ethical statements

Ethical approval for the Ghanaian studies was obtained from the Committee on Human Research, Publication and Ethics, School of Medical Sciences/Komfo Anokye Teaching Hospital, Kwame Nkrumah University of Sciences and Technology, Kumasi, Ghana.

Ethical approval for the malaria study in Hamburg was obtained from the Ethics Committee Hamburg, Germany (PV 5537).

Written informed consent was given by a legal guardian/parent or the participants themselves prior to inclusion in the studies. The studies were carried out in accordance with the principles laid down in the Declaration of Helsinki.

2.11 Software

Table 13: Software

Software	Company	Usage
FlowJo 10 for Mac	BD Bioscience	Analysis of flow cytometric data
BD FACS DIVA 6.2	BD Bioscience	Flow cytometric data acquisition
CytExpert	Beckman Coulter	Flow cytometric data acquisition
GraphPad Prism 9	GraphPad	Statistical analyses and creation of graphs

3   Methods

3.1   Blood collection

All blood samples were taken by trained professionals and collected into heparinized blood collection tubes.

3.2   Centrifugation steps

Unless stated otherwise, cells were sedimented by centrifugation at 4 °C and 420 xg for 5 min.

3.3   Detection of *Plasmodium falciparum* (*Pf*) infections

An ongoing *Pf* infection was investigated by means of an HRP2-based rapid diagnostic test and/or a thick or thin blood smear performed by trained personnel at the University hospital Hamburg Eppendorf (UKE) or the Kumasi Centre for Collaborative Research, Ghana (KCCR). For a thin blood smear, a small drop of blood was spread on a slide and air-dried. For a thick blood smear, a drop of blood was applied onto a slide and only slightly stirred before air-drying it. The dried smears were stained with 4 % Giemsa-solution. A classical Giemsa staining is performed by initial fixation of the dried blood smears in methanol for 2-5 min. After air-drying, the smears are incubated in Giemsa solution for 15 min. and washed twice in 1x PBS. Giemsa stains the cell cores in blue and other cell parts in different shades of red. Cells were examined under an oil immersion microscope (100 x magnification) and erythrocytes infected with *Pf* parasites were counted in relation to either red blood cells or leukocytes to calculate the parasitemia. With a thin blood smear, the parasitemia can be determined by calculating the percentage of infected erythrocytes from all counted erythrocytes. In contrast, the thick blood smear can only be used to determine an acute *Pf* infection, but not to accurately calculate the parasitemia because of the high cell density in the blood smear. Due to differences in the smear and counting methods used by the personnel in Ghana, the parasitemia could not be correlated with data from the regulatory T cell analyses.

3.4 Detection of COVID-19 infections

An ongoing COVID-19 infection was determined by quantitative polymerase chain reaction (qPCR) with specific primers by trained professionals at the university hospital in Hamburg, Eppendorf (UKE).

3.5 Ex vivo staining of human whole blood

For the analyses of T cell phenotypes, ex vivo stainings of fresh venous whole blood (samples of adults ≤ 8 hours old; samples of Ghanaian children ≤ 18 hours old) were performed and analyzed by flow cytometry. In the case of the Ghanaian children, 25-100 µl of whole blood were used for the stainings, depending on the amount of obtained material. If less than 100 µl were used, samples were filled up to 100 µl with 1x DPBS. For the adult patients and donors, 100 µl of whole blood were used. Surface antibodies were added to the whole blood in a 5 ml FACS tube and incubated for 30 min at 4 °C. Detailed information on the antibody panels is given below (Table 14). Red blood cell lysis and fixation of cells were performed by adding 2 ml 1x RBC lysis fixation solution (BioLegend) to each sample. After subsequent vortexing and incubation at room temperature (RT) for 15 min, samples were centrifuged, the supernatant was discarded and the cells were washed twice with 2 ml cold FACS buffer with centrifugation steps between the washing steps. For the panel "GrzB" (GrzB production by CD8$^+$ T cells), cells were then stained with intracellular antibodies using the FoxP3 transcription factor staining buffer kit (eBioscience) according to the manufacturers' protocol. To this end, the supernatant was discarded after the final washing step and the cell pellet was solved in 1 ml of freshly prepared fixation/permeabilization working solution (1 part of FoxP3 Fixation/Permeabilization Concentrate + 3 parts of FoxP3 Fixation/Permeabilization diluent). Cells were fixed and permeabilized for 30-60 min at 4 °C in the dark and subsequently washed twice by adding 2 ml of 1x Permeabilization Buffer. Cells were solved in 100 µl of 1x Permeabilization Buffer and intracellular antibodies were added (Table 14). Staining was performed at 4 °C in the dark and cells were washed twice with 2 ml of 1x Permeabilization Buffer. All cell samples were taken up in 200 µl of cold FACS buffer and analyzed at a flow cytometer. Samples from adults were analyzed using a CytoFlex S (Beckman Coulter) or a LSR Fortessa (BD Bioscience) and samples from Ghanaian children using a CytoFlex S (Beckman Coulter) that was brought to Ghana beforehand. The samples from the previous study, investigating CD8$^+$ T cell responses in

Ghanaian children, were transported to Hamburg and analyzed at a LSRII (BD Bioscience), since no flow cytometer was available at the study site in Ghana at that time. Because fresh blood samples contain only a few dead cells, which can be excluded during the subsequent data analysis by gating, no live/dead staining was performed. Analysis of the flow cytometric data was done with FlowJo for Mac, version 10 (BD Bioscience). Cells were gated for lymphocytes, single cells, CD3+ T cells, CD4+ and CD8+ T cells and subsequently for the other markers (Figure 4). Gates for markers other than CD3, CD4 and CD8 were set according to fluorescence minus one controls (FMO), where up to three antibodies were left out to exclude any fluorescence overlaps. When two or three antibodies were omitted, care was taken to ensure that the corresponding fluorochromes were excited by different lasers. To guarantee a correct output of marker frequencies of small T cell populations such as Tr1 cells, samples with less than 10 cells of the respective cell population were excluded from subsequent marker analyses.

Table 14: Antibody panels used for whole blood ex vivo stainings

The antigens are indicated with their respective fluorochromes, followed by the corresponding clones in parentheses.

Panel "GrzB"	Panel "REG"
(CD8+GrzB+ T cells)	(Regulatory T cells)
surface	surface
CD4 BV510 (OKT4)	CD3 APC-Cy7 (HIT3a)
CD8 AF700 (RPA-T8)	CD4 BV510 (RPA-T4)
CD39 BV421 (A1)	CD8 AF700 (RPA-T8)
CD38 PE (HB-7)	CD25 PE-Cy7 (BC96)
PD-1 PerCP-Cy5.5 (EH12.2H7)	CD127 PerCP-Cy5.5 (A019D5)
	CCR5 PE (J418F1)
intracellular	CD49b FITC (P1E6-C5)
CD3 APC-Cy7 (HIT3a)	CD39 PE-Dazzle (A1)
GrzB AF647 (GB11)	LAG-3 APC (3DS223H)
	PD-1 BV421 (EH12.2H7)
	TIM-3 BV650 (F38-2E2)
	TIGIT BV605 (A15153G)

A Gating of T cells
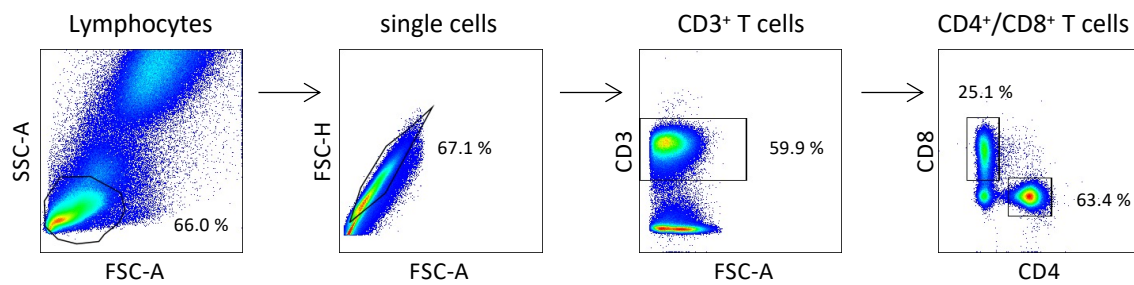
B Gating of T cell surface markers
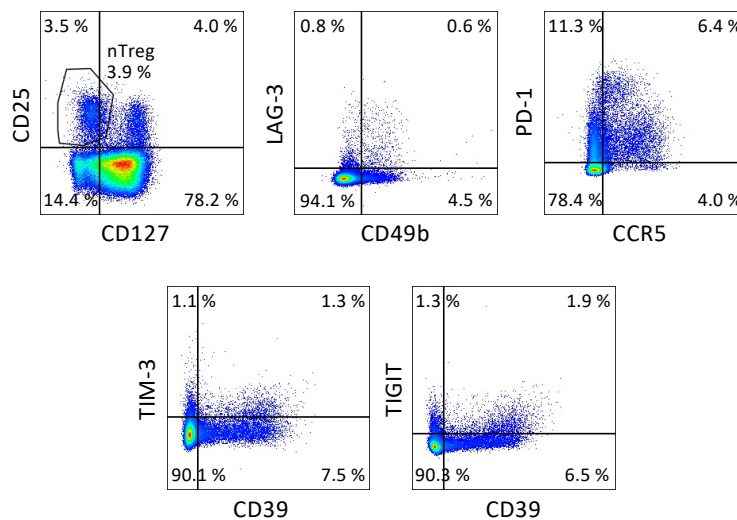
Figure 4: Gating strategy of ex vivo whole blood stainings

(**A**) Lymphocytes were gated based on their position in the forward and sideward scatter areas (FSC-A and SSC-A). Single cells were selected based on the FSC-A against the FSC-height (FSC-H). CD3+ T cells were gated against FSC-A and subsequently divided into CD4+ and CD8+ T cells. Example dot plots of a malaria patient are shown. (**B**) CD4+ and CD8+ T cells were gated for different surface markers. Example dot plots of CD4+ T cells of a malaria patient stained with the "REG-Panel" are shown. Total percentages higher or lower than 100 % occur due to rounding.

3.6   Investigating T cell phenotypes with the t-distributed stochastic neighbor embedding method (t-SNE)

The t-distributed stochastic neighbor embedding method (t-SNE) was used as another approach to visualize the flow cytometric data obtained from ex vivo T cell stainings. Each data point represents a single cell which is displayed in a two-dimensional space in such a way that all similarities of the original, high-dimensional dataset are preserved (174). With t-SNE analysis, it is possible to visualize certain clusters of cells inside a bigger cell population. The t-SNE tool within the FlowJo software was used for the analyses. Cells were gated manually for

lymphocytes, single cells and CD3$^+$ T cells. T cells were downsampled to 20,000 events and concatenated for each group. Only patients with a sufficient number of T cells, comparable cytometer parameters and properly stained markers were included in the analysis. The concatenated events were further downsampled to a total number of 360,000 events. T-SNE was performed based on all measured compensated parameters. To depict the individual cell populations based on their expression of surface molecules, manual gating was applied to the t-SNE plot.

3.7 Isolation of peripheral blood mononuclear cells (PBMCs)

Human peripheral blood mononuclear cells (PBMCs) were isolated from fresh, heparinized whole blood ($\leq$ 8h old) by density gradient centrifugation. To this end, the blood was diluted in an equal volume of 1x PBS and carefully and slowly layered on top of 15 ml ficoll-paque in a 50 ml SepMate™ tube (Stemcell Technologies). The SepMate™ tubes were used according to the manufacturers' protocol. The gradient density centrifugation was performed at 1200 xg and RT for 15 min with brake and acceleration set to the highest level. Due to the membrane of the SepMate™ tubes, which acts as a physical barrier between the sedimented cells and the PBMCs, the centrifugation step can be performed with the centrifuges' brakes turned on. After centrifugation, the erythrocytes and granulocytes are sedimented while the PBMCs are located at the interface between the ficoll and the plasma/PBS mixture. The supernatant was transferred into fresh 50 ml tubes, filled up to 50 ml with X-VIVO 15 cell culture medium and centrifuged at 420 xg and RT for 15 min. After discarding the supernatant, the cells were washed twice with 50 ml X-VIVO 15 with centrifugation steps between the washing steps as described before. At the end, the cells were diluted in cRPMI, counted and stored on ice until further use.

3.8 Determination of cell counts

To determine cell counts, 5-10 µl of the cell suspension were diluted in an equal volume of trypan blue solution. If necessary, cells were diluted in PBS before mixing them with trypan blue. The cells/trypan blue mix was applied to a Neubauer counting chamber (depth 0.1 mm)

and cells in four big squares were counted. The concentration of the cell solution and the total cell count were determined by the following formula:

$$C = \frac{cell\ count\ in\ 4\ big\ squares}{4} \times d \times 10^4 \frac{cells}{ml}$$

$$N = \frac{cell\ count\ in\ 4\ big\ squares}{4} \times d \times 10^4 \times V$$

C = concentration of cell suspension [cells/ml]

N = total cell count

d = dilution factor

V = volume of cell suspension [ml]

3.9 Freezing and thawing of PBMCs

Isolated human PBMCs were diluted at a concentration of $2x\ 10^7$ cells/ml in human AB serum. An equal volume of human AB serum with 20 % DMSO was added to the cell suspension dropwise at a speed of approximately 1 ml/5 sec. The cell suspension was mixed by gently swiveling the tube while adding the serum/DMSO mixture. Thus, a final cell concentration of $1x\ 10^7$ cells/ml and a final content of 10 % DMSO was obtained. The cells were frozen in cryo vials at aliquots of 1 ml in a Mister Frosty freezing container at -80 °C for 24 h. Afterwards, the cells were transferred to liquid nitrogen for permanent storage.

Human PBMCs were thawed according to a previously described protocol (175). The cells were incubated at 37 °C in a water bath for 10 min. Afterwards, the cells of one vial were transferred to a 50 ml tube and 9 ml of prewarmed cRPMI (37 °C) were added dropwise at a speed of approximately 1 ml/5 s. The cell suspension was mixed by gently swiveling the tube while adding the cRPMI. The cells were centrifuged and washed twice with 10 ml cRPMI. After the first washing step, cells from one donor were pooled if more than one tube was thawed. After counting, the cells were diluted at a concentration of $2x\ 10^6$ cells/ml in cRPMI and left to rest at 37 °C for 18h overnight in an angle of 5° over horizontal in a maximum volume of 10 ml per 50 ml tube (

Figure 5). The lid of the tube was slightly opened by turning it one time to guarantee a constant gas exchange. After the resting period, the cells were washed with 10 ml of cRPMI, counted and prepared for subsequent assays.
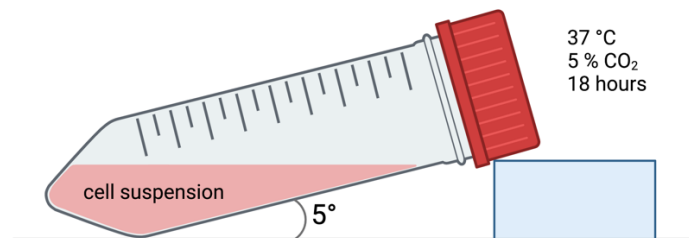
Figure 5: Setup of the PBMCs' resting procedure after thawing
After thawing, the PBMCs were rested overnight at 37 °C and 5 % CO_2 in a maximum volume of 10 ml in a 50 ml reaction tube in a 5° angle over horizontal (175). To guarantee a constant gas exchange, the lid was left slightly open. Created with BioRender.com.

3.10 Suppression-Assays

3.10.1 Isolation of T cells by magnetic bead-based cell separation (MACS)

CD4$^+$ and CD8$^+$ T cells were isolated from human PBMCs with the *MACS CD4 T cell isolation kit human* or the *MACS CD8 T cell isolation kit human* (Miltenyi Biotec) according to the manufacturers' protocol. The PBMCs are incubated with biotinylated antibodies against multiple surface antigens except CD4 or CD8. Thus, the respective T cell population remains untouched. By adding magnetic microbeads coupled with α-biotin antibodies, the antibody-labeled CD4$^-$ or CD8$^-$ cells bind to these beads and can be isolated by pouring the cell suspension over a MACS column that has been clamped into a magnet. All antibody-labeled cells remain in the column and the CD4$^+$/CD8$^+$ T cells are negatively selected. After removal of the magnetic field, the CD4$^-$/CD8$^-$ cells can be washed from the column. The cell counts of all cell populations were determined by trypan blue staining. To determine the purity of the isolated T cells by FACS, a small aliquot of the isolated CD4$^+$ T cells was stained with anti-CD4-APC (RPA-T4) and a small portion of the CD8$^+$ T cells was stained with anti-CD8-APC (RPA-T8). The staining protocol was applied as described in section 2.5. The quality of isolation was considered good when the isolated T cells accounted for 90 % or more of the total cell count.

3.10.2 Irradiation of CD4⁻ feeder cells

The CD4⁻ cells obtained by bead-based cell separation were used as feeder cells for the subsequent cell culture experiments. In in vitro assays, stimulation with antibodies or other soluble stimulants is not sufficient to activate isolated T cells. APCs such as macrophages or DCs are also required in the cell culture. These cells are present in the CD4⁻ cell population. The CD4⁻ cells were used as feeder cells for both the CD8⁺ and the CD4⁺ T cell suppression assays. Since only the proliferation of CD4⁺ or CD8⁺ T cells was to be studied, the proliferation of CD4⁻ cells had to be prevented. For this purpose, the cells were irradiated with γ-rays from a 137-cesium source for 560 s at 2,000 rad (20 Gy).

3.10.3 Staining of effector T cells with proliferation dye

For the suppression assays, in which the proliferation of CD4⁺ and CD8⁺ T cells was examined by FACS analysis, portions of the CD4⁺ and CD8⁺ T cells were stained with the proliferation dye eFluor™ 450 (eF450; ThermoFisher Scientific). This dye binds to all cellular proteins that contain primary amines, has a peak excitation of 409 nm and can be detected via FACS with a 450/50 bandpass filter. During cell division, the dye is evenly distributed to the daughter cells, which can be seen as a fluorescence decrease during FACS analysis. This allows visualization of every division step the cells have undergone.

Prior to staining, portions of the CD4⁺ and CD8⁺ T cells were prepared as unstained controls. The remaining T cells were taken up in 1 ml of prewarmed (37 °C) MACS buffer in a 50 ml reaction tube. To ensure an even distribution of the proliferation dye, the reaction tube was held at an angle during addition of 10 nmol/ml eF450. The cell suspension was immediately mixed by vortexing. After 10 min of incubation at 37°C and 5% CO_2, 5 ml of ice-cold cRPMI were added and the cells were incubated on ice for 5 min. This last step stops the incorporation of the dye and prevents excessive cell damage (quenching). The cells were washed three times with 5 mL of ice-cold cRPMI, followed by centrifugation. The cell number was determined and adjusted to 1×10^6 cells/ml.

3.10.4 Sorting of CD4⁺ T cells by FACS

The isolated CD4⁺ T cells were centrifuged and taken up in 1 ml of 1x PBSS. Fluorochrome-labeled antibodies were added according to the table below (Table 15).

Table 15: Antibody panels used for sorting of CD4^{+} T cells

Panel "Sort1" (CD4^{+}PD-1[+/-]CCR5^{+/-} T cells)	Panel "Sort2" (CD4^{+}PD-1[+/-]TIGIT^{+/-} T cells)
CD4 APC (RPA-T4)	CD4 APC/Cy7 (RPA-T4)
CD25 PE/Cy7 (BC96)	CD25 PE (BC96)
CD127 AF488 (A019D5)	CD127 AF488 (A019D5)
PD-1 PerCP/Cy5.5 (EH12.2H7)	PD-1 PerCP/Cy5.5 (EH12.2H7)
CCR5 PE (J418F1)	TIGIT PE/Dazzle (A15153G)

FMOs were used to set the gates for the cell populations to be sorted. They were prepared from 5×10^5 PBMCs each, taken before isolation of the CD4^{+} T cells. For each FMO, all but one antibody of the panel was added and the cells were stained in 100 µl of 1x PBSS. After 30 min of incubation at 4 °C in the dark, cells were washed with 10 ml of 1x PBSS (FMOs: 1 ml) and taken up in 1 ml of 1x PBSS (FMOs: 100 µl). Prior to the sorting procedure, the cell samples were filtered through a 30 µm filter (CellTrics) to prevent clogging of the flow cytometer. The filters were equilibrated with 500 µl of 1x PBSS before adding the cell samples. After the cell suspension had run through, the filters were washed with 1 ml of 1x PBSS (FMOs: 100 µl). The cell suspension to be sorted was divided into two tubes of 1 ml each. Cells were sorted by FACS with an Aria IIIµ (BD) into FACS tubes prefilled with 1 ml of cRPMI. First, nTreg were sorted based on their expression of CD25 and CD127 (CD25^{+}CD127^{lo}). The remaining cells were sorted either for PD-1[+/-]CCR5^{+/-} or PD-1[+/-]TIGIT^{+/-} populations (Figure 6). The cell counts of all sorted cell populations were determined by trypan blue staining and adjusted to 1×10^6 cells/ml.
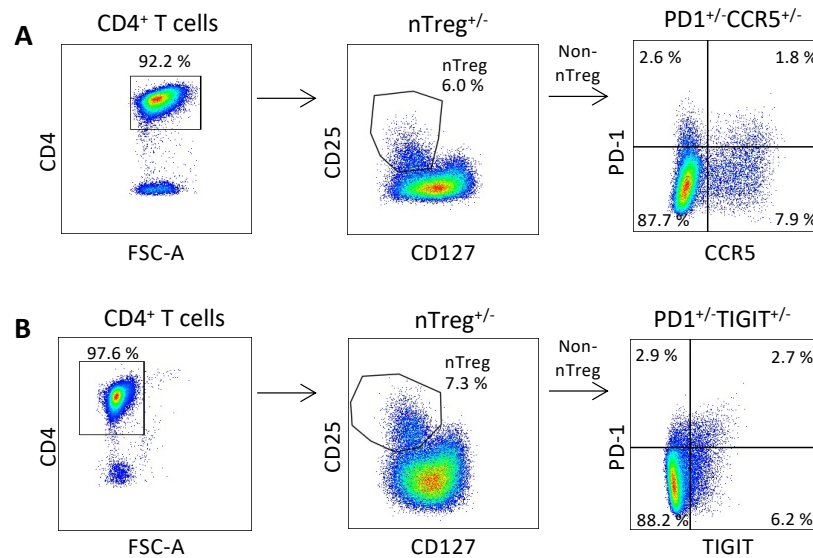
Figure 6: Gating strategy for the sort of CD4$^+$ PD1$^{+/-}$ cell populations

Purified CD4$^+$ T cells of adult malaria patients and healthy donors were sorted by FACS with an Aria IIIµ (BD). nTreg were sorted according to their expression of CD25 and CD127 (CD25^{hi}CD127^{lo}), non-nTreg cells were either sorted for (**A**) PD-1$^{+/-}$CCR5$^{+/-}$ or (**B**) PD-1$^{+/-}$TIGIT$^{+/-}$ subpopulations. Gates were set according to FMOs. Exemplary dot plots of two healthy donors are shown.

3.10.5 Cell stimulation and evaluation of T cell suppression

The sorted CD4$^+$ T cell populations were cultured in 96-well round-bottom plates immediately after isolation. To investigate the suppressive effect of the sorted CD4$^+$ T cells on CD4$^+$ and CD8$^+$ T cells, 2.5 x 10^4 of the eF450-labeled CD4$^+$ or CD8$^+$ T cells were cultured together with the same amount, half the amount (1.25 x 10^4), or without any sorted T cells in cRPMI. All cells were stimulated with 1 µg/ml each of α-CD3 and α-CD28. An unstimulated control of 2.5 x 10^4 eF450-labeled CD4$^+$ and CD8$^+$ T cells and feeder cells each was prepared. Triplicates of each approach were prepared if a sufficient cell number of each sorted population was available. The cells were incubated for 96 h at 37 °C and 5 % CO$_2$.

The 3 samples of the same batch were pooled into FACS tubes and washed with 1 ml of 1x PBS After centrifugation, the cells were taken up in 100 µl live/dead stain (LIVE/DEAD® Fixable Blue Dead Cell Stain dye, diluted 1:1,000 in 1x PBS). The cells were incubated for 30 min at 4 °C in the dark and subsequently washed with 1 ml of FACS buffer. After centrifugation, the cells were taken up in 100 µl of FACS buffer and surface molecules were stained according to the panels below (Table 16). The staining was performed for 30 min at 4 °C in the dark and cells were washed with 2 mL of FACS buffer, centrifuged and taken up in 150 µl of FACS buffer. The cells were analyzed using the LSR II flow cytometer.

Table 16: Antibody panels used for the suppression assays

Panel "Proli1"	Panel "Proli2"
(CD4$^+$PD-1$^{+/-}$CCR5$^{+/-}$ T cells)	(CD4$^+$PD-1$^{+/-}$TIGIT$^{+/-}$ T cells)
For CD4$^+$ responder cells:	For every sample:
CD4 APC (RPA-T4)	CD4 APC-Cy7 (RPA-T4)
	CD8 APC (RPA-T8)
For CD8$^+$ responder cells:	CD25 PE (BC96)
CD8 APC (RPA-T8)	CD127 AF488 (A019D5)
	PD-1 PerCP/Cy5.5 (EH12.2H7)
For every sample:	TIGIT PE/Dazzle (A15153G)
CD25 PE/Cy7 (BC96)	
CD127 AF488 (A019D5)	
PD-1 PerCP/Cy5.5 (EH12.2H7)	
CCR5 PE (J418F1)	

3.11 Analysis of intracellular cytokine production of stimulated T cells

The required number of wells of a 96 well flat bottom plate were prepared with 50 µl of a 10 µg/ml anti-CD3 antibody solution and incubated for 2 h at 37 °C. 50 µl of PBS were used as an unstimulated control. The wells were subsequently washed with 150 µl of PBS. Thawed and rested PBMCs were adjusted to a concentration of 5×10^6 cells/ml and 1×10^6 cells (200 µl) were plated per well. 1 µg/ml anti-CD28 antibody was added to all wells except the unstimulated control. Cells were stimulated for a total of 24 h at 37 °C and 5 % CO_2. For the last 4 h of incubation, 0.2 µl of a 1,000x Brefeldin A solution (Biolegend) and 0.13 µl of a 1,500x GolgiStop solution containing Monensin (BD) were added to each well.

After completion of the incubation, the plate was centrifuged. After every centrifugation step, the supernatant was discarded carefully by pipetting and the cells were solved again by briefly vortexing the plate. The cells were washed with cold PBS and, after a second centrifugation step, solved in 100 µl of a 1:2,000 Zombie NIR Dye solution in PBS. The cells were incubated for 20 min at 4 °C in the dark and washed by adding 150 µl of cold PBS immediately. After centrifugation, the supernatant was discarded and cells were solved in 100 µl of surface antibody mix (Table 17). After incubation for 30 min at 4 °C in the dark, 150 µl of cold FACS

buffer were added to each well and the cells were centrifuged and the supernatant discarded. The cells were fixed and permeabilized in 150 µl of freshly prepared FoxP3 Fixation/Permeabilization Solution (eBioscience) according to the manufacturer's protocol. The cells were incubated for 30-60 minutes at 4 °C in the dark and subsequently washed, first with 100 µl, then with 200 µl of freshly prepared 1x Perm/Wash buffer (eBioscience). 50 µl of CohnII solution (10 µl CohnII + 40 µl 1x Perm/Wash buffer) were added to each well and incubated for 10 min at 4 °C in the dark. Afterwards, 50 µl of a 2x intracellular antibody-mix (Table 17) in 1x Perm/Wash buffer were added to each well and incubated for 30 min at 4 °C in the dark. The cells were washed twice, first with 150 µl and then with 200 µl of 1x Perm/wash buffer, and subsequently solved in 200 µl FACS buffer and analyzed at a LSR Fortessa flow cytometer.

Table 17: Antibody panel used for the intracellular cytokine stainings

Panel "ICS"
surface
CD4 BV510 (OKT4)
CD8 BUV395 (RPA-T8)
CD39 BV711 (A1)
TIM-3 BV650 (F38-2E2)
PD-1 PerCP-Cy5.5 (EH12.2H7)
TIGIT BV605 (A15153G)
CCR5 PerCP-Cy5.5 (J418F1)
CD49b FITC (P1E6-C5)
LAG-3 PE (11C3C65)
intracellular
CD3 BUV737 (SK7)
GrzB AF700 (GB11)
FoxP3 AF647 (259D)
IFN-γ BV785 (4S.B3)
TNF-α PE-Cy7 (MAb11)
IL-10 PE-Dazzle (JES3-19F1)

3.12 Statistics

The software GraphPad Prism 9 was used for all statistical analyses. First, normality of data was analyzed by D'agostino & Pearson test. Statistical significance of normally distributed data was calculated by Kruskal-Wallis test with Dunn's multiple comparisons test while significance of non-normally distributed data was calculated by one-way ANOVA with Tukey's multiple comparisons test. Significant differences are depicted as $*=p \leq 0.05$, $**=p \leq 0.01$, $***=p \leq 0.001$ and $****=p \leq 0.0001$. If no significant differences were found, no note is made in the figures for the sake of clarity.

4 Results

T cells have been shown to play a double-edged role during the immune response against malaria. While their pro-inflammatory functions are needed for a comprehensive control of the parasite burden, they can also cause severe immune-mediated complications like cerebral malaria. Regulatory T cell mechanisms are crucial to counteract this immune-mediated pathology. This study aimed to shed light on the interplay between cytotoxic CD8$^+$ T cells and regulatory T cells during human *Plasmodium falciparum* (*Pf*) malaria. Therefore, the induction of GrzB-producing cytotoxic CD8$^+$ T cells during the blood stage of malaria was investigated in Ghanaian children that were either asymptomatically infected or suffered from mild or severe malaria. Furthermore, different subtypes of counteracting regulatory T cells were analyzed in Ghanaian children as well as adult travelers infected with *Pf*. Particular focus was placed on the role of type 1 regulatory T cells (Tr1), since they were found to be induced during human and mouse malaria. Lastly, differences in the suppressive function of malaria-induced regulatory CD4$^+$FoxP3$^-$PD-1$^+$ T cells co-expressing either CCR5 or TIGIT were investigated.

4.1 The role of cytotoxic CD8$^+$ T cells in disease progression of *P. falciparum* malaria

In experimental cerebral malaria it has been shown that CD8$^+$ T cells sequester in the brain and contribute to the pathology by secreting granzyme B (GrzB) and perforin (157, 176). Their role in human blood-stage malaria remains mostly unclear. When investigating soluble factors in the plasma of Ghanaian children suffering from *Pf* malaria, our group could show that levels of GrzB were elevated in children suffering from severe or mild symptoms compared to children with asymptomatic infection and healthy controls (97). Since GrzB is the main cytokine produced by cytotoxic CD8$^+$ T cells, it was further investigated whether the GrzB found in the plasma of the children was T cell-derived. To this end, ex vivo staining of venous blood from Ghanaian children was performed and levels of intracellular GrzB produced by CD8$^+$ T cells were compared between the different groups (Figure 7).

The proportion of CD8$^+$GrzB$^+$ T cells was significantly higher in children suffering from severe malaria than in children with mild malaria. In general, the level of CD8$^+$GrzB$^+$ T cells was increased in the *Pf*-infected children that showed symptoms compared to children without any

symptoms but with detectable parasitemia (asymptomatic) and healthy children. There was no difference between healthy and asymptomatically infected children (Figure 7A). The frequency of CD8$^+$GrzB$^+$ T cells correlated with the blood parasitemia of the children (Figure 7B). Accordingly, the GrzB content of CD8$^+$ (Figure 7C) and also of CD8$^+$GrzB$^+$ T cells (Figure 7D) was higher in the mild and severe malaria groups compared to asymptomatic and healthy children revealed by higher geometric mean fluorescence intensities (GMFI) of GrzB. Accordingly, not only the frequency of CD8$^+$GrzB$^+$ T cells, but also the amount of GrzB produced by each individual cell increased with disease severity.
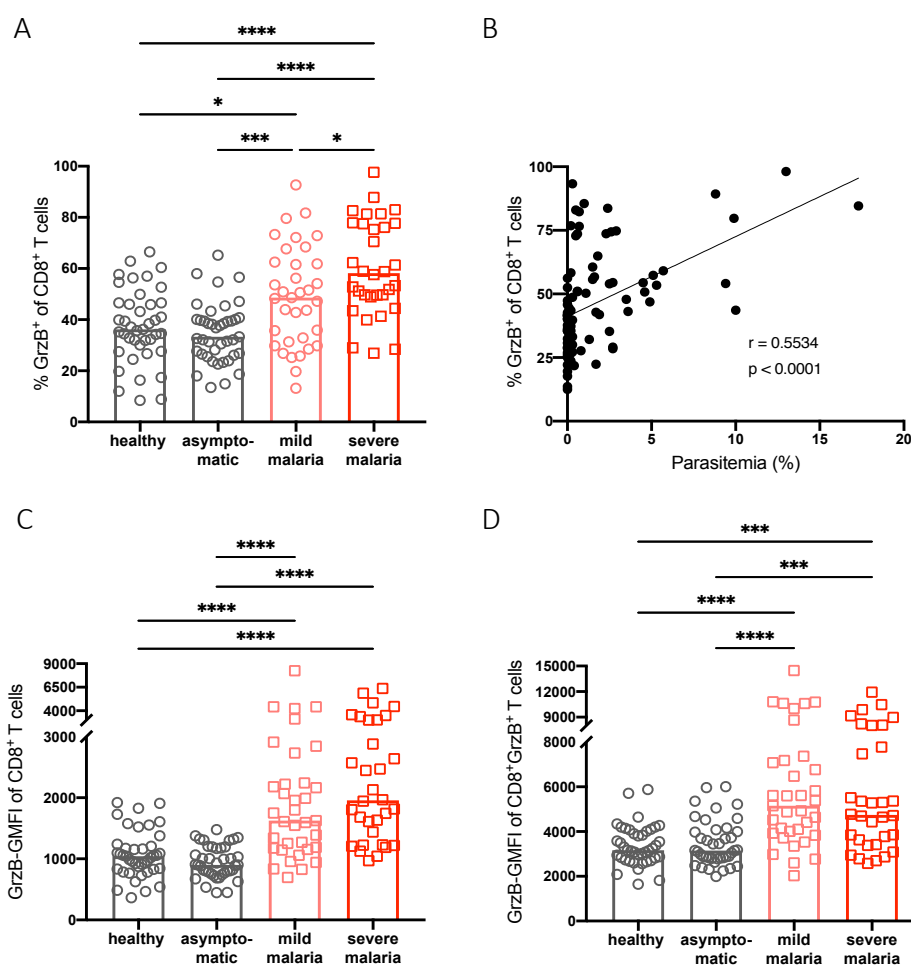
Figure 7: Levels of granzyme B produced by cytotoxic CD8$^+$ T cells are elevated in Ghanaian children suffering from severe malaria.

Whole blood samples of Ghanaian children that are either healthy (n=41) or suffering from an infection with *P. falciparum* without any symptoms (asymptomatic; n=41), mild symptoms (mild malaria; n=35) or severe symptoms (severe malaria; n=32) were stained for the indicated markers and analyzed by flow cytometry. The frequency of granzyme B (GrzB)-producing CD8$^+$ T cells was analyzed (A) and correlated with the parasitemia (B) of all children. The geometric mean fluorescence intensities (GMFI) of GrzB expression of all CD8+ T cells (C) or of GrzB+CD8+ T cells (D) was analyzed. Bars represent the median. Normality of data was analyzed by D'agostino &

Pearson test and group comparisons were done by Kruskal-Wallis test with Dunn's multiple comparisons test or one-way ANOVA with Tukey's multiple comparisons test. Correlation was calculated using nonparametric Spearman correlation (*p ≤ 0.05, **p ≤ 0.01, ***p ≤ 0.001, ****p ≤ 0.0001).

This induction of GrzB-producing cytotoxic CD8⁺ T cells, and therefore the progression of disease severity, must be tightly regulated by regulatory immune mechanisms like the induction of regulatory T cells and the upregulation of co-inhibitory molecules on T cells. To investigate the role of regulatory T cells in the prevention of severe outcomes of malaria, a comprehensive study of regulatory T cell responses in Ghanaian children suffering from mild or severe malaria as well as adult malaria patients was conducted.

4.2 Regulatory T cell responses during human malaria

To investigate the role of regulatory T cells in human *Pf* malaria, samples of different patient cohorts were obtained. Adult travelers who were infected with *Pf* during their stay in a malaria endemic region and developed symptoms after their return to Germany were enrolled as adult malaria patients. To investigate T cell responses in an endemic area for malaria, where children are the most affected group, children suffering either from mild or severe malaria were enrolled in Ghana. To determine whether the observed T cell responses are specific for malaria, results were compared with adult patients suffering from coronavirus disease 2019 (COVID-19). COVID-19 is a novel influenza-like disease that was first described in December 2019 in Wuhan, China and has since spread worldwide, unleashing a pandemic (177). It is caused by the severe acute respiratory syndrome coronavirus 2 (SARS CoV-2) and can result in a severe hyper-inflammatory response, which is a main driver of disease complications and may lead to death (178, 179). Like in malaria, T cells in COVID-19 might also play a dual role in progression and prevention of pathology which makes it interesting to compare T cell characteristics between these two infectious diseases.

4.2.1 The role of natural CD4⁺ regulatory T cells in malaria

One important subset of regulatory T cells is the subset of natural CD4⁺ regulatory T cells (nTreg). Since their role and impact on immune homeostasis during malaria remains controversial, their frequency was analyzed in adult malaria patients and COVID-19 patients

and in children suffering from mild or severe malaria and their corresponding healthy controls. Venous whole blood was stained ex vivo and analyzed by flow cytometry. The CD3$^+$CD4$^+$ nTreg were identified by their high expression of CD25 and their low expression of CD127 (nTreg = CD3$^+$CD4$^+$CD25^{high}CD127^{lo}). The nTreg frequencies were not altered in the patient groups compared to their corresponding healthy controls. Also, there was no difference when comparing adults with children (Figure 8).
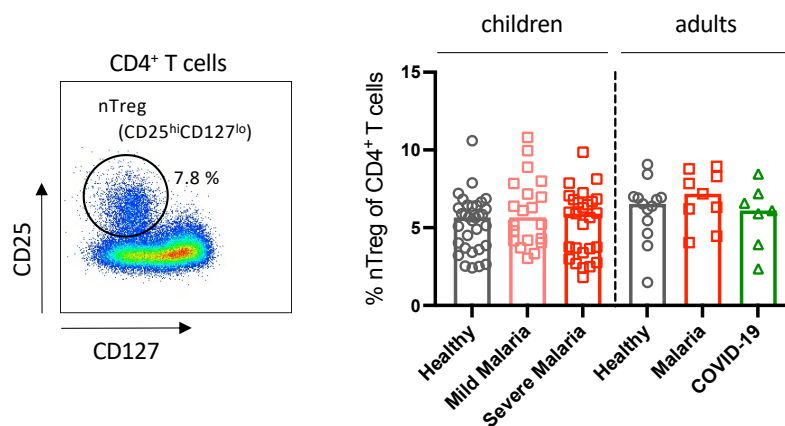
Figure 8: Frequencies of nTreg are similar in children and adults suffering from malaria or COVID-19.
Whole blood samples of adult malaria patients (n=9), COVID-19 patients (n=7) and healthy donors (n=13) and Ghanaian children suffering from mild (n=20) or severe malaria (n=27) and healthy children (n=32) were stained for CD3, CD4, CD25 and CD127. CD3$^+$CD4$^+$ nTreg were identified by their expression of CD25 and CD127 (CD25^{hi}CD127^{lo}). An exemplary dotplot of CD4$^+$ T cells of a healthy adult stained for CD127 and CD25 to identify the nTreg population is shown. Bars represent the median. Normality of data was analyzed by D'agostino & Pearson test and statistical significance was calculated by Kruskal-Wallis test with Dunn's multiple comparisons test (*p ≤ 0.05, **p ≤ 0.01, ***p ≤ 0.001, ****p ≤ 0.0001).

CD4$^+$ nTreg cells were not induced in adults or children suffering from malaria, indicating that other regulatory mechanisms or T cell subsets might play a role in downregulating the pro-inflammatory immune responses. To address this, a comprehensive analysis of the T cell responses in the patient cohorts was conducted.

4.2.2   T cell phenotypes of adult malaria and COVID-19 patients

To get an overview of the induction of regulatory phenotypes on T cells of the studied cohorts, the expression of different co-inhibitory molecules and other surface markers on T cells was investigated further. Our group and others could already show that several co-inhibitory receptors are induced on T cells during acute *Pf* malaria and that the levels of some of these

markers correlate with disease severity (76, 80, 180). To further investigate the phenotypic characteristics of T cells during human malaria, peripheral blood samples of *Pf*-infected adult travelers (n= 12-15) and healthy donors (n= 17) were analyzed for number of T cells and expression of different co-inhibitory molecules and other surface markers, in particular those associated with activation, regulation or differentiation. In addition, marker frequencies were compared with patients suffering from COVID-19 (n= 7). Regarding the expression of co-inhibitory molecules on CD4^{+} and CD8^{+} T cells, the largest differences were seen between the frequencies of TIGIT and LAG-3. TIGIT was most strongly induced on both CD4^{+} and CD8^{+} T cells of COVID-19 patients with significant differences to malaria patients (only on CD4^{+} T cells) and healthy individuals. CD4^{+} T cells of malaria patients also showed increased levels of TIGIT compared to healthy donors. However, LAG-3 frequencies were highest on CD4^{+} as well as CD8^{+} T cells of malaria patients compared to COVID-19 patients and healthy controls, although CD8^{+} T cells showed lower median frequencies of LAG-3 than CD4^{+} T cells (CD4: 6.1 %; CD8: 0.9 %). PD-1 was significantly induced on CD4^{+} T cells of malaria patients, with a trend towards being induced in COVID-19 patients compared to healthy controls. CD8^{+} T cells of COVID-19 patients showed significantly increased levels of PD-1 compared to malaria patients and a trend towards higher levels compared to healthy controls. Similar to LAG-3, TIM-3 was also elevated on CD4^{+} T cells of malaria patients compared to healthy controls and COVID-19 patients, but only significantly increased on CD8^{+} T cells of COVID-19 patients compared to healthy donors (Figure 9A).

CD4^{+} and CD8^{+} T cells of malaria patients expressed higher levels of the C-C chemokine receptor type 5 (CCR5), which can be considered a marker of T cell activation (181, 182) and has also been described as a marker for non-classical FoxP3^{-} regulatory T cells (183, 184), compared to COVID-19 patients and healthy controls. The ectonucleotidase CD39, which functions as an ATPase together with CD73 and thereby regulates T cell functions (133), was upregulated on CD4^{+} T cells of malaria patients compared to healthy controls. Also, CD8^{+} T cells of malaria patients as well as COVID-19 patients showed higher levels of CD39, although this difference was not significant. The integrin CD49b, which has been described as a marker for non-classical FoxP3^{-} Treg cells (61, 185) and CD4^{+} memory precursor T cells that are recruited to the bone marrow (186, 187), was downregulated on both CD4^{+} and CD8^{+} T cells of malaria patients and COVID-19 patients compared to healthy controls, although the difference between COVID-19 patients and healthy donors was not significant. This could point to either a decreased

induction of memory T helper cells or indicate that CD49b⁺ cells have already been recruited from the peripheral blood to the bone marrow in both the malaria and COVID-19 patients. The IL-7 receptor α-chain CD127, which is mostly expressed by naïve and memory T cells but downregulated on activated effector T cells (188), showed lower expression on CD4⁺ T cells of malaria patients compared to COVID-19 patients, with a trend towards lower expression than in healthy donors, indicating a T effector phenotype in malaria patients. Also, CD8⁺ T cells of malaria patients showed lower frequencies of CD127 compared to healthy controls and in trend to COVID-19 patients, which also points towards an effector T cell phenotype (Figure 9B).
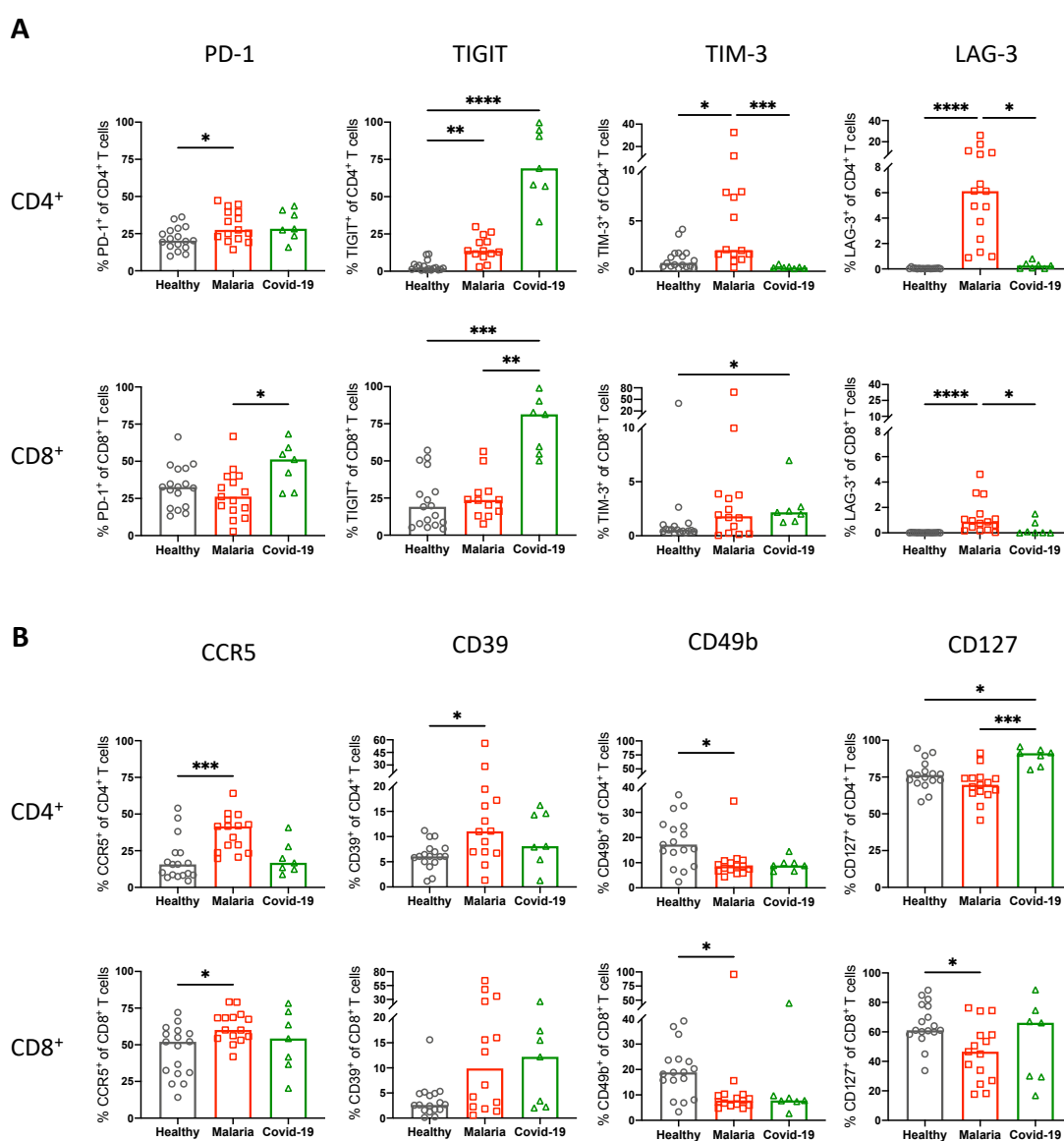

Figure 9: CD4⁺ and CD8⁺ T cells of adult malaria patients, COVID-19 patients and healthy donors show different T cell phenotypes.

Whole blood samples of adult malaria patients (n=12-15), COVID-19 patients (n=7) and healthy donors (n=17) were stained for CD3, CD4 and CD8 to identify T cells and for the indicated co-inhibitory molecules (A) and other surface markers (B) and analyzed by flow cytometry. The bars represent the median. Normality of data was analyzed by D'agostino & Pearson test and statistical significance was determined by Kruskal-Wallis test with Dunn's multiple comparisons test or one-way ANOVA with Tukey's multiple comparisons test (*$p \leq 0.05$, **$p \leq 0.01$, ***$p \leq 0.001$, ****$p \leq 0.0001$).

In summary, T cells of malaria patients showed a more regulatory and activated phenotype compared to healthy individuals and partly also compared to COVID-19 patients. Significant differences could be observed between the T cell phenotypes of malaria patients and COVID-19 patients, especially in the expression of TIGIT and LAG-3.

4.2.3 T cell phenotypes of Ghanaian children suffering from mild or severe malaria

To analyze differences in the T cell characteristics in malaria patients with mild or severe manifestations, children were enrolled at the Agogo Presbyterian Hospital in the Asante Akim North District, a rural area in Ghana. Based on the severity of symptoms and the diagnoses of the doctors, the children were divided into a severe (n=30) or a mild (n=20) malaria group. Children who had their 12-month checkup visit for a different study at the same hospital and were malaria negative were enrolled as healthy controls (n=32). As with the adult cohorts, whole blood samples of the children were stained for FACS analysis and T cells were analyzed for the expression of co-inhibitory molecules as well as activation and differentiation markers (Figure 10).

TIGIT, TIM-3 and LAG-3 were elevated on both CD4$^+$ and CD8$^+$ T cells, while PD-1 was only significantly upregulated on CD4$^+$ T cells of children with severe malaria compared to healthy donors. Children with severe malaria showed higher levels of TIM-3 on their CD4$^+$ T cells and of PD-1, TIGIT and TIM-3 on their CD8$^+$ T cells compared to children with mild malaria. Compared to healthy children, children suffering from mild malaria showed an upregulation of PD-1 and TIGIT on CD4$^+$ T cells and of LAG-3 on both CD4$^+$ and CD8$^+$ T cells (Figure 10A). Overall, it can be said that the children suffering from malaria showed an induction of co-inhibitory molecules on their T cells and that these frequencies were higher in children with severe malaria compared to children with mild malaria. This finding supports the previous study from our group that also found higher levels of co-inhibitors in severe malaria compared to mild malaria (76). Based on the expression of CCR5, the CD4$^+$ and CD8$^+$ T cells of severe malaria patients

showed a more activated phenotype compared to healthy individuals, as seen by an increased frequency of CCR5. Also, the CD8⁺ T cells of mild malaria patients showed a higher frequency of CCR5 than those of healthy children. While the expression of CD39 was not altered on CD4⁺ T cells in the three groups, the CD8⁺ T cells of severe malaria patients showed higher frequencies of CD39 compared to mild malaria patients and healthy children and therefore a more regulatory phenotype. As with the adults, the malaria patients showed decreased frequencies of CD49b on their T cells compared to healthy individuals, also indicating that CD49b⁺ memory T cells had been already recruited from the peripheral blood to the memory T cell niches inside the bone marrow. In contrast to adult malaria patients, the children suffering from malaria showed a much higher expression of CD127 on both CD4⁺ and CD8⁺ T cells compared to healthy children, indicating a more memory-like phenotype of the malaria-experienced T cells (Figure 10B).
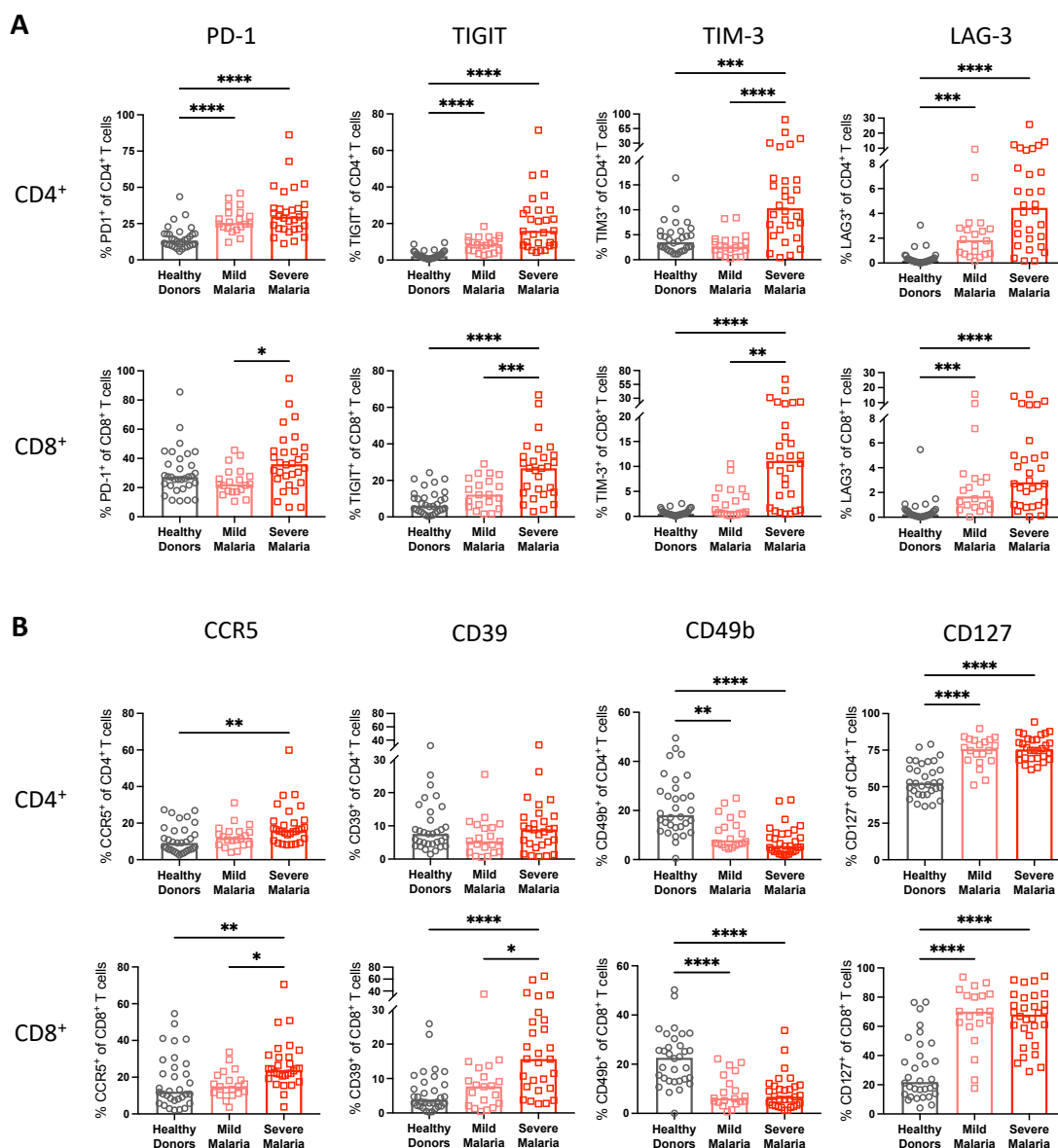
Figure 10: CD4+ and CD8+ T cells of Ghanaian children suffering either from mild or severe malaria show a more regulatory and activated phenotype compared to healthy children.

Whole blood samples of Ghanaian children suffering from mild (n=20) or severe malaria (n=27-30) and healthy children (n=32) were stained for CD3, CD4 and CD8 to identify T cells and for the indicated co-inhibitory molecules (A) and other surface markers (B) and analyzed by flow cytometry. The bars represent the median. Normality of data was analyzed by D'agostino & Pearson test and statistical significance was determined by Kruskal-Wallis test with Dunn's multiple comparisons test or one-way ANOVA with Tukey's multiple comparisons test (*p ≤ 0.05, **p ≤ 0.01, ***p ≤ 0.001, ****p ≤ 0.0001).

4.2.4 Frequencies and characterization of CD4+LAG-3+CD49b+ T cells in malaria patients

The phenotypical analyses of T cells of adults and children suffering from malaria revealed that the co-inhibitor LAG-3 is exclusively upregulated on CD4+ and CD8+ T cells of malaria patients

and is absent in adult COVID-19 patients and healthy individuals. LAG-3, together with CD49b, has been described as a marker of non-classical CD4$^+$FoxP3$^-$ type 1 regulatory T cells (Tr1 cells) (61). To investigate the role of Tr1 cells in malaria, the frequencies of CD4$^+$ T cells co-expressing LAG-3 and CD49b were analyzed in the previously described patient cohorts. In addition to children with malaria, also children suffering from bronchopneumonia (n=11) or febrile seizures (n=5) were also included to examine whether Tr1 cell frequencies differ between patients with different diseases. Bronchopneumonia describes an inflammation of the lungs and is mainly caused by infections with viruses, bacteria or fungi (189). Febrile seizures occur mainly in children between 6 months and 6 years of age. While respiratory tract infections are the most common cause, any febrile illness may trigger febrile seizures in a child that is susceptible to it (190). Only patients with bronchopneumonia or febrile seizures that were malaria negative were included.

When looking at the adult cohorts, only the malaria patients showed an induction of Tr1 cells, while these cells were absent in COVID-19 patients and healthy donors (Figure 11A), as expected considering the lack of LAG-3 expression seen previously (Figure 9A). Tr1 cells were also induced in children suffering from malaria, with significant increases compared to healthy children and children suffering from bronchopneumonia. Also, children with febrile seizures showed lower numbers of Tr1 cells than malaria patients, but not significantly so due to the small sample size. There was no difference in Tr1 cell frequencies between children with mild or severe malaria (Figure 11B).
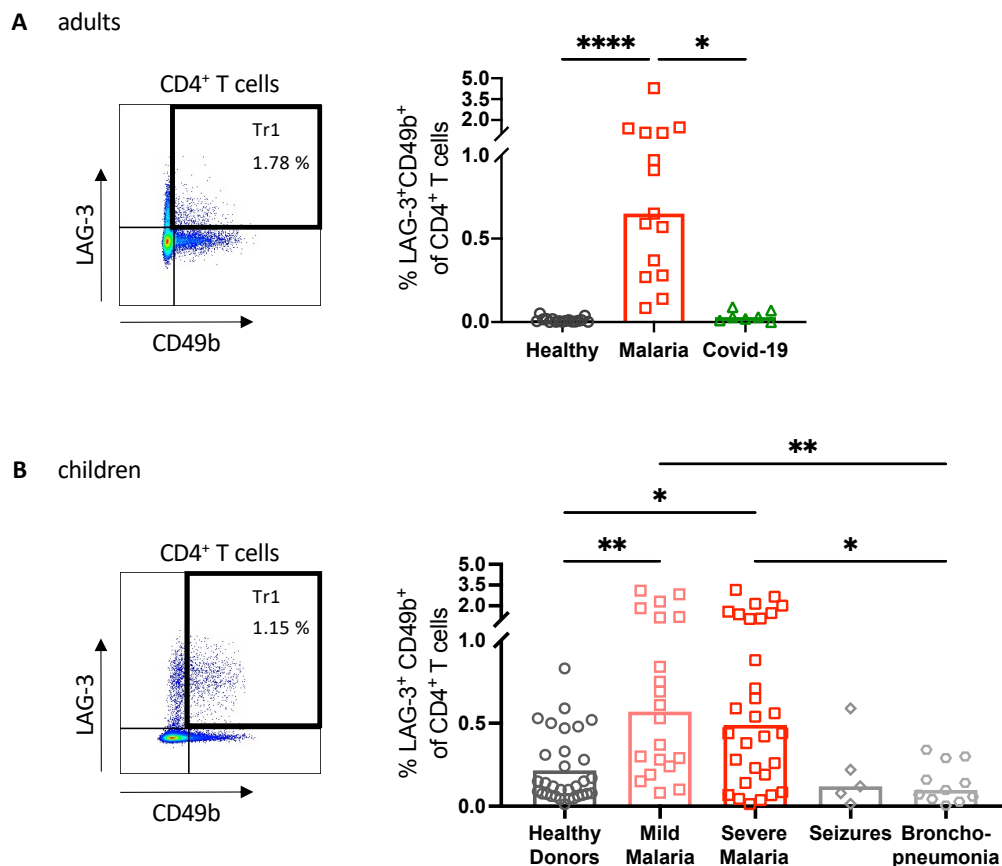
Figure 11: Tr1 cells are induced in acute human malaria.

CD4^{+} T cells of (A) adult malaria patients (n=15), Covid-19 patients (n=7) and healthy donors (n=17) and (B) Ghanaian children suffering from mild (n=20) or severe malaria (n=30), seizures (n=5) or bronchopneumonia (n=11) and healthy children (n=32) were stained for LAG-3 and CD49b and analyzed by flow cytometry. Tr1 cells were identified by co-expression of LAG-3 and CD49b. Exemplary dotplots of malaria patients are shown. The bars represent the median. Normality of data was analyzed by D'agostino & Pearson test and statistical significance was determined by Kruskal-Wallis test with Dunn's multiple comparisons test or one-way ANOVA with Tukey's multiple comparisons test (*p ≤ 0.05, **p ≤ 0.01, ***p ≤ 0.001, ****p ≤ 0.0001).

The induction of CD4^{+}LAG-3^{+}CD49b^{+} Tr1 cells exclusively in malaria patients suggests that they may play a role in the progression of non-sterile immunity, which can protect from severe symptoms. Since there was no difference in the Tr1 cell frequencies between mild and severe malaria cases, their role in regulating overwhelming immune responses in malaria remains unclear. To further characterize the Tr1 cells of malaria patients and to see whether they show different phenotypical properties depending on disease severity, they were analyzed for the expression of the co-inhibitory molecules PD-1, TIGIT and TIM-3 and for the regulatory molecule CD39. Additionally, the expression of CCR5 was examined, which has previously been described to be another marker for human Tr1 cells (183, 184).

Almost all Tr1 cells of adult malaria patients and children with mild or severe malaria expressed PD-1 with respective median frequencies of 98.9 %, 99.1 % and 98.9 % (Figure 12). The same was true for the expression of CCR5, with median frequencies of 98.2 %, 93.1 % and 94.8 %. This conserved expression of PD-1 and CCR5 supports previous studies reporting these to be additional Tr1 cell markers (184, 191). Nearly half of the Tr1 cells of adult malaria patients and children with mild malaria expressed TIGIT, with median frequencies of 46.9 % and 42.4 %, respectively. TIGIT was significantly increased on Tr1 cells of severe malaria cases (median: 68.0 %) compared to mild malaria cases and in trend compared to adult malaria patients. Comparing the frequencies of TIM-3, it was found that Tr1 cells of children suffering from severe malaria showed the highest level of this co-inhibitory molecule (median: 88.7 %) compared to children with mild malaria (median: 67.3 %) and adult malaria patients (median: 48.3 %), with significant differences. Although the median frequency of TIM-3 appeared to be higher on Tr1 cells of mild malaria cases than on those of adult malaria patients, no significance could be detected. Around one third of the Tr1 cells showed expression of CD39 in all three groups, with respective median frequencies of 39.8 %, 35.1 % and 30.9 % and without any differences. Thus, PD-1 and CCR5 were identified as additional markers for malaria-induced Tr1 cells and high expression of TIGIT and TIM-3 on Tr1 cells distinguishes severe from mild malaria cases.
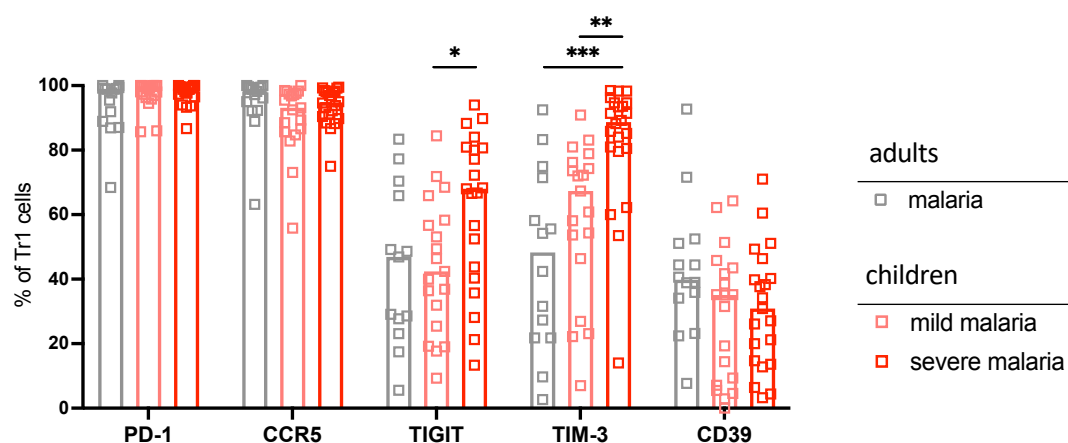
Figure 12: Tr1 cells of malaria patients show specific phenotypic characteristics that differ in the expression of TIGIT and TIM-3.

Tr1 cells (CD4$^+$LAG-3$^+$CD49b$^+$ T cells) of adult malaria patients (n=14-15) and Ghanaian children suffering from mild (n=19) or severe malaria (n=21-22) were stained for different surface molecules and their frequencies were analyzed by flow cytometry. Only patients with a sufficient amount of Tr1 cells (≥ 10) were included in the marker analysis. The bars represent the median. Normality of data was analyzed by D'agostino & Pearson test and

statistical significance was determined using Kruskal-Wallis test with Dunn's multiple comparisons test or one-way ANOVA with Tukey's multiple comparisons test (*p ≤ 0.05, **p ≤ 0.01, ***p ≤ 0.001, ****p ≤ 0.0001).

4.2.5 Frequencies and characterization of CD8⁺LAG-3⁺CD49b⁺ T cells in malaria patients

Recent data from our group in the well-established mouse model of experimental cerebral malaria, in which mice are infected with *Plasmodium berghei ANKA,* showed an induction of not only CD4⁺LAG-3⁺CD49b⁺ but also of CD8⁺LAG-3⁺CD49b⁺ T cells that had suppressive and cytotoxic capacities (62). To elucidate whether CD8⁺ T cells of malaria patients also show phenotypic characteristics of Tr1 cells, their expression of LAG-3 and CD49b was investigated in adult malaria patients (n=15), COVID-19 patients (n=7) and healthy donors (n=17) as well as in Ghanaian children suffering from severe (n=30) or mild malaria (n=20), febrile seizures (n=5) or bronchopneumonia (n=10) and healthy children (n=32).

The frequency of CD8⁺LAG-3⁺CD49b⁺ T cells was significantly increased in adult malaria patients compared to healthy donors and COVID-19 patients, although the total number of these cells was very low (median frequency: 0.12 %). Healthy adults and COVID-19 patients completely lacked CD8⁺LAG-3⁺CD49b⁺ T cells (Figure 13A). In children, the frequencies of CD8⁺LAG-3⁺CD49b⁺ T cells were moderately higher than in adult malaria patients, but no significant differences could be detected between the investigated groups. The median percentages of LAG-3⁺CD49b⁺ among CD8⁺ T cells of children with mild malaria (0.32 %), severe malaria (0.33 %) and bronchopneumonia (0.39 %) were a little higher compared to healthy children (0.12 %) and children with febrile seizures (0.087), but without significance (Figure 13B). Due to the low median percentages in children with febrile seizures and healthy children, it can be said that most of these children lacked CD8⁺LAG-3⁺CD49b⁺ T cells.

A adults

CD8+ T cells

LAG-3+CD49b+
0.4 %

LAG-3

CD49b

% LAG-3+CD49b+ of CD8+ T cells

**** *

Healthy Malaria Covid-19

B children

CD8+ T cells

LAG-3+CD49b+
0.93 %

LAG-3

CD49b

% LAG-3+CD49b+ of CD8+ T cells

Healthy Donors Mild Malaria Severe Malaria Seizures Broncho-pneumonia
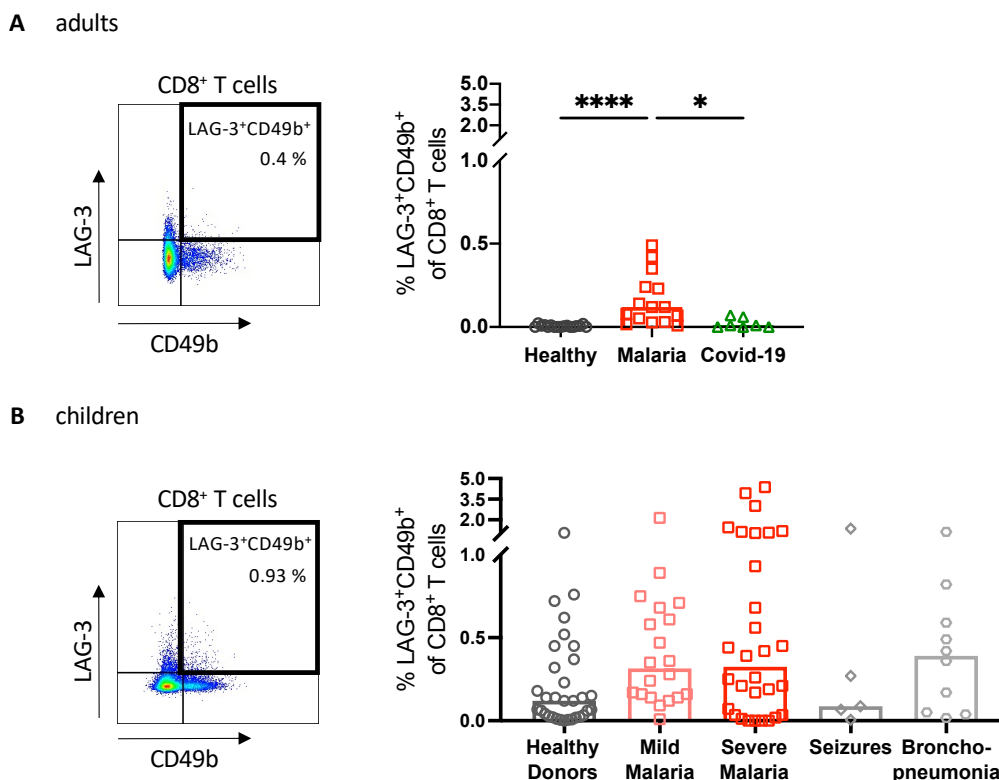
Figure 13: CD8+LAG-3+CD49b+ T cells are induced in adult travelers, but not in children suffering from malaria.

CD8+ T cells of (A) adult malaria patients (n=15), COVID-19 patients (n=7) and healthy donors (n=17) and (B) Ghanaian children suffering from mild (n=20) or severe malaria (n=30), seizures (n=5), bronchopneumonia (n=10) and healthy children (n=32) were stained for LAG-3 and CD49b and analyzed by flow cytometry. The bars represent the median. Normality of data was analyzed by D'agostino & Pearson test and statistical significance was determined using Kruskal-Wallis test with Dunn's multiple comparisons test or one-way ANOVA with Tukey's multiple comparisons test (*p ≤ 0.05, **p ≤ 0.01, ***p ≤ 0.001, ****p ≤ 0.0001).

Since an induction of CD8+LAG-3+CD49b+ T cells was observed in adult malaria patients and these cells were also present in children suffering from malaria, it was investigated whether they had similar phenotypic properties to Tr1 cells. Therefore, as for the Tr1 cells, the CD8+LAG-3+CD49b+ T cells of adult malaria patients (n=8-11) and children with mild (n=17) or severe malaria (n=21-22) were examined for the expression of PD-1, TIGIT, TIM-3, CD39 and CCR5. Again, only patients with sufficient numbers of CD8+LAG-3+CD49b+ T cells, as recorded by FACS (≥ 10), patients were included in this analysis. Similar to Tr1 cells, the vast majority of CD8+LAG-3+CD49b+ T cells also expressed PD-1 and CCR5, with respective median frequencies of 86.5 % and 95.6 % in adult malaria patients, 78.3 % and 79.3 % in mild malaria cases and 92.6 % and 90.1 % in severe malaria cases (Figure 14). In contrast to Tr1 cells, PD-1 was significantly increased on Tr1 cells of children with severe malaria compared to mild malaria,

while the level of CCR5 was higher on CD8$^+$LAG-3$^+$CD49b$^+$ T cells of adult malaria patients as well as severe malaria cases compared to children with mild malaria. Hence, PD-1 and CCR5 are not only markers for Tr1 cells, but also for CD8$^+$LAG-3$^+$CD49b$^+$ T cells of malaria patients, although their expression levels were lower in CD8$^+$LAG-3$^+$CD49b$^+$ T cells. TIGIT was increased on CD8$^+$LAG-3$^+$CD49b$^+$ T cells of children with severe malaria (median: 57.1 %) compared to mild malaria cases. Although the median frequency of adult malaria patients (46.9 %) was similar to that of mild malaria cases (39.3 %), no significance was detected when they were compared to severe malaria patients. Likewise, TIM-3 was increased on CD8$^+$LAG-3$^+$CD49b$^+$ T cells of severe malaria patients compared to mild malaria patients with high significance. Children with mild malaria showed the lowest median frequency of TIM-3 (14.3 %) after adult malaria patients (32.3 %) and children with severe malaria (60.0 %). The median frequencies of TIGIT and TIM-3 were generally lower on CD8$^+$LAG-3$^+$CD49b$^+$ T cells of mild (39.3 % and 14.3 %) and severe malaria cases (57.1 % and 60.0 %) compared to the respective Tr1 cells (mild malaria: 42.4 % and 47.3 %; severe malaria: 68.0 % and 88.7 %). In adult malaria patients, Tr1 and CD8$^+$LAG-3$^+$CD49b$^+$ T cells showed the same median frequency of TIGIT (46.9 %), but the level of TIM-3 was, like in the children, higher on Tr1 cells (48.3 %) than on CD8$^+$LAG-3$^+$CD49b$^+$ T cells (32.3 %). There was no difference in the expression of CD39 between the groups. Roughly one third of the CD8$^+$LAG-3$^+$CD49b$^+$ T cells of mild malaria patients expressed CD39 (39.0 %), while more than half of the CD8$^+$LAG-3$^+$CD49b$^+$ T cells of adult malaria patients (53.0 %) and severe malaria patients (58.6 %) expressed this regulatory molecule. In contrast to TIGIT and TIM-3, CD39 was more highly expressed on CD8$^+$LAG-3$^+$CD49b$^+$ T cells (adult malaria patients: 53.0 %; mild malaria: 39.0 %; severe malaria: 58.6 %) than on Tr1 cells (adult malaria patients: 39.9 %; mild malaria: 35.1 %; severe malaria: 30.9 %). Although CD8$^+$LAG-3$^+$CD49b$^+$ T cells showed many phenotypic similarities to Tr1 cells, they displayed a more heterogenous phenotype, with larger differences between mild and severe malaria cases and adult malaria patients.
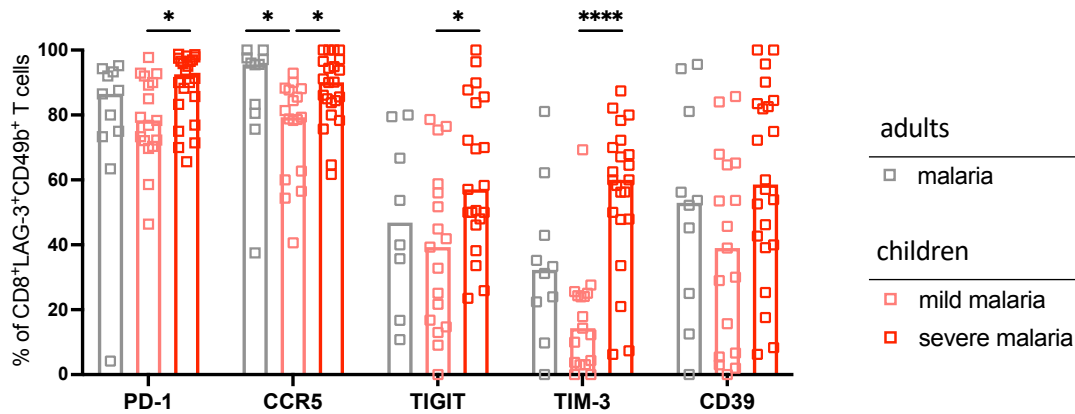
Figure 14: CD8+LAG-3+CD49b+ T cells of malaria patients show Tr1-like characteristics.

CD8+LAG-3+CD49b+ T cells of adult malaria patients (n=8-11) and Ghanaian children suffering from mild (n=17) or severe malaria (n=21-22) were analyzed for their expression of different regulatory molecules. Only patients with a sufficient amount of CD8+LAG-3+CD49b+ ($\geq$ 10) were included in the marker analysis. The bars represent the median. Normality of data was analyzed by D'agostino & Pearson test and statistical significance was determined using Kruskal-Wallis test with Dunn's multiple comparisons test or one-way ANOVA with Tukey's multiple comparisons test (*p $\leq$ 0.05, **p $\leq$ 0.01, ***p $\leq$ 0.001, ****p $\leq$ 0.0001).

4.2.6 Comparison of malaria-induced PD-1+ and LAG-3+CD49b+ T cells

The main characteristics of Tr1 cells are the production of IL-10 and thereby the suppression of T cell functions (58). Thus, to clearly identify a T cell as a Tr1 cell, functional analyses are necessary. Due to the low amount of LAG-3+CD49b+ T cells and limited patient material, a different subset of FoxP3- regulatory T cells was investigated further. Our group identified CD4+PD-1+ T cells that co-express the co-inhibitory molecule cytotoxic T-lymphocyte-associated protein 4 (CTLA-4) are induced in malaria patients and are able to suppress effector T cell proliferation in a dose-dependent manner (80). These cells were also present in healthy adults, where they showed similar properties (data not yet published). Since the majority of malaria-induced Tr1 and CD8+LAG-3+CD49b+ T cells co-expressed PD-1, it was assumed that LAG-3+CD49b+ T cells represent a subpopulation of PD-1+ T cells. To investigate similarities between CD4+PD-1+ T cells and Tr1 cells, the expression of CCR5, TIGIT, TIM-3 and LAG-3 on CD4+PD-1+ T cells of adult malaria patients (n=13-15) and healthy donors (n=17) and of children with mild (n=20) or severe malaria (n=28-30) was examined.

CCR5, TIGIT, TIM-3 and LAG-3 were significantly increased on CD4+PD-1+ T cells of adult malaria patients compared to healthy donors (Figure 15A). The majority of CD4+PD-1+ T cells of adult malaria patients expressed CCR5 (median 76.4 %) and roughly one third co-expressed TIGIT

(median 29.1 %). Only small proportions expressed TIM-3 or LAG-3. In healthy donors, CCR5 was co-expressed by more than one third of the CD4$^+$PD-1$^+$ T cells (median 38.1 %) and also a co-expression of TIGIT was also observed on a small subset of these cells (median 7.37 %). TIM-3 was only expressed by very few cells and LAG-3 was completely absent on CD4$^+$PD-1$^+$ T cells of adult healthy donors. In Ghanaian children, CCR5, TIGIT, TIM-3 and LAG-3 were significantly increased on CD4$^+$PD-1$^+$ T cells of severe malaria patients compared to mild malaria patients (Figure 15B). While the frequencies of CCR5 in mild (median 33.3 %) and severe malaria cases (median 44.8 %) were lower than in adult malaria patients (median 76.4 %), the levels of TIGIT and TIM-3 were higher in severe malaria patients compared to adult malaria patients, with respective medians of 43.5 % and 32.55 %. The median frequencies of LAG-3 were similar in severe malaria (13.1 %) and adult malaria patients (16.8 %), while they were lower in children with mild malaria (7.0 %). In summary, the CD4$^+$PD-1$^+$ T cells of malaria patients showed phenotypic similarities to Tr1 cells, but the levels of most of the investigated surface molecules were lower.
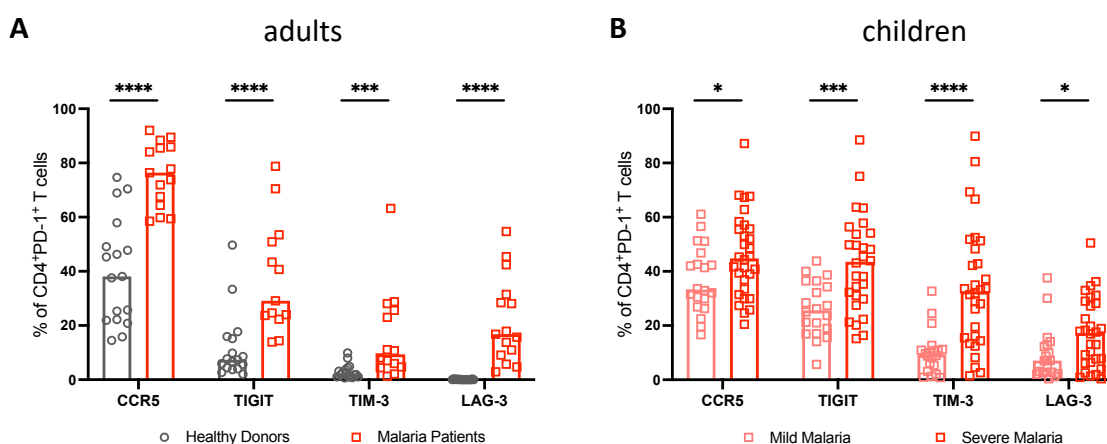
Figure 15: CD4$^+$PD-1$^+$ T cells of malaria patients and healthy donors exhibit a Tr1-like phenotype.

The expression of CCR5, TIGIT, TIM-3 and LAG-3 on CD4$^+$PD-1$^+$ of (A) adult healthy donors (n=17) and *P. falciparum*-infected travelers (n=13-15) and of (B) Ghanaian children with either mild (n=20) or severe malaria (n=28-30) was examined. The bars represent the median. Normality of data was analyzed by D'agostino & Pearson test and statistical significance was determined using Mann Whitney or unpaired t test (*p ≤ 0.05, **p ≤ 0.01, ***p ≤ 0.001, ****p ≤ 0.0001).

To better visualize phenotypic characteristics and co-expression of surface markers on T cells and on LAG-3$^+$CD49b$^+$ T cells in particular, the t-distributed stochastic neighbor embedding

method (t-SNE) was used. T-SNE allows the visualization of high-dimensional data, like flow cytometric data with many parameters, by nonlinear dimensionality reduction. Here, each data point is displayed in a two-dimensional space in such a way that all similarities of the original, high-dimensional dataset are preserved (174). In flow cytometry, this means that cells with similar properties are depicted closer to one another, while more different cells are localized at a greater distance. The t-SNE tool within FlowJo was used for the analysis. Cells of children with mild (n=18) or severe malaria (n=23) were manually gated for lymphocytes, single cells and CD3$^+$ T cells. Only patients with a sufficient number of T cells, comparable cytometer parameters and properly stained markers were included in the analysis. T cells were downsampled to 20,000 events and concatenated for each group. The concatenated events of severe malaria patients were further downsampled to obtain a total number of 360,000 events that was used for the t-SNE algorithm for both the mild and the severe malaria cases. T-SNE was performed based on all measured compensated parameters. To depict the individual cell populations based on their expression of surface molecules, they were first gated manually. Afterwards, the manual gating was applied to the t-SNE plot. Besides LAG-3$^+$CD49b$^+$ T cells and different surface markers, PD-1$^+$CCR5$^+$ and PD-1$^+$TIGIT$^+$ T cells were also analyzed, since CCR5 and TIGIT were found to be markers that are highly co-expressed with PD-1 in malaria patients and healthy donors.

In mild malaria patients, two clear populations of Tr1 and CD8$^+$LAG-3$^+$CD49b$^+$ T cells could be detected (Figure 16A). The Tr1 cells formed a specific cluster of cells, separated from the other CD4$^+$ T cells, while the CD8$^+$LAG-3$^+$CD49b$^+$ T cells did not show that clear separation. Also, in this analysis the expression of PD-1, CCR5, TIM-3 and TIGIT on Tr1 cells was visible. Interestingly, the Tr1 cells were divided into two subsets. The larger subset expressed all the investigated markers except CD39, while the smaller subset also showed expression of CD39. Thus, the expression of CD39 seemed to distinguish subpopulations of Tr1 cells. Furthermore, Tr1 cells were recognizably part of the PD-1$^+$CCR5$^+$ and the PD-1$^+$TIGIT$^+$ T cell subsets. In general, PD-1, TIGIT and CCR5 were distributed much more broadly among T cells than LAG-3 and CD49b, the key markers for Tr1 cells. In severe malaria patients, a specific Tr1 cell cluster with the same properties as in mild malaria patients was visible (Figure 16B). They also expressed the markers PD-1, CCR5, TIM-3 and TIGIT and could be distinguished into two subsets based on the expression of CD39. Again, the population expressing CD39 was smaller than the one lacking CD39. In contrast to mild malaria patients, the CD8$^+$ LAG-3$^+$CD49b$^+$ T cells of severe malaria

patients formed three distinct clusters instead of just one. These clusters were not only spatially separated from each other, but also from the other CD8⁺ T cells. Hence, these CD8⁺LAG-3⁺CD49b⁺ T cells showed more diversity compared to Tr1 cells and compared to mild malaria patients, as these cells did not appear in one single cluster, but were rather distributed among the CD8⁺ T cells. One cluster of CD8⁺LAG-3⁺CD49b⁺ T cells expressed all the investigated markers, while another cluster expressed all markers except CD39. The smallest cluster expressed only PD-1 and CCR5. Interestingly, severe malaria patients showed higher overlaps between PD-1 and TIGIT expression than mild malaria patients and thus more cell clusters that co-expressed PD-1 and TIGIT, especially on CD4⁺ T cells.
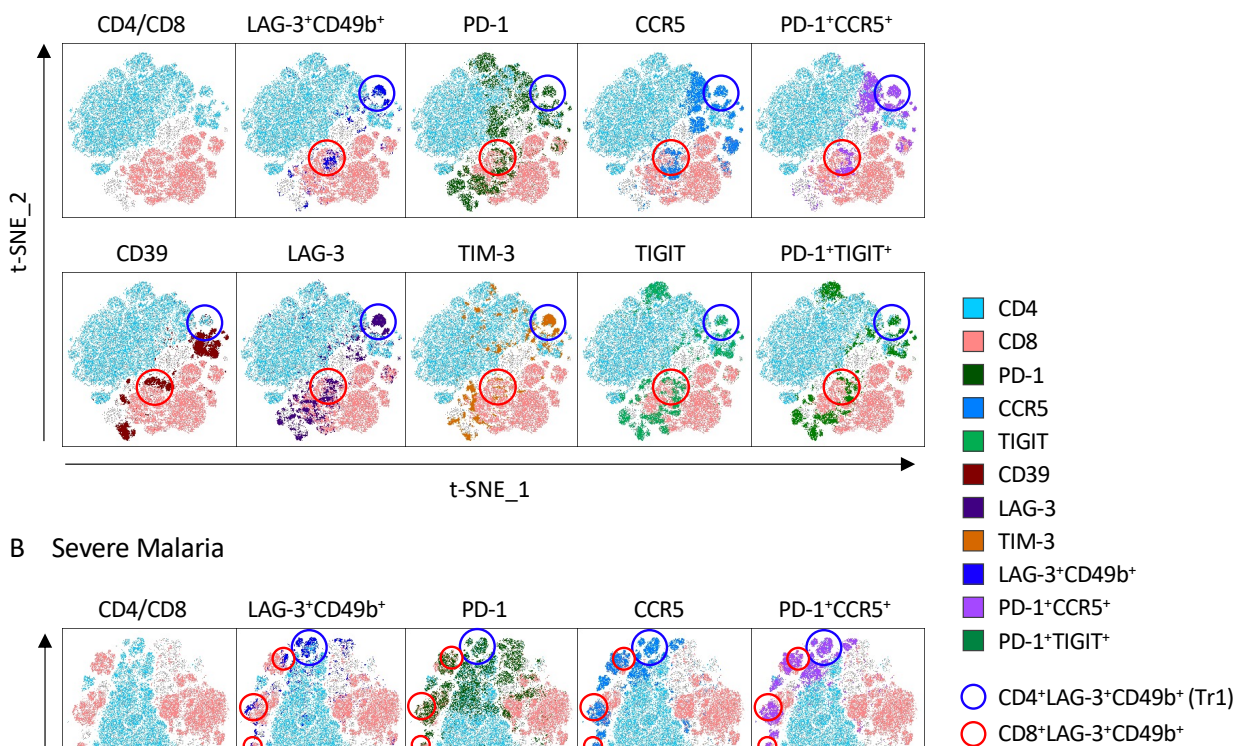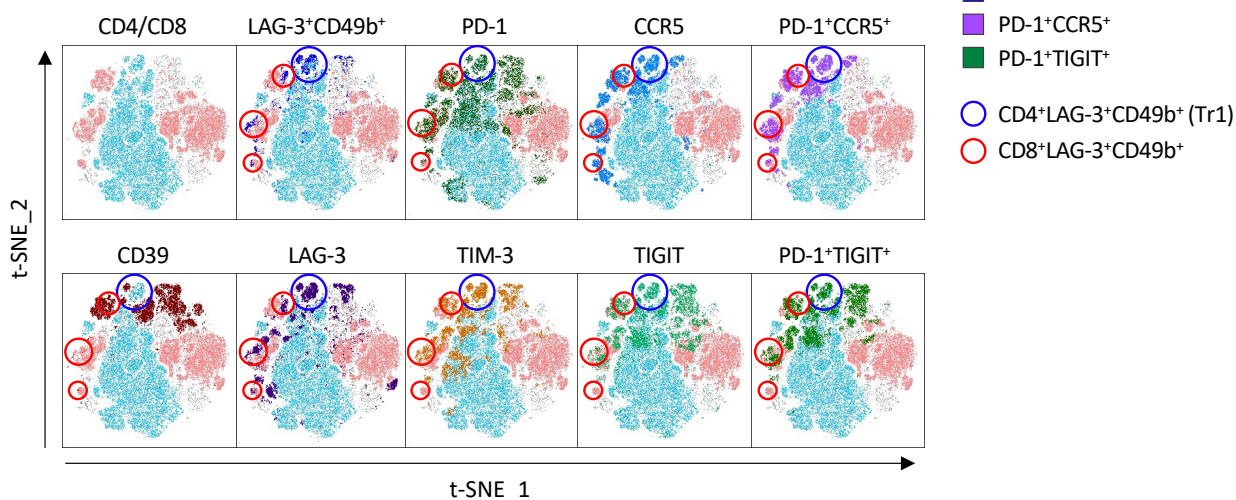
Figure 16: Tr1 cells of children suffering from malaria show a specific phenotype, while CD8⁺LAG-3⁺CD49b⁺ T cells are more heterogenous.

CD3⁺ T cells of Ghanaian children suffering from (A) mild (n=18) or (B) severe malaria (n=23) were downsampled to 20,000 cells, concatenated, and downsampled to a total of 360,000 events using the FlowJo software, in which the t-distributed stochastic neighbor embedding method (t-SNE) was performed. Manual gating of T cell subsets expressing CD4, CD8, PD-1, CCR5, CD39, LAG-3, TIM-3 or TIGIT and of LAG-3⁺CD49b⁺, PD-1⁺CCR5⁺ and PD-1⁺TIGIT⁺ populations was applied to the t-SNE plots. CD4⁺ T cells are depicted in light blue and CD8⁺ T cells in light red. Every surface marker and subpopulations are depicted in a specific color. Tr1 cells are marked by blue circles and CD8⁺LAG-3⁺CD49b⁺ T cells by red circles.

To investigate, whether the observed phenotypic characteristics and marker co-expressions are also present in adult malaria patients, the t-SNE analysis was performed for this patient cohort as well. The CD3⁺ T cells of 7 adult malaria patients were down sampled and concatenated as for the children. In total 140,000 events were used for the analysis. Due to the fact that the adult samples were measured on two different flow cytometers with different parameters, only a small number of patients with matching parameters could be used for this analysis. The patients measured on the BD Fortessa were used. Similar to the children, the Tr1 cells of adult malaria patients clustered together and mainly showed co-expression mainly of PD-1 and CCR5, and partially of TIGIT, CD39 and TIM-3 (Figure 17). They were not as clearly separated into two subpopulations, as defined by CD39 expression, as in mild or severe malaria patients. Tr1 cells of adult malaria patients also showed co-expression of PD-1 and CCR5 as well as of PD-1 and TIGIT. In contrast to children suffering from malaria, adult malaria patients did not show any cluster of CD8⁺LAG-3⁺CD49b⁺ T cells. As revealed by classical gating, the overall percentages of CD8⁺LAG-3⁺CD49b⁺ T cells were lower in adults than in children (Figure 13) and in case of the adults, lower T cell numbers were used in the t-SNE analysis. This may have led to the loss of small cell populations in the t-SNE plot. Similar to mild malaria patients, the adult travelers did not show as strong of an overlap in the expression of PD-1 and TIGIT as the severe malaria patients did. Thus, the adult malaria patients also had PD-1⁺ T cells that lack TIGIT. In summary, the t-SNE analyses showed that Tr1 cells form a specific cell cluster with distinct phenotypes that varies only slightly between adults and children suffering from *P. falciparum* malaria. In contrast to Tr1 cells, CD8⁺LAG-3⁺CD49b⁺ T cells show a more heterogenous phenotype whose diversity increases with disease severity.

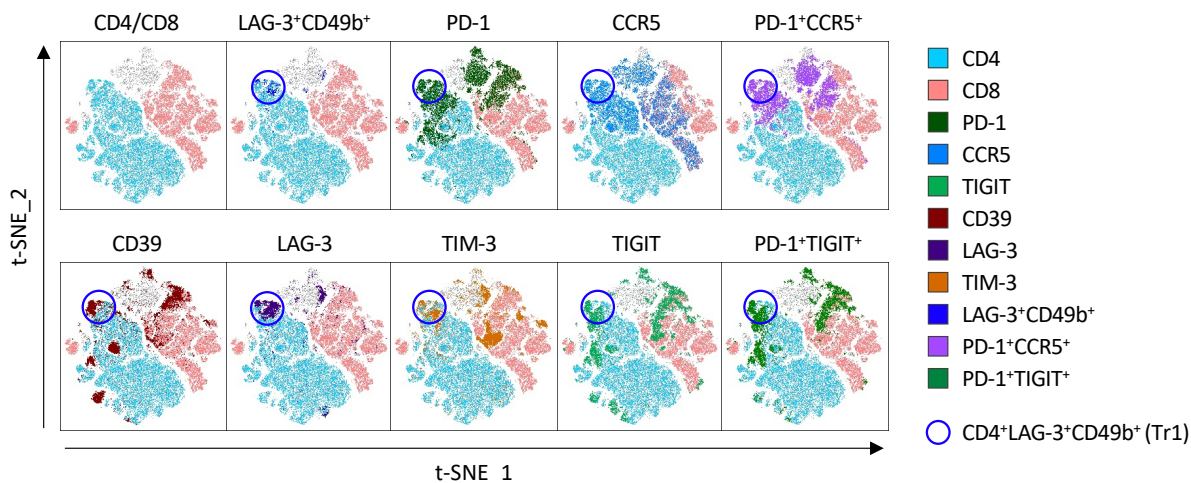Figure 17: Tr1 cells of adult malaria patients show a specific phenotype, while CD8$^+$LAG-3$^+$CD49b$^+$ T cells are not visible via t-distributed stochastic neighbor embedding (t-SNE).

CD3$^+$ T cells of adult travelers suffering from *P. falciparum* malaria (n=7) were downsampled to 20,000 cells and concatenated. A total of 140,000 events was used for the t-distributed stochastic neighbor embedding method (t-SNE) using the FlowJo software. Manual gating of T cell subsets expressing CD4, CD8, PD-1, CCR5, CD39, LAG-3, TIM-3 or TIGIT and of LAG-3$^+$CD49b$^+$, PD-1$^+$CCR5$^+$ and PD-1$^+$TIGIT$^+$ populations was applied to the t-SNE plots. CD4$^+$ T cells are depicted in light blue and CD8$^+$ T cells in light red. Every surface marker and subpopulations are depicted in a specific color. Tr1 cells are marked by a blue circle. A specific cluster of CD8$^+$LAG-3$^+$CD49b$^+$ T cells could not be detected.

The t-SNE analyses revealed that LAG-3$^+$CD49b$^+$ T cells are subpopulations of PD-1$^+$CCR5$^+$ and PD-1$^+$TIGIT$^+$ T cells. To investigate how many LAG-3$^+$CD49$^+$ T cells belong to the PD-1$^+$CCR5$^+$ or the PD-1$^+$TIGIT$^+$ subsets, these frequencies were examined in adult malaria patients (n=8-15) and children suffering from mild (n=17-19) or severe malaria (n=21-22). Only patients with sufficient amounts of Tr1 or CD8$^+$LAG-3$^+$CD49b$^+$ T cells (n≥ 10) and properly stained samples were included in the analyses.

The CD4$^+$PD-1$^+$CCR5$^+$ T cell subset contained almost all of the Tr1 cells of the three cohorts without any differences between the groups (Figure 18A). The CD8$^+$PD-1$^+$CCR5$^+$ T cells of severe malaria patients contained significantly more LAG-3$^+$CD49b$^+$ cells than those of mild malaria patients. Also, the adult malaria patients showed higher levels of PD-1$^+$CCR5$^+$ cells among their CD8$^+$LAG-3$^+$CD49b$^+$ T cells than mild malaria patients, but not significantly so. Both the Tr1 and the CD8$^+$LAG-3$^+$CD49b$^+$ T cells of children with severe malaria showed significantly higher levels of PD-1$^+$TIGIT$^+$ compared to children with mild malaria (Figure 18B). The frequencies in adult malaria patients were similar to those of mild malaria patients, but without any significant

differences to the severe malaria patients. Thus, PD-1$^+$CCR5$^+$ T cell subsets contained all of the Tr1 and most of the CD8$^+$LAG-3$^+$CD49b$^+$ T cells. In comparison, the PD-1$^+$TIGIT$^+$ subsets contained a lower percentage of the LAG-3$^+$CD49b$^+$ T cells than the PD-1$^+$CCR5$^+$ T cell subsets. The percentage of LAG-3$^+$CD49$^+$ T cells that were PD-1$^+$TIGIT$^+$ was significantly higher in patients with severe malaria than in patients with mild malaria.
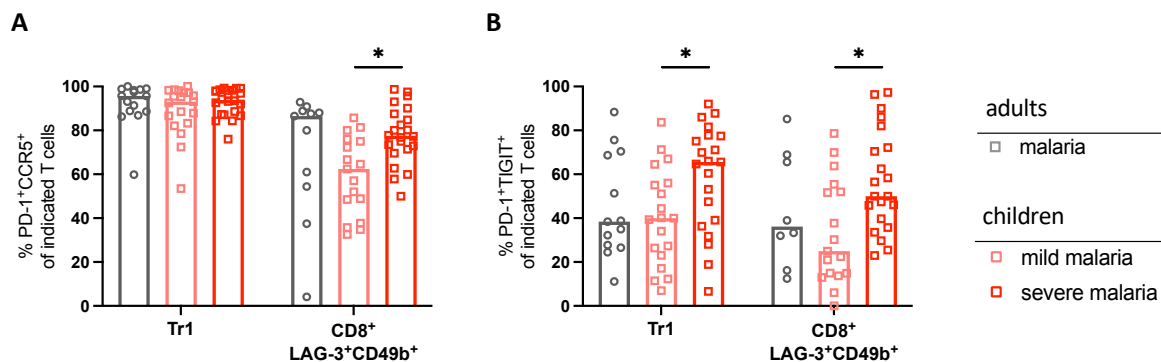
Figure 18: LAG-3$^+$CD49b$^+$ T cells differ in their affiliation to PD-1$^+$ T cell subsets.

Tr1 cells and CD8$^+$LAG-3$^+$CD49b$^+$ T cells of adult malaria patients (n=8-15) and children with mild (n=17-19) or severe malaria (n=21-22) were analyzed for their co-expression of (A) PD-1 and CCR5 and (B) PD-1 and TIGIT. Only patients with a sufficient amount of Tr1 or CD8$^+$LAG-3$^+$CD49b$^+$ T cells ($\geq$ 10) were included in the analysis. The bars represent the median. Normality of data was analyzed by D'agostino & Pearson test and statistical significance was determined using Kruskal-Wallis test with Dunn's multiple comparisons test or one-way ANOVA with Tukey's multiple comparisons test (*p $\leq$ 0.05, **p $\leq$ 0.01, ***p $\leq$ 0.001, ****p $\leq$ 0.0001).

To further investigate the proportions of PD-1$^+$ T cells that co-expressed CCR5 or TIGIT, their frequencies were determined in adult malaria patients (n=12-15) and healthy donors (n=17) and in healthy children (n=32) and children suffering from mild (n=20) or severe malaria (n=28-30).

CD4$^+$PD-1$^+$CCR5$^+$ T cells were significantly induced in adult malaria patients (median: 22.1 %) compared to healthy controls (Figure 19A). In contrast to Tr1 cells, these cells were clearly present in healthy donors with a median frequency of 7.0 %. CD8$^+$PD-1$^+$CCR5$^+$ T cells were present in both healthy individuals and malaria patients without any difference. Their level was similar to that of CD4$^+$PD-1$^+$CCR5$^+$ T cells in malaria patients. Children suffering from malaria showed significant induction of CD4$^+$PD-1$^+$CCR5$^+$ T cells compared to healthy children (median: 4.8 %), but their frequency in mild (median: 10.2 %) and severe cases

(median: 12.1 %) was not altered (Figure 19B). In contrast, CD8$^+$PD-1$^+$CCR5$^+$ T cells were significantly induced in severe malaria patients (median: 17.1 %) compared to mild malaria patients (median: 7.6 %) and healthy controls (median: 5.9 %). There was no difference between mild malaria cases and healthy individuals. CD4$^+$PD-1$^+$TIGIT$^+$ T cells were also induced in adult malaria patients compared to their corresponding healthy donors. Their median frequency was lower overall in healthy individuals (1.5 %) and malaria patients (9.8 %) than of CD4$^+$PD-1$^+$CCR5$^+$ T cells (healthy: 7.0 %; malaria patients: 22.1 %). As in PD-1$^+$CCR5$^+$ T cells, there was no difference between healthy donors and malaria patients in the frequency of CD8$^+$PD-1$^+$TIGIT$^+$ T cells (Figure 19C). Again, their level was the same as that of CD4$^+$PD-1$^+$TIGIT$^+$ T cells in malaria patients. Children with severe (median: 13.1 %) or mild malaria (median: 7.7 %) showed higher levels of CD4$^+$PD-1$^+$TIGIT$^+$ T cells compared to healthy children (median: 1.7 %) and there was a trend for the level to be higher in children suffering from severe malaria compared to mild malaria cases (Figure 19D). CD8$^+$PD-1$^+$TIGIT$^+$ T cells were only significantly induced in children with severe malaria (median: 18.4 %) compared to healthy donors (median: 3.6 %), although there seemed to be a trend towards reduced frequencies in mild malaria cases (median: 9.5 %). In the case of PD-1$^+$TIGIT$^+$ T cells, their levels were comparable between children and adults. This data showed that CD4$^+$PD-1$^+$CCR5$^+$ and CD4$^+$PD-1$^+$TIGIT$^+$ T cells are induced during malaria in adults and children, while CD8$^+$ T cells co-expressing PD-1 and CCR5 or PD-1 and TIGIT are only induced during malaria in children. Both of the investigated PD-1$^+$ T cell populations were also present in healthy donors, which makes them highly feasible for *in vitro* experiments.
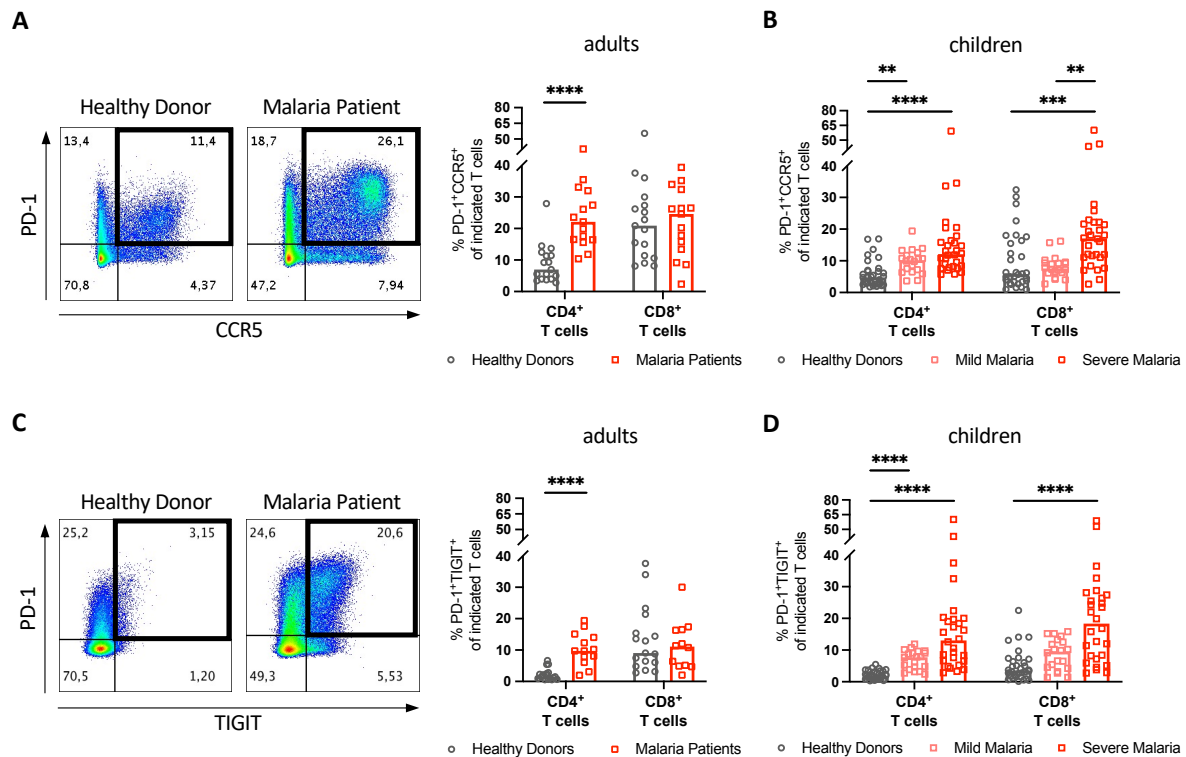
Figure 19: CD4+PD-1+ T cells that co-express CCR5 or TIGIT are induced in malaria patients.

The frequencies of PD-1+CCR5+ T cells were compared between (A) adult malaria patients (n=15) and the respective healthy donors (n=17) and between (B) children suffering from mild (n=20) or severe malaria (n=30) and healthy children (n=32). Additionally, the frequencies of PD-1+TIGIT+ T cells were compared between (C) adult malaria patients (n=12-13) and healthy individuals (n=17) and between (D) children suffering from mild (n=20) or severe malaria (n=28) and healthy children (n=32). Exemplary dot plots of adult healthy donors and malaria patients are shown. The bars represent the median. Normality of data was analyzed by D'agostino & Pearson test. Statistical significance in adults was determined by Mann Whitney or unpaired t test and in children by Kruskal-Wallis test with Dunn's multiple comparisons test (*p ≤ 0.05, **p ≤ 0.01, ***p ≤ 0.001, ****p ≤ 0.0001).

4.3 Suppressive capacities of CD4+PD-1+ T cell subsets that co-express TIGIT or CCR5

Since PD-1+ T cells co-expressing CCR5 or TIGIT were found to contain most of the LAG-3+CD49b+ T cells, but are present in much higher frequencies in malaria patients and healthy donors, their suppressive capacities were examined in *in vitro* suppression assays. Since the material obtained from the Ghanaian children was very limited and not enough for any in vitro experiments, cells of adult healthy donors and malaria patients were used.

4.3.1 Suppressive capacities of CD4$^+$PD-1$^{+/-}$CCR5$^{+/-}$ T cells

First, the suppressive properties of CD4$^+$PD-1$^{+/-}$CCR5$^{+/-}$ T cells were analyzed. In addition to four adult healthy donors, blood samples from two adult malaria patients were obtained. PBMCs were isolated from fresh venous blood and CD4$^+$ T cells and CD4$^-$ cells were separated by a magnetic bead-based isolation assay. Afterwards, the CD4$^+$ T cells were sorted for nTreg (CD25^{hi}CD127^{lo}) and nTreg$^-$ cells were sorted into PD-1$^{+/-}$CCR5$^{+/-}$ populations (Figure 6A). A proportion of the isolated CD4$^+$ T cells was stained with the proliferation dye eFluor^{TM} 450 (eF450) to monitor any changes in their proliferative behavior. Irradiated CD4$^-$ cells, which consisted of all remaining PBMCs, including antigen presenting cells, were used as feeder cells. The labeled CD4$^+$ T cells were incubated with the sorted CD4$^+$ T cell populations and stimulated with anti-CD3 and anti-CD28 antibodies for four days. Proliferation of T effector cells was assessed by flow cytometry (Figure 20A). The amount of proliferated cells incubated alone was set as 0.0 % suppression (Figure 20B). The suppression of CD4$^+$PD-1$^-$CCR5$^+$ T cells was only analysed in healthy donors.

In malaria patients, Treg cells suppressed the CD4$^+$ T cell proliferation the most with a median suppression of 81.0 % (Figure 20C). Of the CD4$^+$PD-1$^{+/-}$CCR5$^{+/-}$ populations, the double positive T cells exhibited the strongest suppressive capacities with a median suppression of 53.4 %. In healthy donors, the PD-1$^+$CCR5$^+$ and the nTreg cells suppressed the CD4$^+$ T cell proliferation in a similar manner, with 36.7 % and 42.1 % respective suppression. The PD-1 single positive cells showed higher suppressive capacities in malaria patients compared to healthy donors, while the double negative cells displayed almost no suppressive function in both groups.
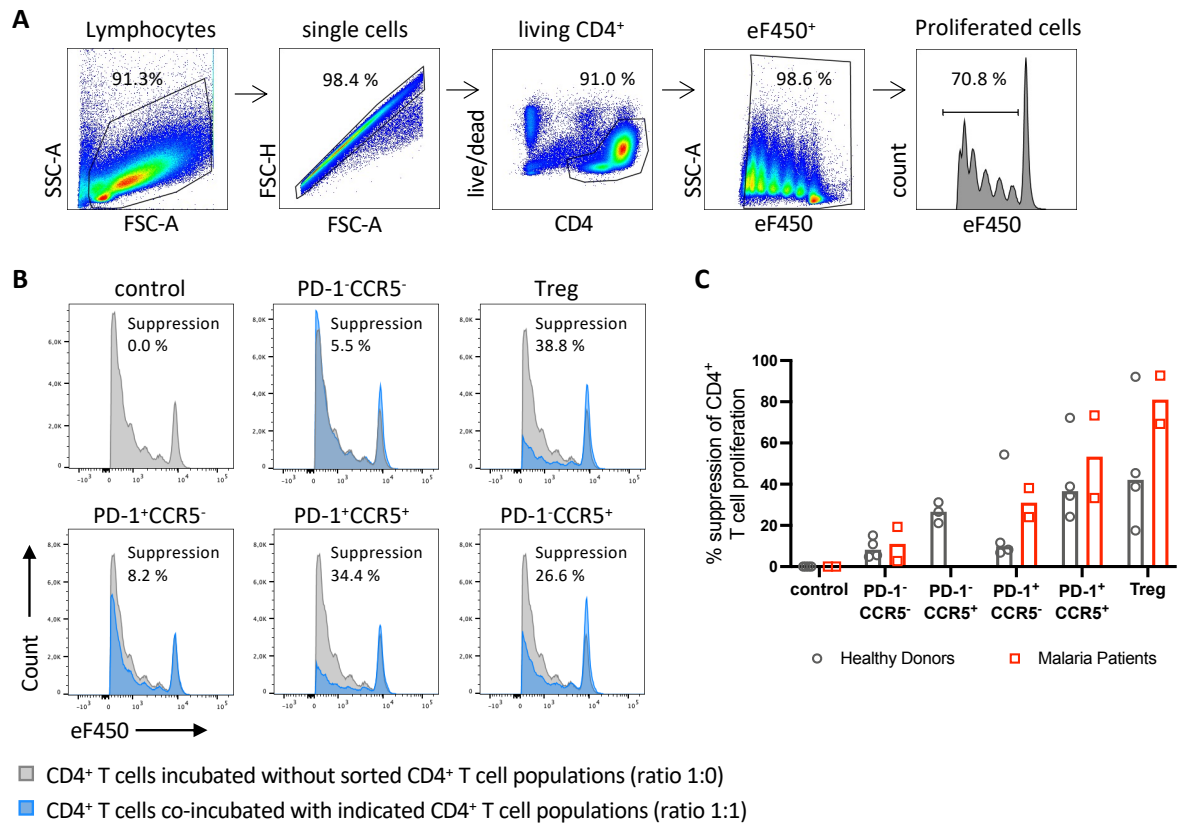
Figure 20: CD4$^+$PD-1$^+$CCR5$^+$ T cells suppress CD4$^+$ T cell proliferation similarly to Treg cells.

Suppressive capacities of CD4$^+$PD-1$^{+/-}$CCR5$^{+/-}$ T cells on CD4$^+$ T cells were analyzed in healthy donors (n=4) and *P. falciparum* infected travelers (n=2). CD4$^+$ T cells were labeled with the proliferation dye eF450 and co-incubated with autologous, FACS-sorted Treg or CD4$^+$Treg$^-$PD-1$^{+/-}$CCR5$^{+/-}$ T cell populations in a 1:1 ratio. Cells were stimulated with soluble anti-CD3 and anti-CD28 antibodies for four days. (A) Living CD4$^+$ singlet T lymphocytes were gated for eF450$^+$ cells and the frequency of proliferated cells. (B) Proliferation of CD4$^+$ T cells incubated with sorted CD4$^+$PD-1$^{+/-}$CCR5$^{+/-}$ populations was assessed (blue histograms). Suppression of CD4$^+$ T cell proliferation was determined relative to CD4$^+$ T cells incubated alone (control; grey histograms). One out of four independent experiments of a healthy donor is shown. (C) Suppressive capacities of sorted CD4$^+$ T cell populations were compared between healthy donors and malaria patients. PD-1$^-$CCR5$^+$ cells were only analyzed in healthy donors in three independent experiments. Statistical significance could not be determined due to the small sample size.

Additionally, it was investigated whether the suppressive capacities of CD4$^+$PD-1$^+$CCR5$^+$ T cells are dose-dependent. To this end, the CD4$^+$ effector T cells were incubated with the sorted T cell populations in a 1:1 and 1:0.5 ratio and the suppression was assessed as before. The suppressive capacity of the double negative cells was not assessed this time, since they were mainly used as a control. As before, the suppression of CD4$^+$PD-1$^-$CCR5$^+$ T cells was only analysed in healthy donors. In healthy donors, all the CD4$^+$PD-1$^{+/-}$CCR5$^{+/-}$ populations showed dose-dependent suppressive activity (Figure 21A). When adding only half the amount of sorted

T cells, their suppressive capacity was visibly reduced. Interestingly, CD4+PD-1-CCR5+ T cells showed higher suppression of CD4+ T cell proliferation compared to CD4+PD-1+CCR5-. In malaria patients, the suppressive capacities of the sorted CD4+ T cells were generally stronger compared to healthy donors (Figure 21B). PD-1+CCR5+ T cells and Treg cells showed a dose-dependent suppression of CD4+ T cells. Only the PD-1+CCR5- T cells showed more suppression when adding only half the amount of cells.
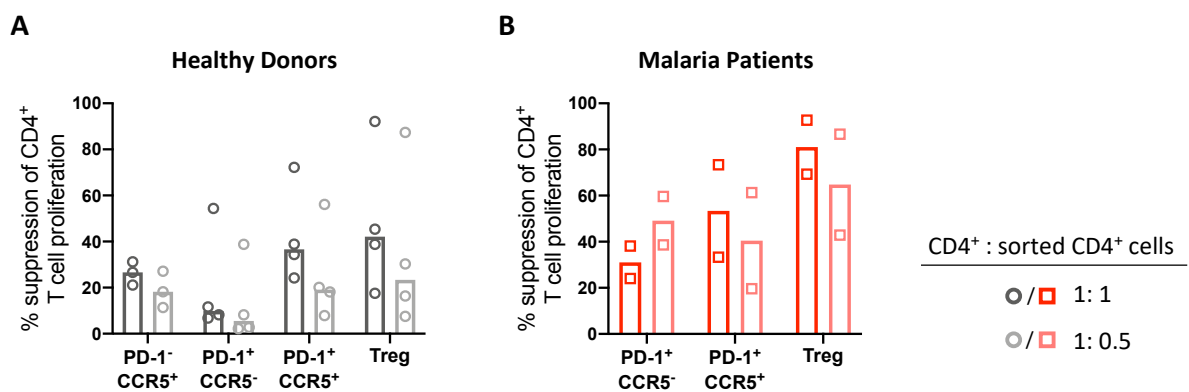
Figure 21: Suppressive capacities of CD4+PD-1+/-CCR5+/- T cells on CD4+ T cells are dose-dependent.

Dose-dependent suppression of CD4+ T cell proliferation by CD4+PD-1+/-CCR5+/- T cells was analyzed in (A) healthy donors (n=3-4) and (B) *P. falciparum* infected travelers (n=2). CD4+ T cells were labeled with the proliferation dye eF450 and co-incubated with FACS-sorted nTreg or CD4+Treg-PD-1+/-CCR5+/- T cell populations in a 1:1 (dark grey circles/dark red squares) or 1:0.5 ratio (light grey circles/light red squares).

To assess whether the CD4+PD-1+/-CCR5+/- T cells are also able to suppress the proliferation of CD8+ T cells, the sorted CD4+ T cell subsets were co-incubated with eF450-labeled autologous CD8+ T cells. Before staining them with eF450, the CD8+ T cells were isolated from PBMCs using a magnetic bead-based assay. This was only done with samples from healthy donors (n=3). Additionally, dose-dependent suppression was analyzed by incubating the cells either at a 1:1 or 1:0.5 ratio. CD8+ T cell proliferation was assessed by flow cytometry (Figure 22A). Again, suppression was calculated based on CD8+ T cells incubated without any regulatory CD4+ T cells (control) (Figure 22B). Treg cells showed the strongest suppression of CD8+ T cell proliferation (Figure 22C). This suppressive effect was dose-dependent and even stronger compared to the suppression of CD4+ T cell proliferation. Similar to the experiment with CD4+ T cells, the CD4+PD-1+CCR5+ T cells had the strongest suppressive effect of the PD-1 and CCR5-expressing

cells, and this was also dose-dependent. The PD-1$^-$CCR5$^+$ and PD-1$^+$CCR5$^-$ cells only showed minor suppression, with dose-dependent effects only in PD-1$^-$CCR5$^+$ cells. As before, the PD-1$^-$CCR5$^-$ cells showed almost no suppressive properties. Accordingly, CD4$^+$PD-1$^+$CCR5$^+$ T cells are regulatory T cells with suppressive capacities similar to Treg cells. Interestingly, CD4$^+$CCR5$^+$ T cells that lack PD-1 also showed weak suppressive effects, mainly on CD4$^+$ T cell proliferation. CD4$^+$PD-1$^+$CCR5$^+$ T cells were not only able to suppress CD4$^+$, but also CD8$^+$ T cell proliferation, and thus seem to play an important role in regulating pro-inflammatory, cytotoxic T cell responses.
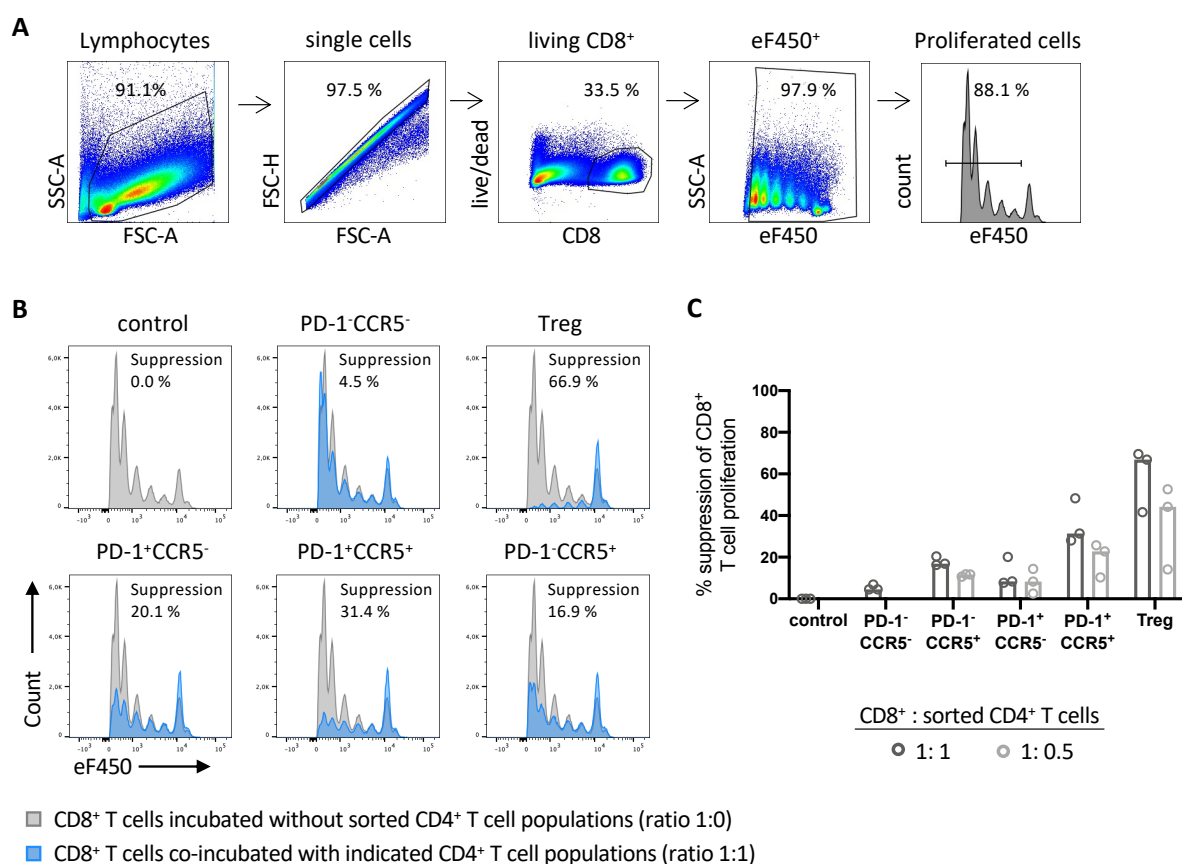
Figure 22: CD4$^+$PD-1$^+$CCR5$^+$ T cells also suppress CD8$^+$ T cell proliferation in a dose-dependent manner.

Suppressive capacities of CD4$^+$PD-1$^+$CCR5$^+$ T cells on CD8$^+$ T cells were analyzed in healthy donors (n=3-4). CD8$^+$ T cells were labeled with the proliferation dye eF450 and co-incubated with autologous, FACS-sorted Treg or CD4$^+$nTreg$^-$PD-1$^{+/-}$CCR5$^{+/-}$ T cell populations in a 1:1 or 1:0.5 ratio. Cells were stimulated with soluble anti-CD3 and anti-CD28 antibodies for four days. (A) Living CD8$^+$ singlet T lymphocytes were gated for eF450$^+$ cells and the frequency of proliferated cells was determined. (B) Proliferation of CD8$^+$ T cells incubated with sorted CD4$^+$PD-1$^{+/-}$CCR5$^{+/-}$ populations was assessed (blue histograms). Suppression of CD8$^+$ T cell proliferation was calculated relative to CD8$^+$ T cells incubated alone (control; grey histograms). One out of three independent experiments is shown. (C) Dose-dependent, suppressive capacities of sorted CD4$^+$ T cell populations on CD8$^+$ T cell proliferation were analyzed. Statistical significance could not be determined due to the small sample size.

4.3.2 Cytokine profile of CD4$^+$PD-1$^{+/-}$CCR5$^{+/-}$ T cells

To further investigate whether the observed differences in the suppressive properties of CD4$^+$PD-1$^{+/-}$CCR5$^{+/-}$ T cells are due to differences in their cytokine production, the cells were stimulated with anti-CD3 and anti-CD28 antibodies and stained intracellularly for GrzB, IL-10, IFN-γ and TNF-α. This was done for healthy donors (n=4) as well as malaria patients (n=5). Additionally, the cells were stained for FoxP3 to exclude nTreg.

The CD4$^+$FoxP3$^-$PD-1$^+$CCR5$^+$ T cells of healthy donors produced higher levels of GrzB, IL-10, IFN-γ and TNF-α compared to the other PD-1/CCR5-expressing cell subsets (Figure 23A). IL-10 and IFN-γ were absent in the double negative cell population, but were produced at very low levels by PD-1 and CCR5 single positive cells. The frequencies of TNF-α were similar between PD-1$^+$ cells co-expressing CCR5 and those without CCR5, while it was lower in CCR5 single positive cells and double negative cells. Similar to healthy donors, the PD-1$^+$CCR5$^+$ cells of malaria patients produced more GrzB and IL-10 than the other T cell subsets although the overall level of IL-10 was very low (Figure 23B). IFN-γ and TNF-α were produced at similar levels in the populations that co-expressed PD-1 and CCR5 and those expressing CCR5 or PD-1 alone. Only the double negative population showed nearly no IFN-γ and very low TNF-α production. Generally, the levels of IL-10, IFN-γ and TNF-α were lower in malaria patients compared to healthy donors. Thus, CD4$^+$ T cells co-expressing PD-1 and CCR5 are activated cells with regulatory functions that produce pro- as well as anti-inflammatory cytokines and therefore show Tr1 cell characteristics in healthy donors as well as in malaria patients.

CD4+ T cells

A Healthy Donors
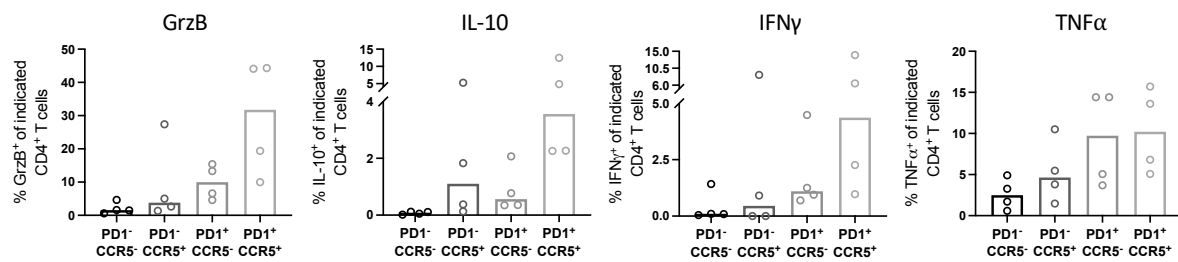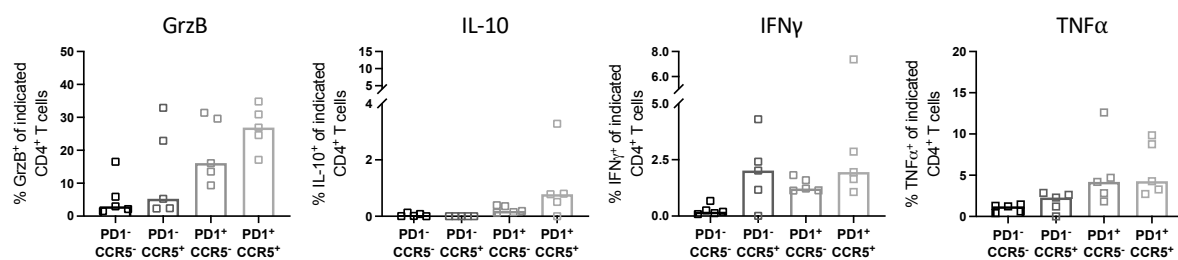
B Malaria Patients

Figure 23: CD4+FoxP3-PD-1+CCR5+ T cells produce more cytokines than their non-double positive counterparts.

CD4+FoxP3-PD-1+/-CCR5+/- T cells of (A) adult healthy donors (n=4) and (B) malaria patients (n=5) were stimulated with aCD3 and aCD28 antibodies and stained intracellularly for GrzB, IFN-γ, IL-10 and TNF-α. Cytokine production was analyzed by flow cytometry. Statistical significance could not be determined due to the small sample size.

4.3.3 Suppressive capacities of CD4+PD-1+/-TIGIT+/- T cells

The suppressive capacities of CD4+PD-1+/-TIGIT+/- T cells were examined in the same way as for the CD4+PD-1+/-CCR5+/- T cells. Due to a lack of samples from malaria patients, only cells of healthy donors were used for these experiments. Again, freshly isolated PBMCs were used to obtain CD4+ T cells and CD4- PBMCs by magnetic bead-based cell isolation. The CD4+ T cells were then sorted by FACS into nTreg cells and the four nTreg- PD-1+/-TIGIT+/- subsets (Figure 6B). As before, the labeled CD4+ T cells were incubated with the sorted CD4+ T cell populations and stimulated with anti-CD3 and anti-CD28 antibodies for four days. Proliferation of T effector cells was assessed by flow cytometry (gating strategy: Figure 20A). The amount of proliferated cells incubated alone was set as 0.0 % suppression (Figure 24A).

As seen before, Treg cells showed the highest median suppressive capacity and this was dose-dependent (Figure 24B). CD4+PD-1+TIGIT- T cells showed the second highest suppressive effect on CD4+ T cell proliferation, and this suppression was also does-dependent. The double

negative, double positive and TIGIT single positive cells had almost no suppressive function, which indicates that TIGIT seems to dampen the suppressive effect, especially of regulatory CD4$^+$PD-1$^+$ T cells.
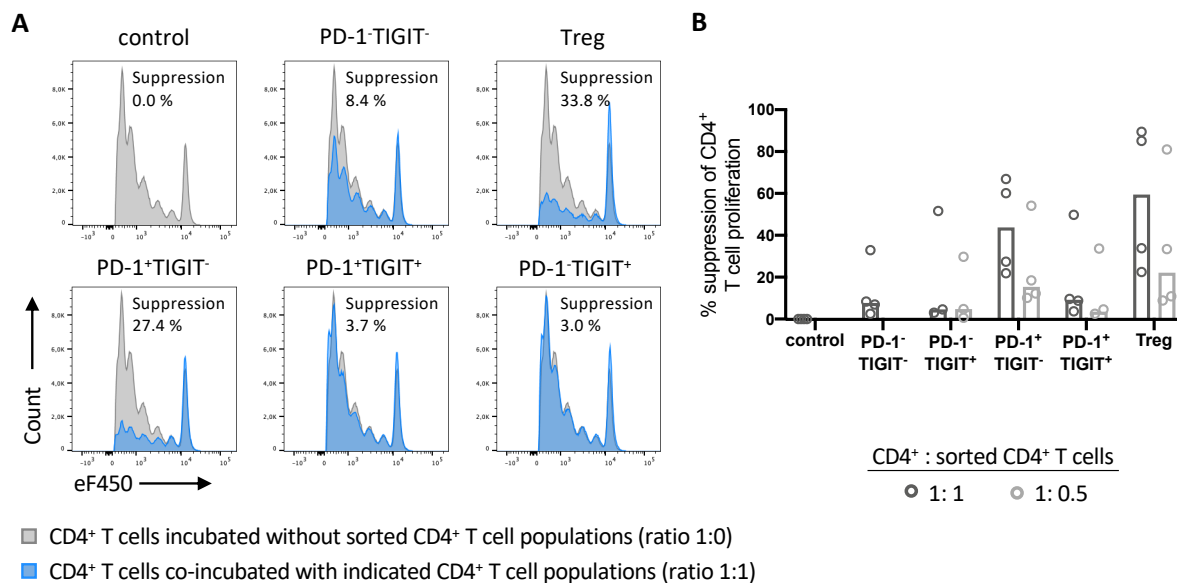
Figure 24: CD4$^+$ T cells that express PD-1 but not TIGIT suppress CD4$^+$ T cell proliferation similar to nTreg cells.

Suppressive capacities of CD4$^+$PD-1$^{+/-}$TIGIT$^{+/-}$ T cells on CD4$^+$ T cell proliferation were analyzed in healthy donors (n=3-4). CD4$^+$ T cells were labeled with the proliferation dye eF450 and co-incubated with autologous, FACS-sorted Treg or CD4$^+$Treg$^-$PD-1$^{+/-}$CCR5$^{+/-}$ T cell populations in a 1:1 or 1:0.5 ratio. Cells were stimulated with soluble anti-CD3 and anti-CD28 antibodies for four days. Gating strategy was used as described before (Figure 20A). (A) Proliferation of CD4$^+$ T cells incubated with sorted CD4$^+$PD-1$^{+/-}$TIGIT$^{+/-}$ populations was assessed (blue histograms). Suppression of CD4$^+$ T cell proliferation was calculated relative to CD4$^+$ T cells incubated alone (control; grey histograms). One out of four independent experiments is shown. (B) Dose-dependent, suppressive capacities of sorted CD4$^+$ T cell populations on CD4$^+$ T cell proliferation were analyzed. Statistical significance could not be determined due to the small sample size.

Afterwards, it was investigated whether the CD4$^+$PD-1$^{+/-}$TIGIT$^{+/-}$ T cells are also able to suppress CD8$^+$ T cell proliferation. To this end, CD8$^+$ T cells were isolated from PBMCs of healthy donors (n=3-4) using a magnetic bead-based method, labeled with eF450 and co-incubated with the autologous sorted CD4$^+$PD-1$^{+/-}$TIGIT$^{+/-}$ T cell populations. CD4$^-$ PBMCs were used as feeder cells. As in the previous suppression assays, Treg cells suppressed the proliferation of CD8$^+$ T cells the most. This suppression was dose-dependent and even stronger compared to the suppression of CD4$^+$ T cell proliferation when comparing the medians. The suppression by PD-1$^+$ T cells that lack TIGIT and those that co-express TIGIT was approximately 50 % lower than that of Treg, and

the double positive cells showed slightly lower suppression compared to the PD-1 single positive cells. TIGIT single positive and double negative cells showed nearly no suppressive effect. In contrast to the experiment with CD4$^+$ effector T cells, CD4$^+$PD-1$^+$TIGIT$^+$ T cells were able to suppress CD8$^+$ T cell proliferation, but not CD4$^+$ T cell proliferation. Thus, the suppression of CD8$^+$ T cell proliferation seems to be more independent from TIGIT than the suppression of CD4$^+$ T cell proliferation.
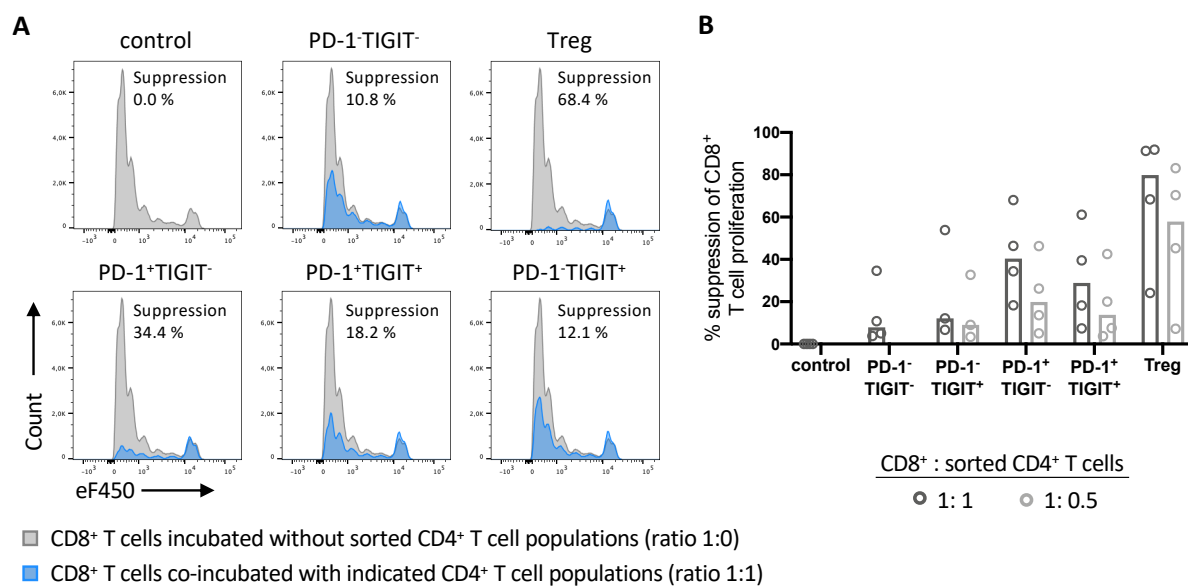
Figure 25: Suppression of CD8$^+$ T cell proliferation by CD4$^+$PD-1$^+$ T cells depends on PD-1, but not TIGIT.

Suppressive capacities of CD4$^+$PD-1$^{+/-}$TIGIT$^{+/-}$ T cells on CD8$^+$ T cell proliferation were analyzed in healthy donors (n=3-4). CD8$^+$ T cells were labeled with the proliferation dye eF450 and co-incubated with autologous, FACS-sorted Treg or CD4$^+$PD-1$^{+/-}$TIGIT$^{+/-}$ Treg$^-$ T cell populations in a 1:1 or 1:0.5 ratio. Cells were stimulated with soluble anti-CD3 and anti-CD28 antibodies for four days. The gating strategy to asses CD8$^+$ T cell proliferation was used as described before (Figure 22A). (A) Proliferation of CD8$^+$ T cells incubated with sorted CD4$^+$PD-1$^{+/-}$TIGIT$^{+/-}$ populations was assessed (blue histograms). Suppression of CD8$^+$ T cell proliferation was calculated relative to CD8$^+$ T cells incubated alone (control; grey histograms). One out of four independent experiments is shown. (B) Dose-dependent, suppressive capacities of sorted CD4$^+$ T cell populations on CD8$^+$ T cell proliferation were analyzed. Statistical significance could not be determined due to the small sample size.

4.3.4   Cytokine profile of CD4$^+$PD-1$^{+/-}$TIGIT$^{+/-}$ T cells

The differences in the production of the cytokines GrzB, IL-10, IFN-γ and TNF-α were also examined for the CD4$^+$PD-1$^{+/-}$TIGIT$^{+/-}$ T cell populations. As before, the cells were stimulated with antibodies directed against CD3 and CD28 and stained intracellularly for the investigated

cytokines. In addition to healthy donors (n=4), cells of malaria patients (n=5) were also used to compare the cytokine profiles and to predict any suppressive function.

In contrast to the PD-1$^+$CCR5$^+$ double positive T cells, the PD-1$^+$TIGIT$^+$ double positive cells of healthy donors produced less GrzB, IL-10, IFN-γ and TNF-α than the PD-1$^+$ cells that lacked TIGIT (Figure 26A). The PD-1$^+$TIGIT$^-$ cells therefore showed the highest levels of the analyzed cytokines. PD-1$^-$ cells exhibited nearly no production of GrzB, IL-10 or IFN-γ and only minor production of TNF-α, independent of TIGIT expression. The cells of malaria patients had a similar cytokine profile regarding GrzB and IFN-γ (Figure 26B). The PD-1$^+$TIGIT$^-$ cells had the highest levels of GrzB and IFN-γ, followed by PD-1$^+$TIGIT$^+$ cells. There was no difference in the levels of IL-10 in the three cell subsets expressing one or both co-inhibitors, and the frequencies of TNF-α were moderately higher in PD-1$^+$ compared to PD-1$^-$ cells, independent of TIGIT expression. In general, the frequencies of IL-10 and IFN-γ were very low. These results support the previous finding that PD-1$^+$ cells are more suppressive when they lack TIGIT, since the PD-1 single positive cells also showed higher levels of pro- and anti-inflammatory cytokines.

CD4$^+$ T cells

A Healthy Donors
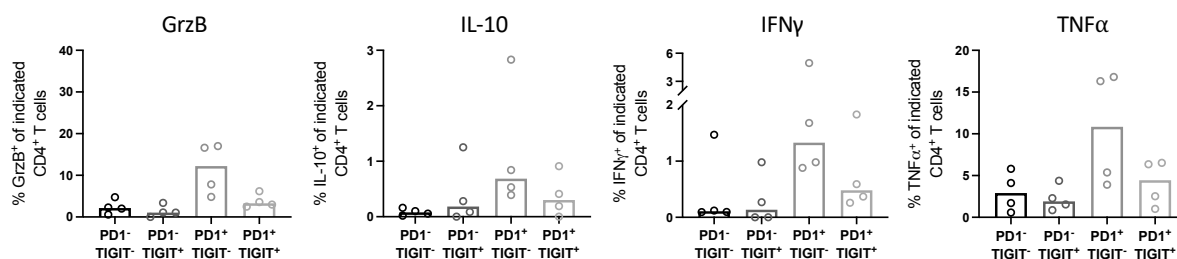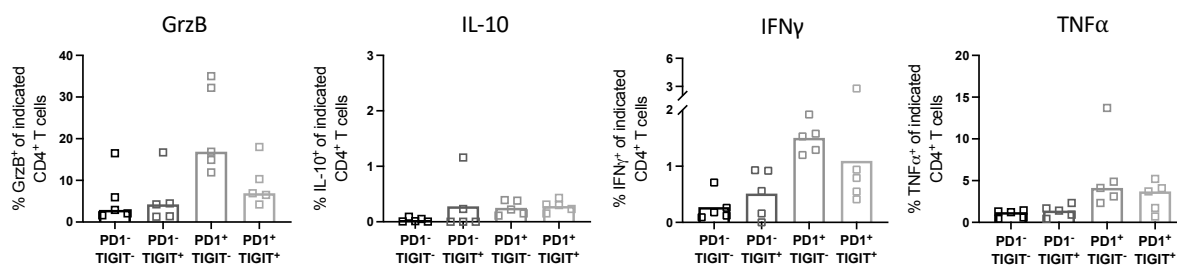
B Malaria Patients

Figure 26: CD4$^+$FoxP3$^-$PD-1$^+$TIGIT$^+$ T cells produce lower amounts of cytokines than their TIGIT$^-$ counterparts.

CD4$^+$FoxP3$^-$PD-1$^{+/-}$TIGIT$^{+/-}$ T cells of (A) adult healthy donors (n=4) and (B) malaria patients (n=5) were stimulated with anti-CD3 and anti-CD28 antibodies and stained intracellularly for GrzB, IFN-γ, IL-10 and TNF-α. Cytokine production was analyzed by flow cytometry. Statistical significance could not be determined due to the small sample size.

4.3.5 Prediction of suppressive activity of CD8⁺PD-1⁺ T cells co-expressing CCR5 or TIGIT based on their cytokine profile

The previous results showed that the CD4$^+$PD-1$^+$ T cells that co-express CCR5 have an increased suppressive function in contrast to the cells that co-express TIGIT. It was also found that CD8$^+$ T cells co-expressing PD-1 and CCR5 or PD-1 and TIGIT are induced in children suffering from severe malaria and are present in adult healthy donors and malaria patients. These cells contained most of the putative regulatory LAG-3$^+$CD49b$^+$ cells. Until now, the suppressive capacities of these cells had not been investigated, but to predict any suppressive function, the production of GrzB, IFN-γ, IL-10 and TNF-α by CD8$^+$PD-1$^{+/-}$CCR5$^{+/-}$ and CD8$^+$PD-1$^{+/-}$TIGIT$^{+/-}$ T cells was analyzed. The cells of adult healthy donors (n=4) and malaria patients (n=5) were stimulated with anti-CD3 and anti-CD28 and stained intracellularly for cytokines as described before.

Similar to CD4$^+$ T cells, CD8$^+$ T cells that co-expressed PD-1 and CCR5 produced higher levels of GrzB and IL-10 than their non-double positive counterparts. This was the case for healthy donors (Figure 27A) as well as malaria patients (Figure 27B). In malaria patients, the double positive cells also produced slightly higher levels of IFN-γ (Figure 27B). The double negative cells showed the lowest levels of GrzB, IFN-γ and TNF-α and no production of IL-10 in both healthy individuals and malaria patients. Thus, CD8$^+$ T cells that co-express PD-1 and CCR5 are also activated cells that produce higher levels of pro- and anti-inflammatory cytokines compared to the non-double positive cells.

CD8+ T cells

A Healthy Donors
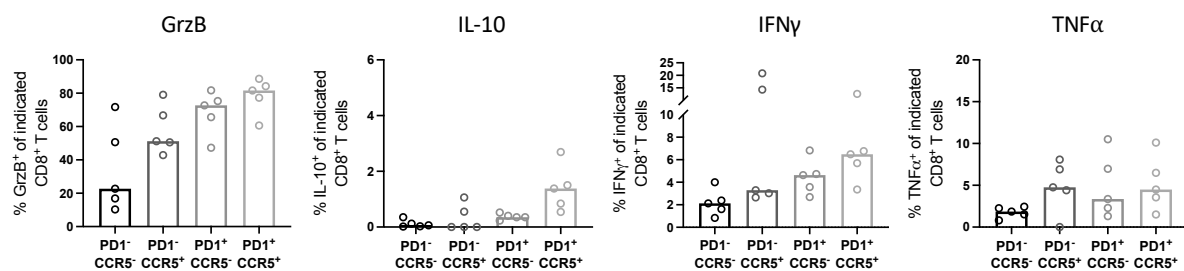
B Malaria Patients

Figure 27: CD8+PD-1+CCR5+ T cells produce higher levels of GrzB and IL-10 than their single-positive counterparts.

CD8+PD-1+/-CCR5+/- T cells of (A) adult healthy donors (n=4) and (B) malaria patients (n=5) were stimulated with anti-CD3 and anti-CD28 antibodies and stained intracellularly for GrzB, IFN-γ, IL-10 and TNF-α. Cytokine production was analyzed by flow cytometry. Statistical significance could not be determined due to the small sample size.
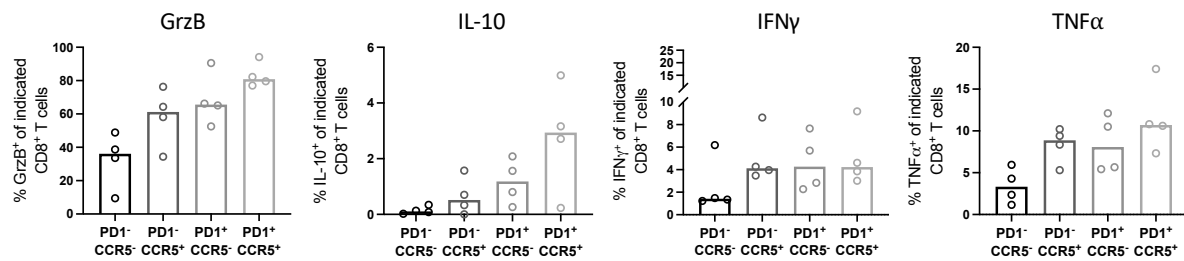
Additionally, CD8+PD-1+/-TIGIT+/- T cells were analyzed for their cytokine profile. PD-1+ cells of healthy donors that lacked TIGIT showed moderately higher levels of GrzB compared to the PD-1 and TIGIT single positive cells (Figure 28A). The double negative cells showed the lowest levels of GrzB. The same GrzB profile could be observed in malaria patients (Figure 28B). While the PD-1 single positive cells of healthy donors also produced the highest amounts of IL-10 and TNF-α, followed by the double positive cells, the levels of IL-10 or TNF-α were not altered between the cells expressing either PD-1 or TIGIT or both co-inhibitors in malaria patients. The double positive cells and the cells of healthy donors did not produce any IL-10, and the TIGIT single positive cells of malaria patients produced only very low amounts of IL-10. There were no visible differences between the three groups expressing either PD-1 or TIGIT or both in the production of IFN-γ in both the healthy donors and the malaria patients. In summary, CD8+PD-1+ T cells also produced pro- and anti-inflammatory cytokines, with increased levels in the cells that co-expressed CCR5, but decreased levels in TIGIT+ cells. Due to the similarity

between the cytokine profiles of CD8$^+$PD-1$^+$ and CD4$^+$PD-1$^+$ T cells, it is highly possible that the CD8$^+$ cells also have suppressive capacities which need to be investigated further.

CD8$^+$ T cells

A   Healthy Donors
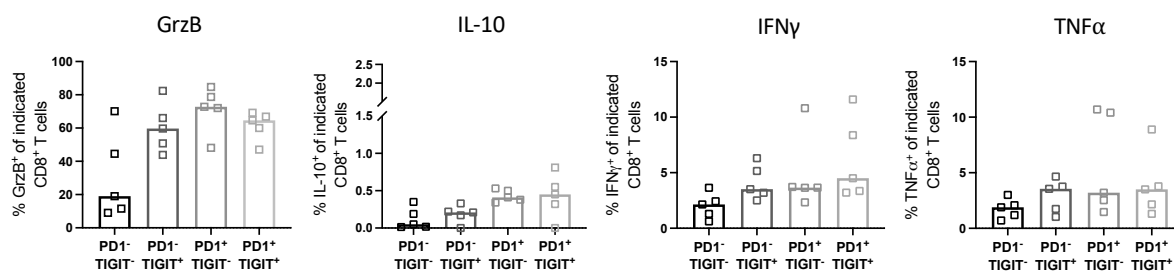
B   Malaria Patients

Figure 28: CD8$^+$ PD-1$^+$TIGIT$^+$ T cells produce lower levels of cytokines than their TIGIT$^-$ counterparts.

CD8$^+$ PD-1$^{+/-}$TIGIT$^{+/-}$ T cells of (A) adult healthy donors (n=4) and (B) malaria patients (n=5) were stimulated with anti-CD3 and anti-CD28 antibodies and stained intracellularly for GrzB, IFN-γ, IL-10 and TNF-α. C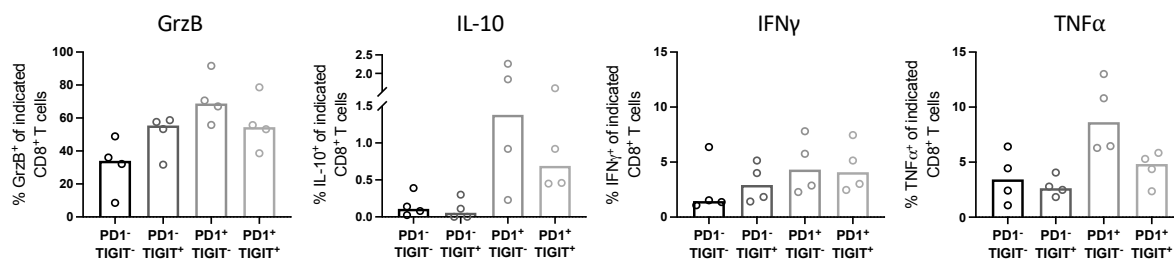ytokine production was analyzed by flow cytometry. Statistical significance could not be determined due to the small sample size.

5 Discussion

The maintenance of an immunological balance between pro- and anti-inflammatory mechanisms is of decisive importance during an infection with the malaria-causing parasite *Plasmodium falciparum* (*Pf*). T cells have not only been shown to be crucial for the development of protective immunity against recurring *Plasmodium* infections but also to contribute to immunopathology that causes severe malaria. It is still unknown why some patients develop severe malaria and others do not. It could be hypothesized that a failure of regulatory mechanisms favors pro-inflammatory immune responses leading to immunopathological effects. Thus, this study aimed to both elucidate the role of cytotoxic CD8$^+$ T cells in the onset of severe human malaria and to identify subsets of regulatory T cells that could counteract this pro-inflammatory immune reaction.

5.1 Granzyme B-producing CD8$^+$ T cells contribute to the development of severe malaria

Several studies in experimental murine malaria have shown evidence that granzyme B (GrzB) production by CD8$^+$ T cells contributes significantly to the onset of severe malaria and to the development of cerebral malaria (157). However, data from human studies addressing this question are scarce. Therefore, the first objective of this study was to shed further light on the role of cytotoxic CD8$^+$ T cells in the development of severe malaria in humans. One of the main effector molecules produced by cytotoxic CD8$^+$ T cells is GrzB that, together with perforin, mediates the induction of apoptosis of infected target cells (37). Our group found elevated levels of GrzB in the plasma of Ghanaian children that were symptomatically infected with *Pf* compared to asymptomatically infected or healthy children (97). When examining the cellular source of the GrzB, the frequency of CD8$^+$ T cells that produce GrzB were found to be elevated in symptomatically infected children compared to asymptomatically infected or healthy children (Figure 7). Additionally, the number of CD8$^+$GrzB$^+$ T cells was higher in children with severe malaria compared to children with mild malaria. This data indicated that cytotoxic CD8$^+$ T cells contribute to disease severity and are the main source of the GrzB found in the plasma of *Pf*-infected children. Concurrent with the data of our study, Riggle et. al. found elevated numbers of CD8$^+$ T cells inside the brain vasculature of children who died due to cerebral

malaria in contrast to children who died from other causes (158). Additionally, they showed that these CD8$^+$ T cells were loaded with GrzB and secreted this GrzB onto the brain vasculature, which supports the findings of our study.

Besides CD8$^+$ T cells, γδ T cells or NK cells also produce GrzB in the context of malaria (192, 193). One limitation of this study was that no specific markers for γδ T cells or NK cells were included in the analyses to clearly identify these cell populations and determine how much they contribute to the production of GrzB. As a surrogate analysis, the GrzB production of CD3$^+$CD4$^-$CD8$^-$ as well as CD3$^-$ cells was investigated, which contain γδ T cells and NK cells, respectively. The CD3$^-$ lymphocytes did not show altered levels of GrzB in any of the groups, but CD3$^+$CD4$^-$CD8$^-$ T cells of symptomatically infected children showed higher levels of GrzB compared to asymptomatically infected or healthy children (Supplementary Figure 2 of (97)). However, in contrast to CD8$^+$ T cells, there was no difference in the frequency of GrzB-producing CD3$^+$CD4$^-$CD8$^-$ T cells between children with severe or mild malaria, indicating that CD8$^+$ T cells are the cytotoxic cell subset that influences the development of severe malaria the most.

Higher numbers of CD8$^+$GrzB$^+$ T cells correlated with the parasitemia of the children, showing that an increase in parasitemia results in an increase of CD8$^+$GrzB$^+$ T cells (Figure 7). However, it also means that despite an increasing number of cytotoxic CD8$^+$ T cells, they fail to control the parasitic reproduction. Since erythrocytes lack MHCI molecules, which are needed for CD8$^+$ T cells to recognize and also lyse infected cells, the CD8$^+$ T cells are hindered from fulfilling their cytotoxic and protective function during blood stage *Pf* malaria. This is in contrast to *P. vivax* malaria, where parasites mainly infect pre-erythrocytic reticulocytes that still have MHCI and CD8$^+$ T cells can exert a protective function (194, 195). The activation of CD8$^+$ T cells during blood-stage malaria can be explained by antigen cross-presentation by CD8$^+$ DCs that capture blood-stage parasites and present MHCI-restricted antigens to CD8$^+$ T cells (196). This cross-presentation leads to the induction of parasite-specific CD8$^+$ T cells that contribute to the development of cerebral malaria.

In conclusion, this study and the recent study from Riggle et al. are the first studies that directly link GrzB-producing CD8$^+$ T cells with the onset of severe malaria in humans, supporting previous findings in experimental murine malaria.

5.2 CD4$^+$CD25$^+$CD127^{lo} nTreg do not seem to play a role in controlling overwhelming T cell responses during malaria

On the one hand, the massive activation and expansion of cytotoxic CD8$^+$ T lymphocytes during the blood stage of *Plasmodium* infection contributes to the onset of severe malaria. On the other hand, CD8$^+$ T cells that are specific for liver-stage antigens have been shown to be crucial for sterile immunity (197). It has been suggested that regulatory immune mechanisms activated during the blood stage are important for protection from overwhelming immunopathological mechanisms mediated by cytotoxic CD8$^+$ T cells, but they may also hinder an effective development of antigen-specific CD8$^+$ T cell memory. The role of natural regulatory T cells (nTreg) in immune homeostasis during *Plasmodium* infections has been studied extensively in mice and humans. Due to disparities in the mode of experiments conducted to investigate nTreg in experimental malaria and due to different outcomes of human data, it is still debated whether nTreg cells are friends or foes of *Plasmodium*-infected individuals (198). To further shed light on the role of nTreg during immune reactions against *Plasmodium falciparum*, their frequency was investigated in different malaria patient cohorts in this study. Additionally, the nTreg frequencies of these patients were compared with those of adults suffering from the novel coronavirus disease 2019 (COVID-19), caused by the severe acute respiratory syndrome coronavirus 2 (SARS-CoV-2). It has been shown that an early activation of cytotoxic CD8$^+$ T cells is crucial for effective viral clearance and is correlated with mild disease progression in COVID-19 patients (199, 200). However, an exacerbated T cell activation is associated with poor clinical outcome (201). Therefore, like in malaria, T cells in COVID-19 might also play a dual role in keeping the activation and regulation of pro-inflammatory immune responses in balance, which seems to determine the severity of the disease. Due to these similarities, it is interesting to compare the T cell responses in malaria and COVID-19.

In this study, the nTreg frequencies did not differ between adult malaria patients, COVID-19 patients and healthy controls or between adults and children (Figure 8). This is consistent with previous findings that nTreg levels are not altered in COVID-19 patients and patients suffering from other respiratory viral diseases like influenza or respiratory syncytial virus (RSV) infections and healthy donors (202). However, when distinguishing patients regarding their disease severity, most studies found decreased levels of circulating nTreg in patients with severe COVID-19 (203-205) compared to mild disease and healthy donors, indicating an increased

recruitment of Tregs into inflamed tissue, specifically lung tissue. In contrast to that, other results showed higher nTreg levels in hospitalized patients with severe disease than in mild cases and healthy donors (202, 206). This in turn could indicate an insufficient recruitment of Tregs from the circulation to peripheral inflamed tissues, leading to increased inflammation and more severe disease. One limitation of this study is that, due to the small sample size, the COVID-19 patients were not distinguished based on disease severity. Accordingly, further investigation into the role of nTreg in disease progression is necessary.

No differences in the nTreg frequencies were found between adult malaria patients and their corresponding healthy controls or between Ghanaian children suffering from mild or severe malaria and healthy children (Figure 8). This is in contrast to the majority of other human studies which show an expansion of nTreg in malaria patients compared to healthy donors and an association of lower nTreg frequencies with lower parasitemia and better disease outcomes (198, 207-209). Most of the studies that investigated the role of nTreg in murine malaria used anti-CD25 antibodies to deplete nTreg cells (210-213). Since activated conventional CD4^{+} and CD8^{+} T cells also express CD25 while some FoxP3^{+} nTreg lack CD25, using only an anti-CD25 antibody is not sufficient to specifically deplete nTreg (214). Consequently, this type of nTreg depletion leads to contradictory results. A study by our group using DEREG mice with a transgenic FoxP3-Diphteria toxin receptor, which allows a more selective depletion of FoxP3^{+} nTreg (215), did not show a correlation between depletion of nTreg cells and disease severity or onset of cerebral malaria (CM) in *Plasmodium berghei ANKA* (PbA)-infected C57BL/6 mice (216). This supports the finding of this study that the pathogenicity of activated cytotoxic T cells does not seem to be controlled by nTreg. Furthermore, studies in mice infected with *Plasmodium yoelii* as well as a human study with *Pf*-infected patients suggest a specific kinetic for nTreg cell expansion during malaria. The numbers of nTregs peaked at day 5-7 post infection in BALB/c mice (217), at day 21 post infection in C57BL/6 mice (209) and at day 10 post infection in humans (207). Since it is hard to determine the exact timepoint post infection in humans with naturally acquired *Plasmodium* infection, the timepoint of blood sampling may differ significantly between the patients. This could be the reason why the nTreg frequencies in this study did not differ between the groups like in other studies. When comparing the data of each individual patient before, during and after a febrile malaria episode, Kurup et al. observed an increase of FoxP3^{+}CD4^{+} nTreg cells during acute febrile malaria episodes (209). In this study, no samples of the same patients were available before or after their malaria episode, so no

longitudinal study of nTreg frequencies could be made. Although further data is necessary to completely understand the role of nTreg in the onset of severe malaria, the data of this study as well as other studies suggest that nTreg cells do not play a major role in protecting from overwhelming immunopathological mechanisms during an infection with *P. falciparum*.

5.3 Regulatory T cell phenotypes differ between malaria and COVID-19 patients and based on disease severity in malaria patients

To further analyze other regulatory mechanisms that could counter-regulate the immune pathological effects of CD8^{+} T cells in malaria patients, the focus was set on the induction of co-inhibitory molecules on T cells. The engagement of co-inhibitory receptors with their respective ligands downregulates T cell functions and is an important immune-regulatory mechanism to prevent immunopathology. In this study, upregulation of PD-1, TIGIT, TIM-3 and LAG-3 on CD4^{+} T cells and of TIGIT, TIM-3 and LAG-3 on CD8^{+} T cells of adult malaria patients could be observed compared to healthy individuals (Figure 9A). Of note, these co-inhibitors were also upregulated on T cells of Ghanaian children with symptomatic malaria compared to healthy children (Figure 10A). In addition to co-inhibitory molecules, the regulatory molecule CD39, which exerts its regulatory function by degrading extracellular ATP, was elevated on T cells of adult malaria patients and Ghanaian children with symptomatic malaria (Figure 9 + Figure 10B). When comparing the Ghanaian children with regard to disease severity, T cells of children with severe malaria showed elevated frequencies of co-inhibitory molecules compared to those with mild malaria (Figure 10A) and CD39 was also upregulated on CD8^{+} T cells of children with severe malaria (Figure 10B).

Consistent with these findings, the induction of co-inhibitory molecules on T cells of *Pf*-infected patients has also been shown by others (77, 80, 218). Furthermore, upregulation of different co-inhibitors on CD4^{+} T cells of patients suffering from severe malaria compared to patients with mild malaria has been observed before (76). Expression of co-inhibitory molecules is an important mechanism to regulate immune homeostasis. However, their excessive upregulation has been associated with T cell exhaustion in chronic viral infections and cancer (67, 100). Dysfunctional or exhausted T cells show diminished effector functions such as reduced IL-2-production, proliferation and cytotoxicity and also an impaired ability to transition into memory cells (219). Many studies have described exhausted T cells in the context of malaria (74, 77,

220). However, in human infections this definition was based mostly on the expression of co-inhibitory molecules such as PD-1, CTLA-4, LAG-3 and TIM-3 that were previously identified as markers of T cell exhaustion in chronic settings (68, 98, 99, 221). It should be noted that malaria resembles an acute, rather than a chronic infection and expression of these co-inhibitory molecules may have different implications here.

Functional analyses of T cell exhaustion in malaria are restricted to experimental murine models. Indeed, the administration of blocking antibodies against LAG-3 in PDL-1-deficient mice infected with *P. yoelii*, for example, improved parasite clearance (222). Likewise, co-blockade of PDL-1 and LAG-3 enhanced anti-parasitic CD4^{+} T cell responses and parasite clearance in *P. yoelii*-infected C57BL/6 mice (74). Notably, *P. yoelii* infection in mice is usually used to study a more chronic setting with a high and persistent antigen load over several weeks, in which T cell dysfunction is more likely. A more acute mouse model of malaria is the infection of C57BL/6 mice with *P. berghei* ANKA (*Pb*A) (223). These mice develop experimental cerebral malaria (ECM) approximately 5 days post infection and die of severe cerebral complications soon after, mimicking symptoms of cerebral malaria in humans, the most severe complication of infections with *P. falciparum*. Interestingly, BALB/c mice infected with *Pb*A, which are normally ECM-resistant, develop characteristic signs of cerebral malaria after administration of blocking antibodies against CTLA4 or PDL-1 and show accumulation of parasites in the brain (79). This further indicates an immunosuppressive role of co-inhibitory receptors in malaria.

In contrast, our group recently showed that CD8^{+}LAG-3^{+} T cells of C57Bl/6 mice infected with *Pb*A are more cytotoxic than their LAG-3^{-} counterparts (82) and that co-inhibitory-rich CD4^{+} as well as CD8^{+} T cells of these mice are capable of suppressing the proliferation of naïve T cells in vitro (62). To further support this, we also showed that CD4^{+}PD-1^{+}CTLA4^{+} T cells of *Pf*-infected patients have similar suppressive capacities to LAG-3^{+} cells in mice and express high levels of IFN-γ and IL-10 as well as the proliferation marker Ki67 (80). These results indicate that these co-inhibitory-rich cells are not exhausted but represent highly functional regulatory T cells that are induced during mouse and human malaria.

Co-inhibitor expression on T cells of adult malaria patients was also compared to that of COVID-19 patients. Particularly striking was the strong induction of TIGIT on CD4^{+} and CD8^{+} T cells of COVID-19 patients compared to malaria patients and healthy donors (Figure 9A). Other studies that investigated the expression of TIGIT on T cells of COVID-19 patients achieved conflicting results. While some studies found no differences in the TIGIT expression on T cells

of COVID-19 patients and healthy individuals (218, 224), other studies also described elevated TIGIT levels in COVID-19 patients, as seen in our results (225, 226). Besides our study, one other study from Herrmann et al. compared TIGIT expression levels of COVID-19 and malaria patients (218). Here, the frequency of TIGIT was not altered in COVID-19 patients compared to malaria patients and healthy individuals. However, a tendency toward lower levels in COVID-19 patients compared to malaria patients was observed. One possible explanation for these conflicting results could be a difference in the average age of the patient cohorts. TIGIT levels were found to correlate with the COVID-19 patients' ages, with older individuals having higher levels of TIGIT on their T cells compared to younger ones (226). Additionally, the kinetic of the expression of every co-inhibitor plays a major role. Since the exact time point of the start of infection in malaria or COVID-19 patients is difficult to determine, the time point of when the blood samples were taken might differ significantly between the studies. Accordingly, this could influence the expression levels of co-inhibitors on T cells.

TIGIT is also upregulated on T cells of Ghanaian children suffering from severe malaria compared to mild malaria cases and healthy children (Figure 10A). Although the upregulation of multiple co-inhibitory molecules is associated with T cell dysfunction, in an acute setting such as malaria or COVID-19 it might also define activated T cells transitioning from naïve cells toward effector cells. Many co-inhibitors have been described to be upregulated on activated as well as antigen-specific T cells (105). In this study, T cells were analyzed in bulk, so the expression pattern of co-inhibitory receptors on antigen-specific T cells might be different. This needs to be investigated further.

TIGIT competes with CD226 for the ligands CD155 and CD112 presented on APCs but binds them with much higher affinity. The binding of TIGIT to its ligands induces the production of anti-inflammatory IL-10 by tolerogenic DCs (103), suppresses pro-inflammatory Th1 and Th17 cell responses and thus shifts the immune response toward a Th2 cell-like response (105). The engagement of CD226 promotes cytotoxicity in CD8$^+$ T cells and thus favors a pro-inflammatory anti-parasitic or anti-viral immune response. Therefore, a downregulation of TIGIT with simultaneous upregulation of CD226 would support a proinflammatory immune response and thus better viral clearance but might also contribute to the onset of severe clinical symptoms. This could explain the lower levels of TIGIT found in critical COVID-19 patients by some studies. On the other hand, elevated levels of co-inhibitory receptors have been described as markers for T cell exhaustion in chronic viral infections and cancer. In chronic LCMV infection in mice,

dysfunctional CD8^{+} T cells co-express TIGIT with PD-1, TIM-3 and LAG-3 (227-229) and exhausted virus-specific CD4^{+} T cells of patients with chronic hepatitis C virus (HCV) infection have been shown to express TIGIT together with PD-1 (230). Although further studies are needed on the function and cytokine production, the very high levels of TIGIT on CD4^{+} and CD8^{+} T cells in COVID-19 patients found in our study suggest a dysfunctional phenotype. These varying levels of TIGIT expression in malaria and COVID-19 patients are one of the major distinctions found in this study, hinting at a distinct difference in T cell profiles between these viral and parasitic diseases.

Another major finding of this study was that LAG-3 is exclusively upregulated on CD4^{+} and CD8^{+} T cells of malaria patients and is absent in healthy donors and COVID-19 patients (Figure 9A). LAG-3 was also upregulated on T cells of Ghanaian children suffering from malaria compared to healthy children (Figure 10A). LAG-3 has been described as a marker of induced regulatory T cells in mice and humans (61, 62) and our data suggests a specific role of those cells during malaria but not COVID-19. Another study that compared malaria and COVID-19 patients also found elevated levels of LAG-3 on CD4^{+} T cells of malaria patients compared to COVID-19 patients and healthy donors (218), which supports our findings. Furthermore, they also found higher levels of LAG-3 on CD8^{+} T cells of COVID-19 patients as well as malaria patients compared to healthy donors. Several other studies also observed at least minor levels of LAG-3^{+} cells in healthy donors while this study didn't observe any LAG-3 expression in healthy donors or COVID-19 patients. There are several possible explanations for these discrepancies between the results of this current study and previous findings. Detection sensitivity, antibody clones and fluorochrome selection may have an impact on the measured amount of LAG-3. Additionally, the mode of experiment might also influence the expression levels, as most of the other studies used isolated and frozen PBMCs and this current study used fresh whole blood for the analysis.

Similarly, TIM-3 expression on CD4^{+} T cells and TIGIT and TIM-3 expression on CD8^{+} T cells were significantly upregulated in children suffering from severe malaria compared to mild malaria cases. These findings are in contrast to previous results showing increased levels of TIM-3 on CD4^{+} T cells of mild malaria cases compared to severe malaria cases (76).

Since the classification and distribution of the malaria patients into mild and severe cases depends first on the diagnosis of the doctor and second on the timepoint of the start of the treatment, the classification might differ between the studies. A patient showing mild malaria

symptoms on the day of sampling and at the start of treatment could have shown severe symptoms one day later. This could explain the discrepancies between the studies regarding the significance of the different expression levels of co-inhibitory molecules in malaria patients. However, all studies show that co-inhibitory molecules are clearly upregulated in *Pf*-infected patients, even when comparing them to patients suffering from autoimmune liver diseases or chronic viral diseases like human immune deficiency virus (HIV), hepatitis B (HBV) or hepatitis C virus (HCV) (102).

TIM-3 has been described as a marker for differentiated IFN-γ-producing CD4^{+} Th1 and cytotoxic CD8^{+} T cells (120, 123). Additionally, T cells in chronic HIV infection or cancer that express high levels of TIM-3 have been shown to be dysfunctional (231). Nevertheless, a strong T cell activation can also lead to an upregulation of TIM-3 without affecting T cell functionality (232, 233). Whether the observed upregulation of TIM-3 in malaria patients is associated with T cell dysfunction was not further addressed in this study, which is a limitation. It has been shown before that blockade of TIM-3 leads to better parasite clearance and reduced cerebral pathology in *PbA*-infected mice (234). This further indicates a significant role of TIM-3 in dampening an effective immune response during malaria.

Taken together, a strong upregulation of multiple co-inhibitory molecules can be observed on both CD4^{+} and CD8^{+} T cells in malaria patients. It has been shown in mice and humans that most of these molecules are transiently expressed and their level decreases with antigen withdrawal, be it through natural parasite clearance or drug-based treatment (62).

Despite the high expression of co-inhibitory molecules on T cells and thus the induction of regulatory T cells that correlates with the severity of malaria, those T cells fail to counteract the immunopathological effects of cytotoxic CD8^{+} T cells as seen by the significant increase of GrzB^{+}-producing CD8^{+} T cells in Ghanaian children with severe malaria. Our studies in mice and humans hint at the fact that those co-inhibitory-rich T cells are not only suppressive but also exert highly cytotoxic functions and thus contribute to immunopathology themselves. Therefore, the question of whether these cells are beneficial or disadvantageous to malaria patients still remains to be elucidated.

5.4 T cells with Tr1 cell characteristics are induced in malaria patients

In this study, LAG-3 was exclusively upregulated in adult malaria patients compared to COVID-19 patients and healthy donors. Furthermore, Ghanaian children suffering from malaria had higher frequencies of LAG-3$^+$ T cells than healthy children (Figure 10A). LAG-3 together with the integrin CD49b have been described as surface markers for mouse and human Tr1 cells (61). Besides the classical FoxP3$^+$ nTreg, Tr1 cells represent another subset of T cells with regulatory capabilities. The role of nTreg in preventing immunopathology in malaria remains controversial; however, whether Tr1 cells may be an important regulator of the anti-malarial immune response has not yet been investigated thoroughly. Indeed, CD4$^+$ T cells co-expressing LAG-3 and CD49b were upregulated in adult malaria patients, while they were absent in healthy donors and COVID-19 patients (Figure 11A). Furthermore, Ghanaian children suffering from malaria showed increased frequencies of Tr1 cells compared to healthy children and children suffering from febrile seizures or bronchopneumonia (Figure 11B). These results show that Tr1 cells are induced during malaria, indicating that they may have an important immune regulatory function during this disease. Tr1 cells are CD4$^+$FoxP3$^-$ cells and mainly produce the anti-inflammatory cytokine IL-10. Additionally, they have been described to co-produce IL-10 together with IFN-γ (61, 235). Interestingly, the induction of IFN-γ$^+$IL-10$^+$ T cells has been described in the context of malaria. Children in Gambia that had only minor numbers of these cells developed a more severe disease, indicating an important regulatory function of IFN-γ$^+$IL-10$^+$ T cells in controlling immunopathology during malaria (236). When analyzing LAG-3 and CD49b irrespective of their co-expression, CD4$^+$LAG-3$^+$ T cells were increased in *Pf*-infected adults and children compared to the corresponding healthy controls or patients suffering from other diseases. On the other hand, the frequency of CD49b was decreased in malaria patients (Figure 9B + Figure 10B). Hence, the induction of Tr1 cells in malaria patients is dependent on the upregulation of LAG-3 but not CD49b. Recently, our group could demonstrate that the suppressive capacity of LAG-3 expressing CD4$^+$ T cells was independent from the expression of CD49b in *Pb*A-infected C57BL/6 mice (62). CD49b is an integrin involved in cell adhesion to collagens (237). So far, its expression has been associated with Tr1 cells mostly in the context of chronic inflammatory conditions (61, 183, 238, 239). However, in peripheral blood or other organs this integrin may not be required or upregulated. Therefore,

it is conceivable that CD49b-expressing CD4$^+$ T cells migrate into organs, explaining the decrease of CD49b$^+$ T cells in peripheral blood.

One limitation of this study is the lack of IL-10-stainings of malaria-induced Tr1 cells. The staining of IL-10 is difficult from a technical perspective. Additionally, in the Ghanaian study setting the patient material was too limited for any stimulation protocols. Therefore, further studies are required to analyze whether the induced CD4$^+$LAG-3$^+$CD49b$^+$ T cells indeed produce IL-10.

Nonetheless, it has been shown that plasma IL-10 levels are increased in malaria patients [163]. Furthermore, when examining the malaria-induced T cells, PD-1 and CCR5 were found to be expressed on almost all of the CD4$^+$LAG-3$^+$CD49b$^+$ T cells (Figure 12), a property previously described for IL-10-producing Tr1 cells [240]. With their immune modulatory properties, Tr1 cells may be important regulators that influence the clinical outcome of *Pf* infections.

There were no differences in the frequencies of CD4$^+$LAG-3$^+$CD49b$^+$ T cells between mild and severe malaria cases. However, the cells of these patient groups showed different phenotypes regarding their co-expression of other co-inhibitory molecules. Interestingly, CD4$^+$LAG-3$^+$CD49b$^+$ T cells of patients with severe malaria showed higher frequencies of the co-inhibitory receptors TIGIT and TIM-3 than those cells of mild malaria patients. TIGIT and TIM-3 expression is associated with an exhausted phenotype in T cells [105]. Therefore, TIGIT and TIM-3 may describe Tr1 cells with impaired regulatory function that fail to prevent immunopathology in malaria, explaining their high frequencies in patients suffering from severe malaria. However, functional analyses of these cells are needed to further elucidate and compare their regulatory properties.

5.5 CCR5 but not TIGIT identifies highly suppressive CD4$^+$PD-1$^+$ regulatory T cells

To analyze whether the TIGIT and TIM-3-expressing Tr1 cells found predominantly in patients suffering from severe malaria do indeed have lower suppressive capacities than their TIGIT$^-$ and TIM3$^-$ counterparts, these cells would need to be isolated from patients' blood to perform functional suppression assays. Due to the technical complexity and the large amount of blood required to isolate sufficient cell numbers, adult patients suffering from acute, symptomatic infection are needed as blood donors. Patients fitting these criteria are returning travelers from

malaria-endemic regions admitted to the University Hospital in Hamburg. However, due to travel restrictions implemented during the COVID-19 pandemic, it was not possible to recruit sufficient numbers of patients with acute malaria for functional assays. To circumvent this issue, FoxP3$^-$ cells with suppressive capacities that could be obtained from healthy donors were used to study the influence of expressed co-inhibitory molecules on their suppressive function. CD4$^+$PD-1$^+$FoxP3$^-$ T cells have been described as a regulatory subset of T cells that is induced in malaria patients, but is also present in healthy donors at lower levels (80). Since PD-1 and CCR5 were identified as additional markers of malaria-induced Tr1 cells, they were chosen to isolate these regulatory cells in an effort to best represent Tr1 cells. Indeed, CD4$^+$LAG-3$^+$CD49b$^+$ T cells are a subset of CD4$^+$PD-1$^+$CCR5$^+$ cells, as revealed by clustering analysis (Figure 16 + Figure 17). TIGIT, as the second most expressed co-inhibitory molecule (after PD-1) on CD4$^+$ T cells, was used as a representative marker for cells expressing multiple co-inhibitory molecules. Accordingly, the CD4$^+$PD-1$^+$TIGIT$^+$ T cells isolated from healthy donors were used to simulate the TIGIT-expressing Tr1 cells identified in patients with severe malaria.

Interestingly, CD4$^+$PD-1$^+$CCR5$^+$ T cells showed the highest suppressive capacities among the sorted CD4$^+$PD-1$^{+/-}$CCR5$^{+/-}$ cell populations. They were able to suppress CD4$^+$ as well as CD8$^+$ T cell proliferation in a similar manner to nTreg (Figure 20 + Figure 22). Supporting the results from the healthy donors, CD4$^+$PD-1$^{+/-}$CCR5$^{+/-}$ T cells isolated from two malaria patients displayed the same pattern in suppressive capacity (Figure 20). Notably, the suppressive capacity in patient-derived T cells was generally higher than in healthy donors, implicating that suppressive capacity may be increased upon acute infection. However, given the small sample size, further experiments are required to solidify this conclusion.

CCR5 is a chemokine receptor that has gained attention as a co-receptor for the cell entry of HIV-1 (241). However, its function in the immune system is the recognition of certain chemokines, among them CCL3, CCL4 and CCL5 (242). Accordingly, CCR5 is involved in cell trafficking processes, guiding immune cells to the site of inflammation, and may be used as an activation marker on T cells. Here, it was found that CCR5 appears to be a marker for suppressive capacity in CD4$^+$ T cells. This is in line with previous results which demonstrated that CCR5^{high} nTreg isolated from tissue samples of patients with colorectal cancer exhibited a higher suppressive function than CCR5^{low} nTregs (243). However, it remains unknown whether CCR5 itself is important for the regulatory abilities of Tregs or whether it is mainly a sign of increased activation of cells with intrinsically stronger suppressive capacities. It has been shown

before that CCR5 is important for the recruitment of Tregs to peripheral organs in the context of colorectal cancer. However, it did not influence the tumor growth or disease outcome (244). Thus, it seems that CCR5 is an additional marker for highly functional regulatory T cells which is important for cell trafficking to the sites of inflammation but does not have an impact on their regulatory function itself.

In contrast, CD4$^+$PD-1$^+$ T cells co-expressing TIGIT showed impaired regulatory properties compared to their TIGIT$^-$ counterparts (Figure 24 + Figure 25). Simultaneous blockade of TIGIT and PD-1 has been shown to result in increased cytokine production of CD8$^+$ tumor-infiltrating T cells in murine colon carcinomas (228) and increased proliferation, cytokine production and degranulation in patients with melanoma (245). These results highlight a potential synergistic effect of the two co-inhibitors. Therefore, it is conceivable that the expression of multiple co-inhibitory molecules on CD4$^+$ T cells results in decreased function and thereby reduced suppressive capacity.

In correlation with their suppressive capacities, CD4$^+$PD-1$^+$CCR5$^+$ T cells isolated from healthy donors produced the highest levels of GrzB, IL-10 and IFN-γ in in vitro stimulation assays (Figure 23A). The expression of both pro- (IFN-γ, GrzB) and anti-inflammatory (IL-10) molecules from the same cell population is another parallel to Tr1 cells. A similar trend could be seen in malaria patients, where CD4$^+$PD-1$^+$CCR5$^+$ T cells produced the highest amount of GrzB and IL-10, whilst IFN-γ production was upregulated in all PD-1- and/or CCR5-expressing populations compared to the double negative population (Figure 23B).

Interestingly, in line with the results of the suppression assays, CD4$^+$PD-1$^+$TIGIT$^-$ T cells showed higher levels of GrzB, IL-10, IFN-γ and TNF-α compared to cells expressing TIGIT (Figure 26). In malaria patients, CD4$^+$PD-1$^+$TIGIT$^-$ T cells showed increased levels of GrzB and IFN-γ compared to TIGIT$^+$ populations. This again indicates that overexpression of TIGIT is a marker for reduced T cell function in both malaria patients and healthy individuals.

Notably, a similar pattern in cytokine expression was found in CD8$^+$PD-1$^{+/-}$CCR5$^{+/-}$ and CD8$^+$PD-1$^{+/-}$TIGIT$^{+/-}$ T cell populations of healthy donors and malaria patients (Figure 28). Whilst CD8$^+$ T cells are usually known for their cytotoxic rather than suppressive functionality, our group demonstrated that malaria-induced CD8$^+$ T cells expressing multiple co-inhibitory molecules in murine experimental malaria have suppressive capacities (62). In general, the expression pattern of co-inhibitory molecules is similar in CD8$^+$ and CD4$^+$ T cells in malaria patients, indicating functional similarities between the two T cell subsets.

Another group described human CD8^{+}HLA-DR^{+} T cells that co-expressed PD-1, CTLA-4 and TIGIT and suppressed the proliferation of autologous PBMCs (246). This indicates that, in addition to CD4^{+} T cells, CD8^{+} T cells expressing co-inhibitory molecules may exhibit a suppressive capacity that might influence the immune response to malaria. However, the question of whether human CD8^{+}PD-1^{+} T cells exert a suppressive function remains to be further investigated.

The exact mechanism of cell suppression by CD4^{+}PD-1^{+}FoxP3^{-} T cells remains elusive. One possible mechanism of suppression is the production of anti-inflammatory cytokines like IL-10 and TGF-β, which have been described as mediators of suppression in nTreg (44, 161). However, despite the increased IL-10 production by CD4^{+}PD-1^{+} T cells, our group showed that their suppressive function is independent of IL-10 alone (80). Another mode of regulation is the expression of CD39, which is upregulated on CD4^{+} and CD8^{+} T cells of malaria patients (Figure 9B + Figure 10B). However, CD39 was not revealed as an additional marker for induced regulatory T cells in this study, although other studies suggest CD39 as a marker for Tr1 cells (247). The exact mechanism of how co-inhibitory molecules exert extrinsic suppressive functions remains incompletely understood. Our group showed that cell-cell contact is required for CD4^{+}PD-1^{+}CTLA-4^{+} T cells to suppress other cells (80). Whilst individual antibody-mediated blockade of PD-1, CTLA4 and TGF-β did not show an effect on the suppressive capacities of those regulatory T cells, it is conceivable that simultaneous blockade may show an effect. Similarly, in tumor therapy, blockade of multiple co-inhibitory molecules increases anti-tumor effector functions, implying synergistic pathways (71, 245). A similar synergistic effect is conceivable in the suppressive function of malaria-induced regulatory T cells.

Taken together, we found elevated levels of T cells expressing multiple co-inhibitory molecules in both the CD4^{+} and CD8^{+} T cell compartment of malaria patients. In CD4^{+} T cells these cells closely resembled Tr1 cells, as identified by their expression of LAG-3 and CD49b. Cells with a similar phenotype were found in healthy donors, identified by co-expression of PD-1 and CCR5. These cells are highly functional and suppressive in both healthy donors and malaria patients. In addition, CCR5 is an additional marker for highly suppressive and functional regulatory T cells that are induced in malaria patients but are also present in healthy donors. Importantly, co-expression of TIGIT is an indicator for reduced suppressive function and cytokine production. Increased frequencies of CD4^{+}PD-1^{+}TIGIT^{+} T cells, as found in Ghanaian children who suffered from severe malaria, indicate an impaired immune regulation in those patients. It could be

hypothesized that due to their decreased suppressive capabilities, the immune response cannot be contained, leading to immunopathology and severe clinical outcome. In light of increasing drug resistance in malaria parasites, resulting in impaired drug efficacy, immunotherapy could provide an alternative, parasite-independent malaria treatment. Identifying how these induced regulatory T cells interact with other cells and how their functionality is regulated could be of great importance to treat malaria and improve the clinical outcome of severe cases in the future.

6 References

1. World malaria report 2022. Geneva: World Health Organization; 2022. Licence: CC BY-NC-SA 3.0 IGO.

2. World malaria report 2020: 20 years of global progress and challenges. Geneva: World Health Organization; 2020. Licence: CC BY-NC-SA 3.0 IGO.

3. World malaria report 2021. Geneva: World Health Organization; 2021. Licence: CC BY-NC-SA 3.0 IGO.

4. Desai M., ter Kuile F.O., Nosten F., McGready R., Asamoa K., Brabin B., and Newman R.D. 2007. Epidemiology and burden of malaria in pregnancy. *Lancet Infect Dis* 7: 93-104.

5. Ahmed M.A., and Cox-Singh J. 2015. Plasmodium knowlesi - an emerging pathogen. *ISBT Sci Ser* 10: 134-140.

6. Ashley E.A., Pyae Phyo A., and Woodrow C.J. 2018. Malaria. *Lancet* 391: 1608-1621.

7. Tuteja R. 2007. Malaria - an overview. *FEBS J* 274: 4670-4679.

8. Mer M., Dünser M.W., Giera R., and Dondorp A.M. 2020. Severe malaria. Current concepts and practical overview: What every intensivist should know. *Intensive Care Med* 46: 907-918.

9. Idro R., Marsh K., John C.C., and Newton C.R.J. 2010. Cerebral Malaria: Mechanisms of Brain Injury and Strategies for Improved Neurocognitive Outcome. *Pediatr Res* 68: 267-274.

10. Birbeck G.L., Molyneux M.E., Kaplan P.W., Seydel K.B., Chimalizeni Y.F., Kawaza K., and Taylor T.E. 2010. Blantyre Malaria Project Epilepsy Study (BMPES) of neurological outcomes in retinopathy-positive paediatric cerebral malaria survivors: a prospective cohort study. *Lancet Neurol* 9: 1173-1181.

11. Storm J., and Craig A.G. 2014. Pathogenesis of cerebral malaria--inflammation and cytoadherence. *Front Cell Infect Microbiol* 4: 100-100.

12. Dunst J., Kamena F., and Matuschewski K. 2017. Cytokines and Chemokines in Cerebral Malaria Pathogenesis. *Front Cell Infect Microbiol* 7: 324.

13. Moxon C.A., Wassmer S.C., Milner D.A., Chisala N.V., Taylor T.E., Seydel K.B., Molyneux M.E., Faragher B., Esmon C.T., Downey C., Toh C.-H., Craig A.G., and Heyderman R.S. 2013. Loss of endothelial protein C receptors links coagulation and inflammation to parasite sequestration in cerebral malaria in African children. *Blood* 122: 842-851.

14. Cowman A.F., Healer J., Marapana D., and Marsh K. 2016. Malaria: Biology and Disease. *Cell* 167: 610-624.

15. Amino R., Giovannini D., Thiberge S., Gueirard P., Boisson B., Dubremetz J.-F., Prévost M.-C., Ishino T., Yuda M., and Ménard R. 2008. Host Cell Traversal Is Important for Progression of the Malaria Parasite through the Dermis to the Liver. *Cell Host Microbe* 3: 88-96.

16. Phillips M.A., Burrows J.N., Manyando C., Van Huijsduijnen R.H., Van Voorhis W.C., and Wells T.N.C. 2017. Malaria. *Nat Rev Dis Primers* 3: 17050.

17. Gilson P.R., and Crabb B.S. 2009. Morphology and kinetics of the three distinct phases of red blood cell invasion by Plasmodium falciparum merozoites. *Int J Parasitol* 39: 91-96.

18. White N.J. 2011. Determinants of relapse periodicity in Plasmodium vivax malaria. *Malar J* 10: 297.

19. Cowman A.F., Berry D., and Baum J. 2012. The cellular and molecular basis for malaria parasite invasion of the human red blood cell. *J Cell Biol* 198: 961-971.

20. Bousema T., and Drakeley C. 2011. Epidemiology and Infectivity of Plasmodium falciparum and Plasmodium vivax Gametocytes in Relation to Malaria Control and Elimination. *Clin Microbiol Rev* 24: 377-410.

21. Nicholson L.B. 2016. The immune system. *Essays Biochem* 60: 275-301.

22. Vivier E., Tomasello E., Baratin M., Walzer T., and Ugolini S. 2008. Functions of natural killer cells. *Nat Immunol* 9: 503-510.

23. Alberts B., Johnson A., Lewis J., Raff M., Roberts K., and Walter P. 2002. B Cells and Antibodies. In: *Molecular Biology of the Cell*, 4th ed. New York: Garland Science.

24. Ribot J.C., Lopes N., and Silva-Santos B. 2021. γδ T cells in tissue physiology and surveillance. *Nat Rev Immunol* 21: 221-232.

25. Alcover A., Alarcón B., and Di Bartolo V. 2018. Cell Biology of T Cell Receptor Expression and Regulation. *Annu Rev Immunol* 36: 103-125.

26. Abbas A.K., Lichtman A.H., Pillai S., Baker D.L., and Baker A. 2018. *Cellular and Molecular Immunology*. 9th ed. Elsevier, Philadelphia, PA.

27. Freedman A.S., Freeman G., Horowitz J.C., Daley J., and Nadler L.M. 1987. B7, a B-cell-restricted antigen that identifies preactivated B cells. *J Immunol* 139: 3260-3267.

28. Freeman G.J., Gray G.S., Gimmi C.D., Lombard D.B., Zhou L.J., White M., Fingeroth J.D., Gribben J.G., and Nadler L.M. 1991. Structure, expression, and T cell costimulatory

activity of the murine homologue of the human B lymphocyte activation antigen B7. *J Exp Med* 174: 625-631.

29. Freeman G.J., Borriello F., Hodes R.J., Reiser H., Gribben J.G., Ng J.W., Kim J., Goldberg J.M., Hathcock K., Laszlo G., and et al. 1993. Murine B7-2, an alternative CTLA4 counter-receptor that costimulates T cell proliferation and interleukin 2 production. *J Exp Med* 178: 2185-2192.

30. Freeman G.J., Gribben J.G., Boussiotis V.A., Ng J.W., Restivo V.A., Jr., Lombard L.A., Gray G.S., and Nadler L.M. 1993. Cloning of B7-2: a CTLA-4 counter-receptor that costimulates human T cell proliferation. *Science* 262: 909-911.

31. Azuma M., Ito D., Yagita H., Okumura K., Phillips J.H., Lanier L.L., and Somoza C. 1993. B70 antigen is a second ligand for CTLA-4 and CD28. *Nature* 366: 76-79.

32. Gross J.A., Callas E., and Allison J.P. 1992. Identification and distribution of the costimulatory receptor CD28 in the mouse. *J Immunol* 149: 380-388.

33. Hathcock K.S., Laszlo G., Pucillo C., Linsley P., and Hodes R.J. 1994. Comparative analysis of B7-1 and B7-2 costimulatory ligands: expression and function. *J Exp Med* 180: 631-640.

34. Thompson C.B., Lindsten T., Ledbetter J.A., Kunkel S.L., Young H.A., Emerson S.G., Leiden J.M., and June C.H. 1989. CD28 activation pathway regulates the production of multiple T-cell-derived lymphokines/cytokines. *Proc Natl Acad Sci U S A* 86: 1333-1337.

35. Boise L.H., Minn A.J., Noel P.J., June C.H., Accavitti M.A., Lindsten T., and Thompson C.B. 1995. CD28 costimulation can promote T cell survival by enhancing the expression of Bcl-XL. *Immunity* 3: 87-98.

36. Chaplin D.D. 2010. Overview of the immune response. *J Allergy Clin Immunol* 125: S3-23.

37. Peters P.J., Borst J., Oorschot V., Fukuda M., Krahenbuhl O., Tschopp J., Slot J.W., and Geuze H.J. 1991. Cytotoxic T lymphocyte granules are secretory lysosomes, containing both perforin and granzymes. *J Exp Med* 173: 1099-1109.

38. Mosmann T.R., Cherwinski H., Bond M.W., Giedlin M.A., and Coffman R.L. 1986. Two types of murine helper T cell clone. I. Definition according to profiles of lymphokine activities and secreted proteins. *J Immunol* 136: 2348-2357.

39. Saravia J., Chapman N.M., and Chi H. 2019. Helper T cell differentiation. *Cell Mol Immunol* 16: 634-643.

40. Stevens T.L., Bossie A., Sanders V.M., Fernandez-Botran R., Coffman R.L., Mosmann T.R., and Vitetta E.S. 1988. Regulation of antibody isotype secretion by subsets of antigen-specific helper T cells. *Nature* 334: 255-258.

41. Harrington L.E., Hatton R.D., Mangan P.R., Turner H., Murphy T.L., Murphy K.M., and Weaver C.T. 2005. Interleukin 17–producing CD4+ effector T cells develop via a lineage distinct from the T helper type 1 and 2 lineages. *Nat Immunol* 6: 1123-1132.

42. Sakaguchi S., Sakaguchi N., Asano M., Itoh M., and Toda M. 1995. Immunologic self-tolerance maintained by activated T cells expressing IL-2 receptor alpha-chains (CD25). Breakdown of a single mechanism of self-tolerance causes various autoimmune diseases. *J Immunol* 155: 1151-1164.

43. Hori S., Nomura T., and Sakaguchi S. 2003. Control of Regulatory T Cell Development by the Transcription Factor Foxp3. *Science* 299: 1057-1061.

44. Asseman C., Mauze S., Leach M.W., Coffman R.L., and Powrie F. 1999. An Essential Role for Interleukin 10 in the Function of Regulatory T Cells That Inhibit Intestinal Inflammation. *J Exp Med* 190: 995-1004.

45. Hesse M., Piccirillo C.A., Belkaid Y., Prufer J., Mentink-Kane M., Leusink M., Cheever A.W., Shevach E.M., and Wynn T.A. 2004. The Pathogenesis of Schistosomiasis Is Controlled by Cooperating IL-10-Producing Innate Effector and Regulatory T Cells. *J Immunol* 172: 3157-3166.

46. Powrie F., Carlino J., Leach M.W., Mauze S., and Coffman R.L. 1996. A critical role for transforming growth factor-beta but not interleukin 4 in the suppression of T helper type 1-mediated colitis by CD45RB(low) CD4+ T cells. *J Exp Med* 183: 2669-2674.

47. Belkaid Y., Piccirillo C.A., Mendez S., Shevach E.M., and Sacks D.L. 2002. CD4+CD25+ regulatory T cells control Leishmania major persistence and immunity. *Nature* 420: 502-507.

48. Green E.A., Gorelik L., McGregor C.M., Tran E.H., and Flavell R.A. 2003. CD4+CD25+ T regulatory cells control anti-islet CD8+ T cells through TGF-β–TGF-β receptor interactions in type 1 diabetes. *Proc Natl Acad Sci U S A* 100: 10878-10883.

49. Scheffold A., Huhn J., and Hofer T. 2005. Regulation of CD4+CD25+ regulatory T cell activity: it takes (IL-)two to tango. *Eur J Immunol* 35: 1336-1341.

50. Sakaguchi S. 2004. Naturally arising CD4+ regulatory t cells for immunologic self-tolerance and negative control of immune responses. *Annu Rev Immunol* 22: 531-562.

51. Sawant D.V., and Vignali D.A. 2014. Once a Treg, always a Treg? *Immunol Rev* 259: 173-191.

52. Fontenot J.D., Gavin M.A., and Rudensky A.Y. 2003. Foxp3 programs the development and function of CD4+CD25+ regulatory T cells. *Nat Immunol* 4: 330-336.

53. Curotto de Lafaille M.A., and Lafaille J.J. 2009. Natural and adaptive foxp3+ regulatory T cells: more of the same or a division of labor? *Immunity* 30: 626-635.

54. Roncarolo M.G., Yssel H., Touraine J.L., Betuel H., De Vries J.E., and Spits H. 1988. Autoreactive T cell clones specific for class I and class II HLA antigens isolated from a human chimera. *J Exp Med* 167: 1523-1534.

55. Roncarolo M.G., Gregori S., Lucarelli B., Ciceri F., and Bacchetta R. 2011. Clinical tolerance in allogeneic hematopoietic stem cell transplantation. *Immunol Rev* 241: 145-163.

56. Gregori S., Goudy K.S., and Roncarolo M.G. 2012. The cellular and molecular mechanisms of immuno-suppression by human type 1 regulatory T cells. *Front Immunol* 3: 30.

57. Pot C., Apetoh L., and Kuchroo V.K. 2011. Type 1 regulatory T cells (Tr1) in autoimmunity. *Semin Immunol* 23: 202-208.

58. Groux H., O'Garra A., Bigler M., Rouleau M., Antonenko S., de Vries J.E., and Roncarolo M.G. 1997. A CD4+ T-cell subset inhibits antigen-specific T-cell responses and prevents colitis. *Nature* 389: 737-742.

59. Magnani C.F., Alberigo G., Bacchetta R., Serafini G., Andreani M., Roncarolo M.G., and Gregori S. 2011. Killing of myeloid APCs via HLA class I, CD2 and CD226 defines a novel mechanism of suppression by human Tr1 cells. *Eur J Immunol* 41: 1652-1662.

60. Yao Y., Vent-Schmidt J., McGeough M.D., Wong M., Hoffman H.M., Steiner T.S., and Levings M.K. 2015. Tr1 Cells, but Not Foxp3+ Regulatory T Cells, Suppress NLRP3 Inflammasome Activation via an IL-10-Dependent Mechanism. *J Immunol* 195: 488-497.

61. Gagliani N., Magnani C.F., Huber S., Gianolini M.E., Pala M., Licona-Limon P., Guo B., Herbert D.R., Bulfone A., Trentini F., Di Serio C., Bacchetta R., Andreani M., Brockmann L., Gregori S., Flavell R.A., and Roncarolo M.G. 2013. Coexpression of CD49b and LAG-3 identifies human and mouse T regulatory type 1 cells. *Nat Med* 19: 739-746.

62. Brandi J., Lehmann C., Kaminski L.C., Schulze Zur Wiesch J., Addo M., Ramharter M., Mackroth M., Jacobs T., and Riehn M. 2021. T cells expressing multiple co-inhibitory molecules in acute malaria are not exhausted but exert a suppressive function in mice. *Eur J Immunol* 52: 312-327.

63. Roncarolo M.G., Gregori S., Bacchetta R., Battaglia M., and Gagliani N. 2018. The Biology of T Regulatory Type 1 Cells and Their Therapeutic Application in Immune-Mediated Diseases. *Immunity* 49: 1004-1019.

64. Lönnberg T., Svensson V., James K.R., Fernandez-Ruiz D., Sebina I., Montandon R., Soon M.S.F., Fogg L.G., Nair A.S., Liligeto U.N., Stubbington M.J.T., Ly L.-H., Bagger F.O., Zwiessele M., Lawrence N.D., Souza-Fonseca-Guimaraes F., Bunn P.T., Engwerda C.R., Heath W.R., Billker O., Stegle O., Haque A., and Teichmann S.A. 2017. Single-cell RNA-seq and computational analysis using temporal mixture modeling resolves TH1/TFH fate bifurcation in malaria. *Sci Immunol* 2: eaal2192.

65.   Wherry E.J. 2011. T cell exhaustion. *Nat Immunol* 12: 492-499.

66.   Zajac A.J., Blattman J.N., Murali-Krishna K., Sourdive D.J.D., Suresh M., Altman J.D., and Ahmed R. 1998. Viral Immune Evasion Due to Persistence of Activated T Cells Without Effector Function. *J Exp Med* 188: 2205-2213.

67.   Jiang Y., Li Y., and Zhu B. 2015. T-cell exhaustion in the tumor microenvironment. *Cell Death Dis* 6: e1792.

68.   Fourcade J., Sun Z., Benallaoua M., Guillaume P., Luescher I.F., Sander C., Kirkwood J.M., Kuchroo V., and Zarour H.M. 2010. Upregulation of Tim-3 and PD-1 expression is associated with tumor antigen–specific CD8+ T cell dysfunction in melanoma patients. *J Exp Med* 207: 2175-2186.

69.   Baitsch L., Baumgaertner P., Devêvre E., Raghav S.K., Legat A., Barba L., Wieckowski S., Bouzourene H., Deplancke B., Romero P., Rufer N., and Speiser D.E. 2011. Exhaustion of tumor-specific CD8+ T cells in metastases from melanoma patients. *J Clin Invest* 121: 2350-2360.

70.   Swart M., Verbrugge I., and Beltman J.B. 2016. Combination Approaches with Immune-Checkpoint Blockade in Cancer Therapy. *Front Oncol* 6: 233.

71.   Rotte A. 2019. Combination of CTLA-4 and PD-1 blockers for treatment of cancer. *J Exp Clin Cancer Res* 38.

72.   Abers M.S., Lionakis M.S., and Kontoyiannis D.P. 2019. Checkpoint Inhibition and Infectious Diseases: A Good Thing? *Trends Mol Med* 25: 1080-1093.

73.   Gay C.L., Bosch R.J., Ritz J., Hataye J.M., Aga E., Tressler R.L., Mason S.W., Hwang C.K., Grasela D.M., Ray N., Cyktor J.C., Coffin J.M., Acosta E.P., Koup R.A., Mellors J.W., Eron J.J., and Team f.t.A.C.T.S. 2017. Clinical Trial of the Anti-PD-L1 Antibody BMS-936559 in HIV-1 Infected Participants on Suppressive Antiretroviral Therapy. *J Infect Dis* 215: 1725-1733.

74.   Butler N.S., Moebius J., Pewe L.L., Traore B., Doumbo O.K., Tygrett L.T., Waldschmidt T.J., Crompton P.D., and Harty J.T. 2012. Therapeutic blockade of PD-L1 and LAG-3 rapidly clears established blood-stage Plasmodium infection. *Nat Immunol* 13: 188-195.

75.   Jayaraman P., Jacques M.K., Zhu C., Steblenko K.M., Stowell B.L., Madi A., Anderson A.C., Kuchroo V.K., and Behar S.M. 2016. TIM3 Mediates T Cell Exhaustion during Mycobacterium tuberculosis Infection. *PLoS Pathog* 12: e1005490.

76.   Abel A., Steeg C., Aminkiah F., Addai-Mensah O., Addo M., Gagliani N., Casar C., Yar D.D., Owusu-Dabo E., Jacobs T., and Mackroth M.S. 2018. Differential expression pattern of co-inhibitory molecules on CD4(+) T cells in uncomplicated versus complicated malaria. *Sci Rep* 8: 4789.

77.   Illingworth J., Butler N.S., Roetynck S., Mwacharo J., Pierce S.K., Bejon P., Crompton P.D., Marsh K., and Ndungu F.M. 2013. Chronic exposure to Plasmodium falciparum is associated with phenotypic evidence of B and T cell exhaustion. *J Immunol* 190: 1038-1047.

78.   Jacobs T., Graefe S.E., Niknafs S., Gaworski I., and Fleischer B. 2002. Murine malaria is exacerbated by CTLA-4 blockade. *J Immunol* 169: 2323-2329.

79.   Hafalla J.C., Claser C., Couper K.N., Grau G.E., Renia L., de Souza J.B., and Riley E.M. 2012. The CTLA-4 and PD-1/PD-L1 inhibitory pathways independently regulate host resistance to Plasmodium-induced acute immune pathology. *PLoS Pathog* 8: e1002504.

80.   Mackroth M.S., Abel A., Steeg C., Schulze Zur Wiesch J., and Jacobs T. 2016. Acute Malaria Induces PD1+CTLA4+ Effector T Cells with Cell-Extrinsic Suppressor Function. *PLoS Pathog* 12: e1005909.

81.   Costa P.A., Leoratti F.M., Figueiredo M.M., Tada M.S., Pereira D.B., Junqueira C., Soares I.S., Barber D.L., Gazzinelli R.T., and Antonelli L.R. 2015. Induction of Inhibitory Receptors on T Cells During Plasmodium vivax Malaria Impairs Cytokine Production. *J Infect Dis* 212: 1999-2010.

82.   Brandi J., Riehn M., Hadjilaou A., and Jacobs T. 2022. Increased Expression of Multiple Co-Inhibitory Molecules on Malaria-Induced CD8+ T Cells Are Associated With Increased Function Instead of Exhaustion. *Front Immunol* 13: 878320.

83.   Ishida Y., Agata Y., Shibahara K., and Honjo T. 1992. Induced expression of PD-1, a novel member of the immunoglobulin gene superfamily, upon programmed cell death. *EMBO J* 11: 3887-3895.

84.   Freeman G.J., Long A.J., Iwai Y., Bourque K., Chernova T., Nishimura H., Fitz L.J., Malenkovich N., Okazaki T., Byrne M.C., Horton H.F., Fouser L., Carter L., Ling V., Bowman M.R., Carreno B.M., Collins M., Wood C.R., and Honjo T. 2000. Engagement of the PD-1 immunoinhibitory receptor by a novel B7 family member leads to negative regulation of lymphocyte activation. *J Exp Med* 192: 1027-1034.

85.   Vibhakar R., Juan G., Traganos F., Darzynkiewicz Z., and Finger L.R. 1997. Activation-induced expression of human programmed death-1 gene in T-lymphocytes. *Exp Cell Res* 232: 25-28.

86.   Okazaki T., Maeda A., Nishimura H., Kurosaki T., and Honjo T. 2001. PD-1 immunoreceptor inhibits B cell receptor-mediated signaling by recruiting src homology 2-domain-containing tyrosine phosphatase 2 to phosphotyrosine. *Proc Natl Acad Sci U S A* 98: 13866-13871.

87.   Sheppard K.A., Fitz L.J., Lee J.M., Benander C., George J.A., Wooters J., Qiu Y., Jussif J.M., Carter L.L., Wood C.R., and Chaudhary D. 2004. PD-1 inhibits T-cell receptor

induced phosphorylation of the ZAP70/CD3zeta signalosome and downstream signaling to PKCtheta. *FEBS Lett* 574: 37-41.

88. Hui E., Cheung J., Zhu J., Su X., Taylor M.J., Wallweber H.A., Sasmal D.K., Huang J., Kim J.M., Mellman I., and Vale R.D. 2017. T cell costimulatory receptor CD28 is a primary target for PD-1-mediated inhibition. *Science* 355: 1428-1433.

89. Jubel J.M., Barbati Z.R., Burger C., Wirtz D.C., and Schildberg F.A. 2020. The Role of PD-1 in Acute and Chronic Infection. *Front Immunol* 11: 487.

90. Terawaki S., Chikuma S., Shibayama S., Hayashi T., Yoshida T., Okazaki T., and Honjo T. 2011. IFN-α Directly Promotes Programmed Cell Death-1 Transcription and Limits the Duration of T Cell-Mediated Immunity. *J Immunol* 186: 2772-2779.

91. Keir M.E., Butte M.J., Freeman G.J., and Sharpe A.H. 2008. PD-1 and its ligands in tolerance and immunity. *Annu Rev Immunol* 26: 677-704.

92. Francisco L.M., Sage P.T., and Sharpe A.H. 2010. The PD-1 pathway in tolerance and autoimmunity. *Immunol Rev* 236: 219-242.

93. Yamazaki T., Akiba H., Iwai H., Matsuda H., Aoki M., Tanno Y., Shin T., Tsuchiya H., Pardoll D.M., Okumura K., Azuma M., and Yagita H. 2002. Expression of programmed death 1 ligands by murine T cells and APC. *J Immunol* 169: 5538-5545.

94. Keir M.E., Liang S.C., Guleria I., Latchman Y.E., Qipo A., Albacker L.A., Koulmanda M., Freeman G.J., Sayegh M.H., and Sharpe A.H. 2006. Tissue expression of PD-L1 mediates peripheral T cell tolerance. *J Exp Med* 203: 883-895.

95. Brown J.A., Dorfman D.M., Ma F.R., Sullivan E.L., Munoz O., Wood C.R., Greenfield E.A., and Freeman G.J. 2003. Blockade of programmed death-1 ligands on dendritic cells enhances T cell activation and cytokine production. *J Immunol* 170: 1257-1266.

96. Selenko-Gebauer N., Majdic O., Szekeres A., Hofler G., Guthann E., Korthauer U., Zlabinger G., Steinberger P., Pickl W.F., Stockinger H., Knapp W., and Stockl J. 2003. B7-H1 (programmed death-1 ligand) on dendritic cells is involved in the induction and maintenance of T cell anergy. *J Immunol* 170: 3637-3644.

97. Kaminski L.-C., Riehn M., Abel A., Steeg C., Yar D.D., Addai-Mensah O., Aminkiah F., Owusu Dabo E., Jacobs T., and Mackroth M.S. 2019. Cytotoxic T Cell-Derived Granzyme B Is Increased in Severe Plasmodium Falciparum Malaria. *Front Immunol* 10: 2917.

98. Barber D.L., Wherry E.J., Masopust D., Zhu B., Allison J.P., Sharpe A.H., Freeman G.J., and Ahmed R. 2006. Restoring function in exhausted CD8 T cells during chronic viral infection. *Nature* 439: 682-687.

99. Blackburn S.D., Shin H., Haining W.N., Zou T., Workman C.J., Polley A., Betts M.R., Freeman G.J., Vignali D.A.A., and Wherry E.J. 2009. Coregulation of CD8+ T cell

exhaustion by multiple inhibitory receptors during chronic viral infection. *Nat Immunol* 10: 29-37.

100.   Wherry E.J., and Kurachi M. 2015. Molecular and cellular insights into T cell exhaustion. *Nat Rev Immunol* 15: 486-499.

101.   Woo S.R., Turnis M.E., Goldberg M.V., Bankoti J., Selby M., Nirschl C.J., Bettini M.L., Gravano D.M., Vogel P., Liu C.L., Tangsombatvisit S., Grosso J.F., Netto G., Smeltzer M.P., Chaux A., Utz P.J., Workman C.J., Pardoll D.M., Korman A.J., Drake C.G., and Vignali D.A. 2012. Immune inhibitory molecules LAG-3 and PD-1 synergistically regulate T-cell function to promote tumoral immune escape. *Cancer Res* 72: 917-927.

102.   Abel A. 2016. Untersuchung koinhibitorischer Moleküle in der humanen Malaria (Dissertation). Universität Hamburg, Fachbereich Biologie.

103.   Yu X., Harden K., Gonzalez L.C., Francesco M., Chiang E., Irving B., Tom I., Ivelja S., Refino C.J., Clark H., Eaton D., and Grogan J.L. 2009. The surface protein TIGIT suppresses T cell activation by promoting the generation of mature immunoregulatory dendritic cells. *Nat Immunol* 10: 48-57.

104.   Boles K.S., Vermi W., Facchetti F., Fuchs A., Wilson T.J., Diacovo T.G., Cella M., and Colonna M. 2009. A novel molecular interaction for the adhesion of follicular CD4 T cells to follicular DC. *Eur J Immunol* 39: 695-703.

105.   Anderson A.C., Joller N., and Kuchroo V.K. 2016. Lag-3, Tim-3, and TIGIT: Co-inhibitory Receptors with Specialized Functions in Immune Regulation. *Immunity* 44: 989-1004.

106.   Stanietsky N., Simic H., Arapovic J., Toporik A., Levy O., Novik A., Levine Z., Beiman M., Dassa L., Achdout H., Stern-Ginossar N., Tsukerman P., Jonjic S., and Mandelboim O. 2009. The interaction of TIGIT with PVR and PVRL2 inhibits human NK cell cytotoxicity. *Proc Natl Acad Sci U S A* 106: 17858-17863.

107.   Dougall W.C., Kurtulus S., Smyth M.J., and Anderson A.C. 2017. TIGIT and CD96: new checkpoint receptor targets for cancer immunotherapy. *Immunol Rev* 276: 112-120.

108.   Lozano E., Dominguez-Villar M., Kuchroo V., and Hafler D.A. 2012. The TIGIT/CD226 axis regulates human T cell function. *J Immunol* 188: 3869-3875.

109.   Joller N., Lozano E., Burkett P.R., Patel B., Xiao S., Zhu C., Xia J., Tan T.G., Sefik E., Yajnik V., Sharpe A.H., Quintana F.J., Mathis D., Benoist C., Hafler D.A., and Kuchroo V.K. 2014. Treg cells expressing the coinhibitory molecule TIGIT selectively inhibit proinflammatory Th1 and Th17 cell responses. *Immunity* 40: 569-581.

110.   Kurtulus S., Sakuishi K., Ngiow S.F., Joller N., Tan D.J., Teng M.W., Smyth M.J., Kuchroo V.K., and Anderson A.C. 2015. TIGIT predominantly regulates the immune response via regulatory T cells. *J Clin Invest* 125: 4053-4062.

111.   Triebel F., Jitsukawa S., Baixeras E., Roman-Roman S., Genevee C., Viegas-Pequignot E., and Hercend T. 1990. LAG-3, a novel lymphocyte activation gene closely related to CD4. *J Exp Med* 171: 1393-1405.

112.   Huard B., Prigent P., Tournier M., Bruniquel D., and Triebel F. 1995. CD4/major histocompatibility complex class II interaction analyzed with CD4- and lymphocyte activation gene-3 (LAG-3)-Ig fusion proteins. *Eur J Immunol* 25: 2718-2721.

113.   Wang J., Sanmamed M.F., Datar I., Su T.T., Ji L., Sun J., Chen L., Chen Y., Zhu G., Yin W., Zheng L., Zhou T., Badri T., Yao S., Zhu S., Boto A., Sznol M., Melero I., Vignali D.A.A., Schalper K., and Chen L. 2019. Fibrinogen-like Protein 1 Is a Major Immune Inhibitory Ligand of LAG-3. *Cell* 176: 334-347 e312.

114.   Xu F., Liu J., Liu D., Liu B., Wang M., Hu Z., Du X., Tang L., and He F. 2014. LSECtin expressed on melanoma cells promotes tumor progression by inhibiting antitumor T-cell responses. *Cancer Res* 74: 3418-3428.

115.   Hannier S., Tournier M., Bismuth G., and Triebel F. 1998. CD3/TCR complex-associated lymphocyte activation gene-3 molecules inhibit CD3/TCR signaling. *J Immunol* 161: 4058-4065.

116.   Huang C.T., Workman C.J., Flies D., Pan X., Marson A.L., Zhou G., Hipkiss E.L., Ravi S., Kowalski J., Levitsky H.I., Powell J.D., Pardoll D.M., Drake C.G., and Vignali D.A. 2004. Role of LAG-3 in regulatory T cells. *Immunity* 21: 503-513.

117.   Workman C.J., and Vignali D.A. 2005. Negative regulation of T cell homeostasis by lymphocyte activation gene-3 (CD223). *J Immunol* 174: 688-695.

118.   Durham N.M., Nirschl C.J., Jackson C.M., Elias J., Kochel C.M., Anders R.A., and Drake C.G. 2014. Lymphocyte Activation Gene 3 (LAG-3) modulates the ability of CD4 T-cells to be suppressed in vivo. *PLoS One* 9: e109080.

119.   Monney L., Sabatos C.A., Gaglia J.L., Ryu A., Waldner H., Chernova T., Manning S., Greenfield E.A., Coyle A.J., Sobel R.A., Freeman G.J., and Kuchroo V.K. 2002. Th1-specific cell surface protein Tim-3 regulates macrophage activation and severity of an autoimmune disease. *Nature* 415: 536-541.

120.   Hastings W.D., Anderson D.E., Kassam N., Koguchi K., Greenfield E.A., Kent S.C., Zheng X.X., Strom T.B., Hafler D.A., and Kuchroo V.K. 2009. TIM-3 is expressed on activated human CD4+ T cells and regulates Th1 and Th17 cytokines. *Eur J Immunol* 39: 2492-2501.

121.   Gao X., Zhu Y., Li G., Huang H., Zhang G., Wang F., Sun J., Yang Q., Zhang X., and Lu B. 2012. TIM-3 Expression Characterizes Regulatory T Cells in Tumor Tissues and Is Associated with Lung Cancer Progression. *PLoS One* 7: e30676.

122.   Gleason M.K., Lenvik T.R., McCullar V., Felices M., O'Brien M.S., Cooley S.A., Verneris M.R., Cichocki F., Holman C.J., Panoskaltsis-Mortari A., Niki T., Hirashima M., Blazar

B.R., and Miller J.S. 2012. Tim-3 is an inducible human natural killer cell receptor that enhances interferon gamma production in response to galectin-9. *Blood* 119: 3064-3072.

123. Zhu C., Anderson A.C., Schubart A., Xiong H., Imitola J., Khoury S.J., Zheng X.X., Strom T.B., and Kuchroo V.K. 2005. The Tim-3 ligand galectin-9 negatively regulates T helper type 1 immunity. *Nat Immunol* 6: 1245-1252.

124. Nakayama M., Akiba H., Takeda K., Kojima Y., Hashiguchi M., Azuma M., Yagita H., and Okumura K. 2009. Tim-3 mediates phagocytosis of apoptotic cells and cross-presentation. *Blood* 113: 3821-3830.

125. Huang Y.-H., Zhu C., Kondo Y., Anderson A.C., Gandhi A., Russell A., Dougan S.K., Petersen B.-S., Melum E., Pertel T., Clayton K.L., Raab M., Chen Q., Beauchemin N., Yazaki P.J., Pyzik M., Ostrowski M.A., Glickman J.N., Rudd C.E., Ploegh H.L., Franke A., Petsko G.A., Kuchroo V.K., and Blumberg R.S. 2015. CEACAM1 regulates TIM-3-mediated tolerance and exhaustion. *Nature* 517: 386-390.

126. Meyers J.H., Sabatos C.A., Chakravarti S., and Kuchroo V.K. 2005. The TIM gene family regulates autoimmune and allergic diseases. *Trends Mol Med* 11: 362-369.

127. Lee J., Su E.W., Zhu C., Hainline S., Phuah J., Moroco J.A., Smithgall T.E., Kuchroo V.K., and Kane L.P. 2011. Phosphotyrosine-dependent coupling of Tim-3 to T-cell receptor signaling pathways. *Mol Cell Biol* 31: 3963-3974.

128. Sakuishi K., Apetoh L., Sullivan J.M., Blazar B.R., Kuchroo V.K., and Anderson A.C. 2010. Targeting Tim-3 and PD-1 pathways to reverse T cell exhaustion and restore anti-tumor immunity. *J Exp Med* 207: 2187-2194.

129. Zhou Q., Munger M.E., Veenstra R.G., Weigel B.J., Hirashima M., Munn D.H., Murphy W.J., Azuma M., Anderson A.C., Kuchroo V.K., and Blazar B.R. 2011. Coexpression of Tim-3 and PD-1 identifies a CD8+ T-cell exhaustion phenotype in mice with disseminated acute myelogenous leukemia. *Blood* 117: 4501-4510.

130. Wang T.-F., and Guidotti G. 1996. CD39 Is an Ecto-(Ca2+, Mg2+)-apyrase *J Biol Chem* 271: 9898-9901.

131. Beavis P.A., Stagg J., Darcy P.K., and Smyth M.J. 2012. CD73: a potent suppressor of antitumor immune responses. *Trends Immunol* 33: 231-237.

132. Cauwels A., Rogge E., Vandendriessche B., Shiva S., and Brouckaert P. 2014. Extracellular ATP drives systemic inflammation, tissue damage and mortality. *Cell Death Dis* 5: e1102-e1102.

133. Deaglio S., Dwyer K.M., Gao W., Friedman D., Usheva A., Erat A., Chen J.-F., Enjyoji K., Linden J., Oukka M., Kuchroo V.K., Strom T.B., and Robson S.C. 2007. Adenosine generation catalyzed by CD39 and CD73 expressed on regulatory T cells mediates immune suppression. *J Exp Med* 204: 1257-1265.

134. Mandapathil M., Szczepanski M.J., Szajnik M., Ren J., Jackson E.K., Johnson J.T., Gorelik E., Lang S., and Whiteside T.L. 2010. Adenosine and Prostaglandin E2 Cooperate in the Suppression of Immune Responses Mediated by Adaptive Regulatory T Cells. *J Biol Chem* 285: 27571-27580.

135. Gupta P.K., Godec J., Wolski D., Adland E., Yates K., Pauken K.E., Cosgrove C., Ledderose C., Junger W.G., Robson S.C., Wherry E.J., Alter G., Goulder P.J.R., Klenerman P., Sharpe A.H., Lauer G.M., and Haining W.N. 2015. CD39 Expression Identifies Terminally Exhausted CD8+ T Cells. *PLoS Pathog* 11: e1005177.

136. Baer K., Klotz C., Kappe S.H.I., Schnieder T., and Frevert U. 2007. Release of Hepatic Plasmodium yoelii Merozoites into the Pulmonary Microvasculature. *PLoS Pathog* 3: e171.

137. Escalante A.A., Lal A.A., and Ayala F.J. 1998. Genetic Polymorphism and Natural Selection in the Malaria Parasite Plasmodium falciparum. *Genetics* 149: 189-202.

138. Radtke A.J., Kastenmüller W., Espinosa D.A., Gerner M.Y., Tse S.-W., Sinnis P., Germain R.N., Zavala F.P., and Cockburn I.A. 2015. Lymph-Node Resident CD8α+ Dendritic Cells Capture Antigens from Migratory Malaria Sporozoites and Induce CD8+ T Cell Responses. *PLoS Pathog* 11: e1004637.

139. Chakravarty S., Cockburn I.A., Kuk S., Overstreet M.G., Sacci J.B., and Zavala F. 2007. CD8+ T lymphocytes protective against malaria liver stages are primed in skin-draining lymph nodes. *Nat Med* 13: 1035-1041.

140. Carvalho L.H., Sano G.-I., Hafalla J.C.R., Morrot A., De Lafaille M.A.C., and Zavala F. 2002. IL-4-secreting CD4+ T cells are crucial to the development of CD8+ T-cell responses against malaria liver stages. *Nat Med* 8: 166-170.

141. Liehl P., Zuzarte-Luís V., Chan J., Zillinger T., Baptista F., Carapau D., Konert M., Hanson K.K., Carret C., Lassnig C., Müller M., Kalinke U., Saeed M., Chora A.F., Golenbock D.T., Strobl B., Prudêncio M., Coelho L.P., Kappe S.H., Superti-Furga G., Pichlmair A., Vigário A.M., Rice C.M., Fitzgerald K.A., Barchet W., and Mota M.M. 2014. Host-cell sensors for Plasmodium activate innate immunity against liver-stage infection. *Nat Med* 20: 47-53.

142. Roland J., Soulard V.r., Sellier C.l., Drapier A.-M., Di Santo J.P., Cazenave P.-A., and Pied S. 2006. NK Cell Responses to Plasmodium Infection and Control of Intrahepatic Parasite Development. *J Immunol* 177: 1229-1239.

143. Gonzalez-Aseguinolaza G., De Oliveira C., Tomaska M., Hong S., Bruna-Romero O., Nakayama T., Taniguchi M., Bendelac A., Van Kaer L., Koezuka Y., and Tsuji M. 2000. α-Galactosylceramide-activated Vα14 natural killer T cells mediate protection against murine malaria. *Proc Natl Acad Sci U S A* 97: 8461-8466.

144. Reece W.H.H., Pinder M., Gothard P.K., Milligan P., Bojang K., Doherty T., Plebanski M., Akinwunmi P., Everaere S., Watkins K.R., Voss G., Tornieporth N., Alloueche A., Greenwood B.M., Kester K.E., McAdam K.P.W.J., Cohen J., and Hill A.V.S. 2004. A CD4+ T-cell immune response to a conserved epitope in the circumsporozoite protein correlates with protection from natural Plasmodium falciparum infection and disease. *Nat Med* 10: 406-410.

145. Bastos K.R.B., Barboza R., Elias R.M., Sardinha L.R., Grisotto M.G., Marinho C.R.F., Amarante-Mendes G.P., Alvarez J.M., and Lima M.R.D.I. 2002. Impaired Macrophage Responses May Contribute to Exacerbation of Blood-Stage Plasmodium chabaudi chabaudi Malaria in Interleukin-12-Deficient Mice. *J Interferon Cytokine Res* 22: 1191-1199.

146. Horowitz A., Newman K.C., Evans J.H., Korbel D.S., Davis D.M., and Riley E.M. 2010. Cross-Talk between T Cells and NK Cells Generates Rapid Effector Responses to Plasmodium falciparum-Infected Erythrocytes. *J Immunol* 184: 6043-6052.

147. Schofield L., Villaquiran J., Ferreira A., Schellekens H., Nussenzweig R., and Nussenzweig V. 1987. γ Interferon, CD8+ T cells and antibodies required for immunity to malaria sporozoites. *Nature* 330: 664-666.

148. Sam H., and Stevenson M.M. 2001. Early IL-12 p70, but not p40, production by splenic macrophages correlates with host resistance to blood-stage Plasmodium chabaudi AS malaria. *Clin Exp Immunol* 117: 343-349.

149. Yoshimoto T., Yoneto T., Waki S., and Nariuchi H. 1998. Interleukin-12-Dependent Mechanisms in the Clearance of Blood-Stage Murine Malaria Parasite Plasmodium berghei XAT, an Attenuated Variant of P. berghei NK65. *J Infect Dis* 177: 1674-1681.

150. Wenisch C., Parschalk B., Narzt E., Looareesuwan S., and Graninger W. 1995. Elevated Serum Levels of IL-10 and IFN-γ in Patients with Acute Plasmodium falciparum Malaria. *Clin Immunol Immunopathol* 74: 115-117.

151. Bouharoun-Tayoun H., Oeuvray C., Lunel F., and Druilhe P. 1995. Mechanisms underlying the monocyte-mediated antibody-dependent killing of Plasmodium falciparum asexual blood stages. *J Exp Med* 182: 409-418.

152. Blackman M.J., Heidrich H.G., Donachie S., McBride J.S., and Holder A.A. 1990. A single fragment of a malaria merozoite surface protein remains on the parasite during red cell invasion and is the target of invasion-inhibiting antibodies. *J Exp Med* 172: 379-382.

153. Bouharoun-Tayoun H., Attanath P., Sabchareon A., Chongsuphajaisiddhi T., and Druilhe P. 1990. Antibodies that protect humans against Plasmodium falciparum blood stages do not on their own inhibit parasite growth and invasion in vitro, but act in cooperation with monocytes. *J Exp Med* 172: 1633-1641.

154.   Giribaldi G., Ulliers D., Mannu F., Arese P., and Turrini F. 2001. Growth ofPlasmodium falciparuminduces stage-dependent haemichrome formation, oxidative aggregation of band 3, membrane deposition of complement and antibodies, and phagocytosis of parasitized erythrocytes. *Br J Haematol* 113: 492-499.

155.   Nitcheu J., Bonduelle O., Combadiere C., Tefit M., Seilhean D., Mazier D., and Combadiere B. 2003. Perforin-Dependent Brain-Infiltrating Cytotoxic CD8+ T Lymphocytes Mediate Experimental Cerebral Malaria Pathogenesis. *J Immunol* 170: 2221-2228.

156.   Potter S., Chan-Ling T., Ball H.J., Mansour H., Mitchell A., Maluish L., and Hunt N.H. 2006. Perforin mediated apoptosis of cerebral microvascular endothelial cells during experimental cerebral malaria. *Int J Parasitol* 36: 485-496.

157.   Haque A., Best S.E., Unosson K., Amante F.H., de Labastida F., Anstey N.M., Karupiah G., Smyth M.J., Heath W.R., and Engwerda C.R. 2011. Granzyme B Expression by CD8+ T Cells Is Required for the Development of Experimental Cerebral Malaria. *J Immunol* 186: 6148-6156.

158.   Riggle B.A., Manglani M., Maric D., Johnson K.R., Lee M.H., Neto O.L.A., Taylor T.E., Seydel K.B., Nath A., Miller L.H., McGavern D.B., and Pierce S.K. 2020. CD8+ T cells target cerebrovasculature in children with cerebral malaria. *J Clin Invest* 130: 1128-1138.

159.   Howland S.W., Poh C.M., and Rénia L. 2015. Activated Brain Endothelial Cells Cross-Present Malaria Antigen. *PLoS Pathog* 11: e1004963.

160.   Howland S.W., Poh C.M., Gun S.Y., Claser C., Malleret B., Shastri N., Ginhoux F., Grotenbreg G.M., and Rénia L. 2013. Brain microvessel cross-presentation is a hallmark of experimental cerebral malaria. *EMBO Mol Med* 5: 984-999.

161.   Tang Q., Boden E.K., Henriksen K.J., Bour-Jordan H., Bi M., and Bluestone J.A. 2004. Distinct roles of CTLA-4 and TGF-β in CD4+CD25+ regulatory T cell function. *Eur J Immunol* 34: 2996-3005.

162.   Yang L., Pang Y., and Moses H.L. 2010. TGF-β and immune cells: an important regulatory axis in the tumor microenvironment and progression. *Trends Immunol* 31: 220-227.

163.   Peyron F., Burdin N., Ringwald P., Vuillez J.P., Rousset F., and Banchereau J. 1994. High levels of circulating IL-10 in human malaria. *Clin Exp Immunol* 95: 300-303.

164.   Bediako Y., Adams R., Reid A.J., Valletta J.J., Ndungu F.M., Sodenkamp J., Mwacharo J., Ngoi J.M., Kimani D., Kai O., Wambua J., Nyangweso G., de Villiers E.P., Sanders M., Lotkowska M.E., Lin J.W., Manni S., Addy J.W.G., Recker M., Newbold C., Berriman M., Bejon P., Marsh K., and Langhorne J. 2019. Repeated clinical malaria episodes are associated with modification of the immune system in children. *BMC Med* 17: 60.

165. Gonzales S.J., Reyes R.A., Braddom A.E., Batugedara G., Bol S., and Bunnik E.M. 2020. Naturally Acquired Humoral Immunity Against Plasmodium falciparum Malaria. *Front Immunol* 11: 594653.

166. Duffy P.E., and Patrick Gorres J. 2020. Malaria vaccines since 2000: progress, priorities, products. *npj Vaccines* 5: 48.

167. Medica D.L., and Sinnis P. 2005. Quantitative Dynamics of Plasmodium yoelii Sporozoite Transmission by Infected Anopheline Mosquitoes. *Infect Immun* 73: 4363-4369.

168. Nussenzweig R.S., Vanderberg J., Most H., and Orton C. 1967. Protective Immunity produced by the Injection of X-irradiated Sporozoites of Plasmodium berghei. *Nature* 216: 160-162.

169. Mordmuller B., Surat G., Lagler H., Chakravarty S., Ishizuka A.S., Lalremruata A., Gmeiner M., Campo J.J., Esen M., Ruben A.J., Held J., Calle C.L., Mengue J.B., Gebru T., Ibanez J., Sulyok M., James E.R., Billingsley P.F., Natasha K.C., Manoj A., Murshedkar T., Gunasekera A., Eappen A.G., Li T., Stafford R.E., Li M., Felgner P.L., Seder R.A., Richie T.L., Sim B.K., Hoffman S.L., and Kremsner P.G. 2017. Sterile protection against human malaria by chemoattenuated PfSPZ vaccine. *Nature* 542: 445-449.

170. Ishizuka A.S., Lyke K.E., Dezure A., Berry A.A., Richie T.L., Mendoza F.H., Enama M.E., Gordon I.J., Chang L.-J., Sarwar U.N., Zephir K.L., Holman L.A., James E.R., Billingsley P.F., Gunasekera A., Chakravarty S., Manoj A., Li M., Ruben A.J., Li T., Eappen A.G., Stafford R.E., K C N., Murshedkar T., Decederfelt H., Plummer S.H., Hendel C.S., Novik L., Costner P.J.M., Saunders J.G., Laurens M.B., Plowe C.V., Flynn B., Whalen W.R., Todd J.P., Noor J., Rao S., Sierra-Davidson K., Lynn G.M., Epstein J.E., Kemp M.A., Fahle G.A., Mikolajczak S.A., Fishbaugher M., Sack B.K., Kappe S.H.I., Davidson S.A., Garver L.S., Björkström N.K., Nason M.C., Graham B.S., Roederer M., Sim B.K.L., Hoffman S.L., Ledgerwood J.E., and Seder R.A. 2016. Protection against malaria at 1 year and immune correlates following PfSPZ vaccination. *Nat Med* 22: 614-623.

171. Sissoko M.S., Healy S.A., Katile A., Omaswa F., Zaidi I., Gabriel E.E., Kamate B., Samake Y., Guindo M.A., Dolo A., Niangaly A., Niaré K., Zeguime A., Sissoko K., Diallo H., Thera I., Ding K., Fay M.P., O'Connell E.M., Nutman T.B., Wong-Madden S., Murshedkar T., Ruben A.J., Li M., Abebe Y., Manoj A., Gunasekera A., Chakravarty S., Sim B.K.L., Billingsley P.F., James E.R., Walther M., Richie T.L., Hoffman S.L., Doumbo O., and Duffy P.E. 2017. Safety and efficacy of PfSPZ Vaccine against Plasmodium falciparum via direct venous inoculation in healthy malaria-exposed adults in Mali: a randomised, double-blind phase 1 trial. *Lancet Infect Dis* 17: 498-509.

172. Mettens P., Dubois P.M., Demoitié M.-A., Bayat B., Donner M.-N., Bourguignon P., Stewart V.A., Heppner D.G., Garçon N., and Cohen J. 2008. Improved T cell responses to Plasmodium falciparum circumsporozoite protein in mice and monkeys induced by a novel formulation of RTS,S vaccine antigen. *Vaccine* 26: 1072-1082.

173. RTS S.C.T.P. 2015. Efficacy and safety of RTS,S/AS01 malaria vaccine with or without a booster dose in infants and children in Africa: final results of a phase 3, individually randomised, controlled trial. *Lancet* 386: 31-45.

174. Van der Maaten L., and Hinton G. 2008. Visualizing data using t-SNE. *J Mach Learn Res* 9: 2579-2605.

175. Ramachandran H., Laux J., Moldovan I., Caspell R., Lehmann P.V., and Subbramanian R.A. 2012. Optimal thawing of cryopreserved peripheral blood mononuclear cells for use in high-throughput human immune monitoring studies. *Cells* 1: 313-324.

176. Potter S., Chan-Ling T., Ball H.J., Mansour H., Mitchell A., Maluish L., and Hunt N.H. 2006. Perforin mediated apoptosis of cerebral microvascular endothelial cells during experimental cerebral malaria. *Int J Parasitol* 36: 485-496.

177. Zhu N., Zhang D., Wang W., Li X., Yang B., Song J., Zhao X., Huang B., Shi W., Lu R., Niu P., Zhan F., Ma X., Wang D., Xu W., Wu G., Gao G.F., and Tan W. 2020. A Novel Coronavirus from Patients with Pneumonia in China, 2019. *N Engl J Med* 382: 727-733.

178. Del Valle D.M., Kim-Schulze S., Huang H.-H., Beckmann N.D., Nirenberg S., Wang B., Lavin Y., Swartz T.H., Madduri D., Stock A., Marron T.U., Xie H., Patel M., Tuballes K., Van Oekelen O., Rahman A., Kovatch P., Aberg J.A., Schadt E., Jagannath S., Mazumdar M., Charney A.W., Firpo-Betancourt A., Mendu D.R., Jhang J., Reich D., Sigel K., Cordon-Cardo C., Feldmann M., Parekh S., Merad M., and Gnjatic S. 2020. An inflammatory cytokine signature predicts COVID-19 severity and survival. *Nat Med* 26: 1636-1643.

179. Mehta P., McAuley D.F., Brown M., Sanchez E., Tattersall R.S., and Manson J.J. 2020. COVID-19: consider cytokine storm syndromes and immunosuppression. *Lancet* 395: 1033-1034.

180. Doe H.T., Kimura D., Miyakoda M., Kimura K., Akbari M., and Yui K. 2016. Expression of PD-1/LAG-3 and cytokine production by CD4+ T cells during infection with Plasmodium parasites. *Microbiol Immunol* 60: 121-131.

181. Bleul C.C., Wu L., Hoxie J.A., Springer T.A., and Mackay C.R. 1997. The HIV coreceptors CXCR4 and CCR5 are differentially expressed and regulated on human T lymphocytes. *Proc Natl Acad Sci U S A* 94: 1925-1930.

182. Wu L., Paxton W.A., Kassam N., Ruffing N., Rottman J.B., Sullivan N., Choe H., Sodroski J., Newman W., Koup R.A., and Mackay C.R. 1997. CCR5 Levels and Expression Pattern Correlate with Infectability by Macrophage-tropic HIV-1, In Vitro. *J Exp Med* 185: 1681-1692.

183. Brockmann L., Soukou S., Steglich B., Czarnewski P., Zhao L., Wende S., Bedke T., Ergen C., Manthey C., Agalioti T., Geffken M., Seiz O., Parigi S.M., Sorini C., Geginat J., Fujio K., Jacobs T., Roesch T., Izbicki J.R., Lohse A.W., Flavell R.A., Krebs C., Gustafsson J.-A., Antonson P., Roncarolo M.G., Villablanca E.J., Gagliani N., and Huber S. 2018.

Molecular and functional heterogeneity of IL-10-producing CD4+ T cells. *Nat Commun* 9: 5457.

184. Facciotti F., Gagliani N., Häringer B., Alfen J.S., Penatti A., Maglie S., Paroni M., Iseppon A., Moro M., Crosti M.C., Stölzel K., Romagnani C., Moroni G., Ingegnoli F., Torretta S., Pignataro L., Annoni A., Russo F., Pagani M., Abrignani S., Meroni P., Flavell R., and Geginat J. 2016. IL-10–producing forkhead box protein 3–negative regulatory T cells inhibit B-cell responses and are involved in systemic lupus erythematosus. *J Allergy Clin Immunol* 137: 318-321.e315.

185. Vicente R., Quentin J., Mausset-Bonnefont A.-L., Chuchana P., Martire D., Cren M., Jorgensen C., and Louis-Plence P. 2016. Nonclassical CD4+CD49b+ Regulatory T Cells as a Better Alternative to Conventional CD4+CD25+ T Cells To Dampen Arthritis Severity. *J Immunol* 196: 298-309.

186. Hanazawa A., Hayashizaki K., Shinoda K., Yagita H., Okumura K., Löhning M., Hara T., Tani-ichi S., Ikuta K., Eckes B., Radbruch A., Tokoyoda K., and Nakayama T. 2013. CD49b-dependent establishment of T helper cell memory. *Immunol Cell Biol* 91: 524-531.

187. Kassiotis G., Gray D., Kiafard Z., Zwirner J., and Stockinger B. 2006. Functional Specialization of Memory Th Cells Revealed by Expression of Integrin CD49b. *J Immunol* 177: 968-975.

188. Mahnke Y.D., Brodie T.M., Sallusto F., Roederer M., and Lugli E. 2013. The who's who of T-cell differentiation: Human memory T-cell subsets. *Eur J Immunol* 43: 2797-2809.

189. Fyfe B., and Miller D.V. 2016. Bronchopneumonia. In: *Diagnostic Pathology: Hospital Autopsy*. Elsevier, Philadelphia. III-2-48-III-42-51.

190. Patel N., Ram D., Swiderska N., Mewasingh L.D., Newton R.W., and Offringa M. 2015. Febrile seizures. *Br Med J* 351: h4240.

191. Totsuka T., Kanai T., Makita S., Fujii R., Nemoto Y., Oshima S., Okamoto R., Koyanagi A., Akiba H., Okumura K., Yagita H., and Watanabe M. 2005. Regulation of murine chronic colitis by CD4+CD25- programmed death-1+ T cells. *Eur J Immunol* 35: 1773-1785.

192. Böttger E., Multhoff G., Kun J.F.J., and Esen M. 2012. Plasmodium falciparum-Infected Erythrocytes Induce Granzyme B by NK Cells through Expression of Host-Hsp70. *PLoS One* 7: e33774.

193. Hernández-Castañeda M.A., Happ K., Cattalani F., Wallimann A., Blanchard M., Fellay I., Scolari B., Lannes N., Mbagwu S., Fellay B., Filgueira L., Mantel P.-Y., and Walch M. 2020. γδ T Cells Kill Plasmodium falciparum in a Granzyme- and Granulysin-Dependent Mechanism during the Late Blood Stage. *J Immunol* 204: 1798-1809.

194. Antonelli L.R., Junqueira C., Vinetz J.M., Golenbock D.T., Ferreira M.U., and Gazzinelli R.T. 2020. The immunology of Plasmodium vivax malaria. *Immunol Rev* 293: 163-189.

195. Junqueira C., Barbosa C.R.R., Costa P.A.C., Teixeira-Carvalho A., Castro G., Sen Santara S., Barbosa R.P., Dotiwala F., Pereira D.B., Antonelli L.R., Lieberman J., and Gazzinelli R.T. 2018. Cytotoxic CD8+ T cells recognize and kill Plasmodium vivax–infected reticulocytes. *Nat Med* 24: 1330-1336.

196. Lundie R.J., De Koning-Ward T.F., Davey G.M., Nie C.Q., Hansen D.S., Lau L.S., Mintern J.D., Belz G.T., Schofield L., Carbone F.R., Villadangos J.A., Crabb B.S., and Heath W.R. 2008. Blood-stage Plasmodium infection induces CD8+ T lymphocytes to parasite-expressed antigens, largely regulated by CD8alpha+ dendritic cells. *Proc Natl Acad Sci U S A* 105: 14509-14514.

197. Schmidt N.W., Butler N.S., Badovinac V.P., and Harty J.T. 2010. Extreme CD8 T Cell Requirements for Anti-Malarial Liver-Stage Immunity following Immunization with Radiation Attenuated Sporozoites. *PLoS Pathog* 6: e1000998.

198. Van Braeckel-Budimir N., Kurup S.P., and Harty J.T. 2016. Regulatory issues in immunity to liver and blood-stage malaria. *Curr Opin Immunol* 42: 91-97.

199. Bergamaschi L., Mescia F., Turner L., Hanson A.L., Kotagiri P., Dunmore B.J., Ruffieux H., De Sa A., Huhn O., Morgan M.D., Gerber P.P., Wills M.R., Baker S., Calero-Nieto F.J., Doffinger R., Dougan G., Elmer A., Goodfellow I.G., Gupta R.K., Hosmillo M., Hunter K., Kingston N., Lehner P.J., Matheson N.J., Nicholson J.K., Petrunkina A.M., Richardson S., Saunders C., Thaventhiran J.E.D., Toonen E.J.M., Weekes M.P., Göttgens B., Toshner M., Hess C., Bradley J.R., Lyons P.A., and Smith K.G.C. 2021. Longitudinal analysis reveals that delayed bystander CD8+ T cell activation and early immune pathology distinguish severe COVID-19 from mild disease. *Immunity* 54: 1257-1275.e1258.

200. Notarbartolo S., Ranzani V., Bandera A., Gruarin P., Bevilacqua V., Putignano A.R., Gobbini A., Galeota E., Manara C., Bombaci M., Pesce E., Zagato E., Favalli A., Sarnicola M.L., Curti S., Crosti M., Martinovic M., Fabbris T., Marini F., Donnici L., Lorenzo M., Mancino M., Ungaro R., Lombardi A., Mangioni D., Muscatello A., Aliberti S., Blasi F., De Feo T., Prati D., Manganaro L., Granucci F., Lanzavecchia A., Francesco R.D., Gori A., Grifantini R., and Abrignani S. 2021. Integrated longitudinal immunophenotypic, transcriptional, and repertoire analyses delineate immune responses in patients with COVID-19. *Sci Immunol* 6: eabg5021.

201. Mathew D., Giles J.R., Baxter A.E., Oldridge D.A., Greenplate A.R., Wu J.E., Alanio C., Kuri-Cervantes L., Pampena M.B., D'Andrea K., Manne S., Chen Z., Huang Y.J., Reilly J.P., Weisman A.R., Ittner C.A.G., Kuthuru O., Dougherty J., Nzingha K., Han N., Kim J., Pattekar A., Goodwin E.C., Anderson E.M., Weirick M.E., Gouma S., Arevalo C.P., Bolton M.J., Chen F., Lacey S.F., Ramage H., Cherry S., Hensley S.E., Apostolidis S.A., Huang A.C., Vella L.A., Betts M.R., Meyer N.J., Wherry E.J., Alam Z., Addison M.M., Byrne K.T., Chandra A., Descamps H.C., Kaminskiy Y., Hamilton J.T., Noll J.H., Omran D.K., Perkey E., Prager E.M., Pueschl D., Shah J.B., Shilan J.S., and Vanderbeck A.N. 2020. Deep

immune profiling of COVID-19 patients reveals distinct immunotypes with therapeutic implications. *Science* 369: eabc8511.

202. Vick S.C., Frutoso M., Mair F., Konecny A.J., Greene E., Wolf C.R., Logue J.K., Franko N.M., Boonyaratanakornkit J., Gottardo R., Schiffer J.T., Chu H.Y., Prlic M., and Lund J.M. 2021. A regulatory T cell signature distinguishes the immune landscape of COVID-19 patients from those with other respiratory infections. *Sci Adv* 7: eabj0274.

203. Qin C., Zhou L., Hu Z., Zhang S., Yang S., Tao Y., Xie C., Ma K., Shang K., Wang W., and Tian D.-S. 2020. Dysregulation of Immune Response in Patients With Coronavirus 2019 (COVID-19) in Wuhan, China. *Clin Infect Dis* 71: 762-768.

204. Sadeghi A., Tahmasebi S., Mahmood A., Kuznetsova M., Valizadeh H., Taghizadieh A., Nazemiyeh M., Aghebati-Maleki L., Jadidi-Niaragh F., Abbaspour-Aghdam S., Roshangar L., Mikaeili H., and Ahmadi M. 2021. Th17 and Treg cells function in SARS-CoV2 patients compared with healthy controls. *J Cell Physiol* 236: 2829-2839.

205. Caldrer S., Mazzi C., Bernardi M., Prato M., Ronzoni N., Rodari P., Angheben A., Piubelli C., and Tiberti N. 2021. Regulatory T Cells as Predictors of Clinical Course in Hospitalised COVID-19 Patients. *Front Immunol* 12: 789735.

206. Galván-Peña S., Leon J., Chowdhary K., Michelson D.A., Vijaykumar B., Yang L., Magnuson A.M., Chen F., Manickas-Hill Z., Piechocka-Trocha A., Worrall D.P., Hall K.E., Ghebremichael M., Walker B.D., Li J.Z., Yu X.G., Mathis D., Benoist C., Lavin-Parsons K., Parry B., Lilley B., Lodenstein C., McKaig B., Charland N., Khanna H., Margolin J., Gonye A., Gushterova I., Lasalle T., Sharma N., Russo B.C., Rojas-Lopez M., Sade-Feldman M., Manakongtreecheep K., Tantivit J., and Thomas M.F. 2021. Profound Treg perturbations correlate with COVID-19 severity. *Proc Natl Acad Sci U S A* 118: e2111315118.

207. Walther M., Tongren J.E., Andrews L., Korbel D., King E., Fletcher H., Andersen R.F., Bejon P., Thompson F., Dunachie S.J., Edele F., De Souza J.B., Sinden R.E., Gilbert S.C., Riley E.M., and Hill A.V.S. 2005. Upregulation of TGF-β, FOXP3, and CD4+CD25+ Regulatory T Cells Correlates with More Rapid Parasite Growth in Human Malaria Infection. *Immunity* 23: 287-296.

208. Torcia M.G., Santarlasci V., Cosmi L., Clemente A., Maggi L., Mangano V.D., Verra F., Bancone G., Nebie I., Sirima B.S., Liotta F., Frosali F., Angeli R., Severini C., Sannella A.R., Bonini P., Lucibello M., Maggi E., Garaci E., Coluzzi M., Cozzolino F., Annunziato F., Romagnani S., and Modiano D. 2008. Functional deficit of T regulatory cells in Fulani, an ethnic group with low susceptibility to Plasmodium falciparum malaria. *Proc Natl Acad Sci U S A* 105: 646-651.

209. Kurup S.P., Obeng-Adjei N., Anthony S.M., Traore B., Doumbo O.K., Butler N.S., Crompton P.D., and Harty J.T. 2017. Regulatory T cells impede acute and long-term immunity to blood-stage malaria through CTLA-4. *Nat Med* 23: 1220-1225.

210.   Couper K.N., Blount D.G., Wilson M.S., Hafalla J.C., Belkaid Y., Kamanaka M., Flavell R.A., de Souza J.B., and Riley E.M. 2008. IL-10 from CD4+CD25-Foxp3-CD127-adaptive regulatory T cells modulates parasite clearance and pathology during malaria infection. *PLoS Pathog* 4: e1000004.

211.   Hisaeda H., Maekawa Y., Iwakawa D., Okada H., Himeno K., Kishihara K., Tsukumo S.-I., and Yasutomo K. 2004. Escape of malaria parasites from host immunity requires CD4+CD25+ regulatory T cells. *Nat Med* 10: 29-30.

212.   Vigário A.M., Gorgette O., Dujardin H.C., Cruz T., Cazenave P.-A., Six A., Bandeira A., and Pied S. 2007. Regulatory CD4+CD25+ Foxp3+ T cells expand during experimental Plasmodium infection but do not prevent cerebral malaria. *Int J Parasitol* 37: 963-973.

213.   Amante F.H., Stanley A.C., Randall L.M., Zhou Y., Haque A., McSweeney K., Waters A.P., Janse C.J., Good M.F., Hill G.R., and Engwerda C.R. 2007. A Role for Natural Regulatory T Cells in the Pathogenesis of Experimental Cerebral Malaria. *Am J Pathol* 171: 548-559.

214.   Couper K.N., Blount D.G., de Souza J.B., Suffia I., Belkaid Y., and Riley E.M. 2007. Incomplete depletion and rapid regeneration of Foxp3+ regulatory T cells following anti-CD25 treatment in malaria-infected mice. *J Immunol* 178: 4136-4146.

215.   Lahl K., Loddenkemper C., Drouin C., Freyer J., Arnason J., Eberl G.R., Hamann A., Wagner H., Huehn J., and Sparwasser T. 2007. Selective depletion of Foxp3+ regulatory T cells induces a scurfy-like disease. *J Exp Med* 204: 57-63.

216.   Steeg C., Adler G., Sparwasser T., Fleischer B., and Jacobs T. 2009. Limited Role of CD4+Foxp3+Regulatory T Cells in the Control of Experimental Cerebral Malaria. *J Immunol* 183: 7014-7022.

217.   Abel S., Lückheide N., Westendorf A.M., Geffers R., Roers A., Müller W., Sparwasser T., Matuschewski K., Buer J., and Hansen W. 2012. Strong Impact of CD4+Foxp3+ Regulatory T Cells and Limited Effect of T Cell-Derived IL-10 on Pathogen Clearance during Plasmodium yoelii Infection. *J Immunol* 188: 5467 - 5477.

218.   Herrmann M., Schulte S., Wildner N.H., Wittner M., Brehm T.T., Ramharter M., Woost R., Lohse A.W., Jacobs T., and Schulze zur Wiesch J. 2020. Analysis of Co-inhibitory Receptor Expression in COVID-19 Infection Compared to Acute Plasmodium falciparum Malaria: LAG-3 and TIM-3 Correlate With T Cell Activation and Course of Disease. *Front Immunol* 11: 1870.

219.   Blank C.U., Haining W.N., Held W., Hogan P.G., Kallies A., Lugli E., Lynn R.C., Philip M., Rao A., Restifo N.P., Schietinger A., Schumacher T.N., Schwartzberg P.L., Sharpe A.H., Speiser D.E., Wherry E.J., Youngblood B.A., and Zehn D. 2019. Defining 'T cell exhaustion'. *Nat Rev Immunol* 19: 665-674.

220. Chandele A., Mukerjee P., Das G., Ahmed R., and Chauhan V.S. 2011. Phenotypic and functional profiling of malaria-induced CD8 and CD4 T cells during blood-stage infection with Plasmodium yoelii. *Immunology* 132: 273-286.

221. Joller N., Hafler J.P., Brynedal B., Kassam N., Spoerl S., Levin S.D., Sharpe A.H., and Kuchroo V.K. 2011. Cutting edge: TIGIT has T cell-intrinsic inhibitory functions. *J Immunol* 186: 1338-1342.

222. Furtado R., Chorro L., Zimmerman N., Guillen E., Spaulding E., Chin S.S., Daily J.P., and Lauvau G. 2021. Blockade of LAG-3 in PD-L1-Deficient Mice Enhances Clearance of Blood Stage Malaria Independent of Humoral Responses. *Front Immunol* 11: 3522.

223. Rest J.R. 1982. Cerebral malaria in inbred mice. I. A new model and its pathology. *Trans R Soc Trop Med Hyg* 76: 410-415.

224. Schultheiß C., Paschold L., Simnica D., Mohme M., Willscher E., von Wenserski L., Scholz R., Wieters I., Dahlke C., Tolosa E., Sedding D.G., Ciesek S., Addo M., and Binder M. 2020. Next-Generation Sequencing of T and B Cell Receptor Repertoires from COVID-19 Patients Showed Signatures Associated with Severity of Disease. *Immunity* 53: 442-455.e444.

225. Zheng H.-Y., Zhang M., Yang C.-X., Zhang N., Wang X.-C., Yang X.-P., Dong X.-Q., and Zheng Y.-T. 2020. Elevated exhaustion levels and reduced functional diversity of T cells in peripheral blood may predict severe progression in COVID-19 patients. *Cell Mol Immunol* 17: 541-543.

226. Files J.K., Boppana S., Perez M.D., Sarkar S., Lowman K.E., Qin K., Sterrett S., Carlin E., Bansal A., Sabbaj S., Long D.M., Kutsch O., Kobie J., Goepfert P.A., and Erdmann N. 2021. Sustained cellular immune dysregulation in individuals recovering from SARS-CoV-2 infection. *J Clin Invest* 131.

227. Doering Travis A., Crawford A., Angelosanto Jill M., Paley Michael A., Ziegler Carly G., and Wherry E.J. 2012. Network Analysis Reveals Centrally Connected Genes and Pathways Involved in CD8+ T Cell Exhaustion versus Memory. *Immunity* 37: 1130-1144.

228. Johnston Robert J., Comps-Agrar L., Hackney J., Yu X., Huseni M., Yang Y., Park S., Javinal V., Chiu H., Irving B., Eaton Dan L., and Grogan Jane L. 2014. The Immunoreceptor TIGIT Regulates Antitumor and Antiviral CD8+ T Cell Effector Function. *Cancer Cell* 26: 923-937.

229. Richter K., Agnellini P., and Oxenius A. 2009. On the role of the inhibitory receptor LAG-3 in acute and chronic LCMV infection. *Int Immunol* 22: 13-23.

230. Ackermann C., Smits M., Woost R., Eberhard J.M., Peine S., Kummer S., Marget M., Kuntzen T., Kwok W.W., Lohse A.W., Jacobs T., Boettler T., and Schulze zur Wiesch J. 2019. HCV-specific CD4+ T cells of patients with acute and chronic HCV infection display high expression of TIGIT and other co-inhibitory molecules. *Sci Rep* 9: 10624.

231. Kuchroo V.K., Anderson A.C., and Petrovas C. 2014. Coinhibitory receptors and CD8 T cell exhaustion in chronic infections. *Curr Opin HIV AIDS* 9: 439-445.

232. Rangachari M., Zhu C., Sakuishi K., Xiao S., Karman J., Chen A., Angin M., Wakeham A., Greenfield E.A., Sobel R.A., Okada H., McKinnon P.J., Mak T.W., Addo M.M., Anderson A.C., and Kuchroo V.K. 2012. Bat3 promotes T cell responses and autoimmunity by repressing Tim-3–mediated cell death and exhaustion. *Nat Med* 18: 1394-1400.

233. Ferris R.L., Lu B., and Kane L.P. 2014. Too Much of a Good Thing? Tim-3 and TCR Signaling in T Cell Exhaustion. *J Immunol* 193: 1525-1530.

234. Hou N., Zou Y., Piao X., Liu S., Wang L., Li S., and Chen Q. 2016. T-Cell Immunoglobulin- and Mucin-Domain-Containing Molecule 3 Signaling Blockade Improves Cell-Mediated Immunity Against Malaria. *J Infect Dis* 214: 1547-1556.

235. Haringer B., Lozza L., Steckel B., and Geginat J. 2009. Identification and characterization of IL-10/IFN-gamma-producing effector-like T cells with regulatory function in human blood. *J Exp Med* 206: 1009-1017.

236. Walther M., Jeffries D., Finney O.C., Njie M., Ebonyi A., Deininger S., Lawrence E., Ngwa-Amambua A., Jayasooriya S., Cheeseman I.H., Gomez-Escobar N., Okebe J., Conway D.J., and Riley E.M. 2009. Distinct Roles for FOXP3+ and FOXP3- CD4+ T Cells in Regulating Cellular Immunity to Uncomplicated and Severe *Plasmodium falciparum* Malaria. *PLoS Pathog* 5: e1000364.

237. Carter W.G., Wayner E.A., Bouchard T.S., and Kaur P. 1990. The role of integrins alpha 2 beta 1 and alpha 3 beta 1 in cell-cell and cell-substrate adhesion of human epidermal cells. *J Cell Biol* 110: 1387-1404.

238. Koch K., Koch N., Sandaradura de Silva U., Jung N., Schulze zur Wiesch J., Fätkenheuer G., Hartmann P., Romerio F., and Lehmann C. 2015. Increased Frequency of CD49b/LAG-3+ Type 1 Regulatory T Cells in HIV-Infected Individuals. *AIDS Res Hum Retroviruses* 31: 1238-1246.

239. Kim J., Lee J., Gonzalez J., Fuentes-Duculan J., Garcet S., and Krueger J.G. 2018. Proportion of CD4+CD49b+LAG-3+ Type 1 Regulatory T Cells in the Blood of Psoriasis Patients Inversely Correlates with Psoriasis Area and Severity Index. *J Invest Dermatol* 138: 2669-2672.

240. Alfen J.S., Larghi P., Facciotti F., Gagliani N., Bosotti R., Paroni M., Maglie S., Gruarin P., Vasco C.M., Ranzani V., Frusteri C., Iseppon A., Moro M., Crosti M.C., Gatti S., Pagani M., Caprioli F., Abrignani S., Flavell R.A., and Geginat J. 2018. Intestinal IFN-γ–producing type 1 regulatory T cells coexpress CCR5 and programmed cell death protein 1 and downregulate IL-10 in the inflamed guts of patients with inflammatory bowel disease. *J Allergy Clin Immunol* 142: 1537-1547.e1538.

241. Dragic T., Litwin V., Allaway G.P., Martin S.R., Huang Y., Nagashima K.A., Cayanan C., Maddon P.J., Koup R.A., Moore J.P., and Paxton W.A. 1996. HIV-1 entry into CD4+ cells is mediated by the chemokine receptor CC-CKR-5. *Nature* 381: 667-673.

242. Vangelista L., and Vento S. 2018. The Expanding Therapeutic Perspective of CCR5 Blockade. *Front Immunol* 8: 1981.

243. Ward S.T., Li K.-K., and Curbishley S.M. 2014. A method for conducting suppression assays using small numbers of tissue-isolated regulatory T cells. *MethodsX* 1: 168-174.

244. Ward S.T., Li K.K., Hepburn E., Weston C.J., Curbishley S.M., Reynolds G.M., Hejmadi R.K., Bicknell R., Eksteen B., Ismail T., Rot A., and Adams D.H. 2015. The effects of CCR5 inhibition on regulatory T-cell recruitment to colorectal cancer. *Br J Cancer* 112: 319-328.

245. Chauvin J.M., Pagliano O., Fourcade J., Sun Z., Wang H., Sander C., Kirkwood J.M., Chen T.H., Maurer M., Korman A.J., and Zarour H.M. 2015. TIGIT and PD-1 impair tumor antigen-specific CD8(+) T cells in melanoma patients. *J Clin Invest* 125: 2046-2058.

246. Machicote A., Belen S., Baz P., Billordo L.A., and Fainboim L. 2018. Human CD8(+)HLA-DR(+) Regulatory T Cells, Similarly to Classical CD4(+)Foxp3(+) Cells, Suppress Immune Responses via PD-1/PD-L1 Axis. *Front Immunol* 9: 2788.

247. Mascanfroni I.D., Takenaka M.C., Yeste A., Patel B., Wu Y., Kenison J.E., Siddiqui S., Basso A.S., Otterbein L.E., Pardoll D.M., Pan F., Priel A., Clish C.B., Robson S.C., and Quintana F.J. 2015. Metabolic control of type 1 regulatory T cell differentiation by AHR and HIF1-α. *Nat Med* 21: 638-646.

Danksagungen/ Acknowledgements

Vielen Dank auch an Maren Sandkuhl! Danke für deine großartige Unterstützung im Labor, besonders beim Isolieren der ganzen PBMCs, die schönen Kaffeepausen, die Gespräche und den Austausch bei experimentellen Herausforderungen!

Ein großer Dank geht auch an Christiane Steeg. Danke für deine Unterstützung und deine Expertise bei sämtlichen wissenschaftlichen Fragen. Danke auch für dein offenes Ohr, deinen Optimismus und deine Herzlichkeit!

Danke an Madeleine Hamley, für die super fixen und zuverlässigen Korrekturen meiner englischen Sprache!

Außerdem bedanke ich mich bei Nicole Gilberger, Eva Mertens, Anna Jäger und Oumou Maiga-Ascofaré aus der Infektionsepidemiologie (AG May) für die Zusammenarbeit an den Projekten in Ghana. Vielen Dank für die Bereitstellung von Blutproben aus euren Malaria-Studienkohorten und die Unterstützung bei den organisatorischen Herausforderungen!

Of course, a big thank you also goes to the team from the KCCR in Kumasi and the team in Agogo! Special thanks to John Amuasi and Anthony Afum-Adjei Awuah, for the project organization on site.

A huge thank you to Wilfred Aniagyei for coordinating the lab work and for the great support with just everything! Thank you for enriching my time in Ghana so much, showing me so many things (for example how to eat Kenkey properly) and being a huge support for all of us who are part in this great project!

Medaase!

Ich danke auch den großen und kleineren flauschigen Fellnasen, die mich durch diese Zeit begleitet haben. Danke Moldi, Magnus, Mimi, Frida und Babsi, dass ihr meine Kuschelattacken ertragt, mir geduldig zuhört und mir gute Laune macht!

Ganz besonders danke ich meiner Familie! Liebe Mama, lieber Papa, liebe Sophia, liebe Omi, vielen Dank, dass ihr mich immer bedingungslos Unterstützt und immer für mich da seid! Ich liebe euch sehr!